

國立臺灣大學生命科學院分子與細胞生物學研究所



碩士論文

Graduate Institute of Molecular and Cellular Biology

College of Life Science

National Taiwan University

Master Thesis

藉由定量磷酸化蛋白質體學分析探討 MCM2 在肺癌細胞
中的調控網絡

Quantitative phosphoproteomic analysis uncovers the
regulatory networks of minichromosome maintenance
protein 2 in lung cancer cells

張曉婷

Siao-Ting Chong

指導教授：阮雪芬 博士

Advisor: Dr. Hsueh-Fen Juan, Ph.D.

中華民國 104 年 7 月

July, 2015

誌謝



在兩年的研究所學習過程，隨著論文的付梓，即將劃上句點。這篇論文能順利完成，幸蒙指導教授阮雪芬老師花費精力與時間，不吝地為學生於研究的方向提供指導與教誨。感謝老師在論文的修訂上提供了寶貴且專業的意見，使得本論文的內容更加完備充實。師恩浩瀚，永銘於心。

我還要感謝實驗室的所有成員，所有曾經幫助過我的學長學弟學姊學妹還有好同學，給我許多研究方面建議，幫我解決各式各樣的實驗問題。謝謝你們平常的照顧與幫助，伴我渡過這兩年的研究所生涯。研究室成員們彼此的情誼，我會銘記在心及珍惜這個緣分。

最後我還要感謝我最摯愛的父母，哥哥及三位弟弟，感謝您們的關懷照顧和支持，讓我能專注於課業研究中，願以此與家人共享。

張曉婷

分子與細胞生物學研究所

中華民國一百零四年七月

中文摘要



微小染色體維持蛋白 2 (MCM2) 是 DNA 複製的主要調控因子。MCM2 與其它 MCM 蛋白結合形成六聚體複合物 (MCM2-7)，並發揮具有解旋酶活性的功能。其功能除了用於 DNA 解旋，還會限制 DNA 在每個細胞週期僅複製一次。MCM2 在增殖細胞中表現量高，因此在許多種癌症被廣泛用作生物標誌物。然而，MCM2 的分子調控機制在肺癌細胞中研究甚少。在這項研究中，我們用 A549 (wild-type p53) 和 H1299 (p53-null) 細胞株探討 MCM2 在肺腺癌扮演的角色。研究結果顯示，在 A549 細胞中過表達 MCM2 會促進細胞增殖，而在 H1299 細胞中抑制 MCM2 表達則會減少細胞增殖。接著，我們進行定量磷酸化蛋白質體學來揭示在肺癌細胞中受 MCM2 調控的重要下游基因的網絡。我們在過度表達 MCM2 的 A549 細胞中共鑑定出 594 個磷酸化蛋白及 1494 個磷酸化位點。這些磷酸化位點中，有 164 個磷酸化蛋白具有顯著差異。此外，在低表達 MCM2 的 H1299 細胞中，我們鑑定 588 個磷酸化蛋白及 1599 個磷酸化位點。這些磷酸化位點中，有 82 個磷酸化蛋白有顯著差異。這些有顯著差異的磷酸化蛋白參與了 RNA 剪接，細胞週期和細胞骨架等功能。在表達 MCM2 的 A549 細胞過和低表達 MCM2 的 H1299 細胞中，我們發現一個共同被調控的磷酸化位點，即是絲氨酸-99 (Ser99)，它位在高遷移率族蛋白 HMG- I / HMG -Y (HMGA1) 上。這表明 HMGA1-Ser99 對肺癌細胞有著重要的調節作用。我們的結果提供肺癌細胞受 MCM2 調控的磷酸化蛋白質體，並發現其調控磷酸化網絡。這些研究為肺癌治療提供了新的目標。

關鍵詞：定量磷酸化蛋白質體學、微小染色體維持蛋白 2、調控網絡、肺癌

ABSTRACT



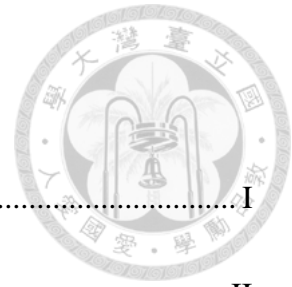
Minichromosome maintenance protein 2 (MCM2) is a licensing factor for DNA replication. It interacts with other MCM proteins to comprise MCM2-7 complex, which acts as a helicase for DNA unwinding and limits DNA replication to one round per cell cycle. MCM2 has been widely used as a biomarker for proliferation in many types of cancer. However, the molecular regulation underlying MCM2 in lung cancer cells is poorly understood. In this study, we investigated the role of MCM2 in lung adenocarcinoma A549 (wild-type p53) and H1299 (null p53) cells. MCM2 overexpression increased cell proliferation in A549 cells while silencing MCM2 decreased cell proliferation in H1299 cells. We performed global quantitative phosphoproteomic analysis to uncover the important downstream networks regulated by MCM2 in lung cancer cells. We identified 1484 phosphorylation sites in 593 phosphoproteins of MCM2-overexpressed A549 cells. Of these phosphosites, 110 phosphoproteins were significantly changed in response to MCM2 overexpression. In addition, we identified 1599 phosphorylation sites in 592 phosphoproteins of MCM2-silenced H1299 cells. Of these phosphosites, 57 phosphoproteins were significantly changed in response to MCM2 silencing. The differentially regulated phosphoproteins are involved in biological functions such as RNA splicing, cell cycle and cytoskeleton regulation. Functional study demonstrated that MCM2 overexpression promoted cell migration in A549 cells. Moreover, silencing MCM2 inhibits cell migration and induces cell cycle arrest in H1299 cells. Furthermore, we observed a common phosphorylation change at Ser-99 of high mobility group protein HMG-I/HMG-Y (HMGA1) in both MCM2 overexpression and silencing, indicating an important regulatory effect of Ser-

99 HMGA1 on lung cancer cells. The phosphoproteomic profiling of MCM2 in lung cancer cells provides new insight about phosphorylation networks regulated by MCM2 and reveals novel targets for lung cancer therapy.



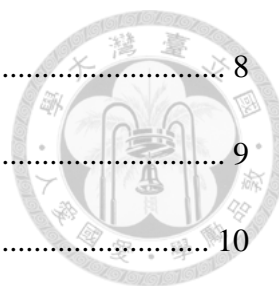
Keywords: Quantitative phosphoproteome, minichromosome maintenance protein-2, regulatory networks, lung cancer cells

Contents

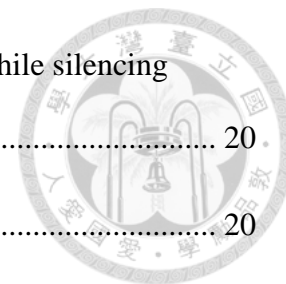


口試委員會審定書	I
誌謝	II
中文摘要	III
ABSTRACT	IV
LIST OF FIGURES	IX
LIST OF TABLES	XI
Chapter 1 INTRODUCTION.....	1
1.1 Lung cancer.....	1
1.2 Minichromosome maintenance protein 2 (MCM2).....	1
1.3 The MCM2 and cancer	2
1.4 Phosphoproteomics	2
1.5 Aim of the study	4
1.6 Experimental Design.....	4
Chapter 2 EXPERIMENTAL PROCESSES	6
2.1 Cell Culture human lung epithelial cells.....	6
2.2 Protein extraction.....	6
2.3 Reduction, Alkylation and Protein Digestion	7
2.4 Dimethyl labelling	7
2.5 Phosphopeptide Enrichment	8

2.6 NanoLC–MS/MS Analysis.....	8
2.7 Data Processing and Analyses	9
2.8 Plasmid construction and transfection	10
2.9 siRNA transfection	10
2.10 Site-directed mutagenesis	11
2.11 MTT and MTS cell viability assay	11
2.12 Colony formation assay	12
2.13 Cell migration assay.....	12
2.14 Cell cycle analysis using flow cytometry	12
2.15 Western blot.....	13
2.16 Statistics analysis	14
Chapter3 RESULTS	15
3.1 Overexpression of MCM2 in A549 increased cell proliferation and silencing MCM2 in H1299 cells decreased cell proliferation.....	15
3.2 P53 might be the up-regulator of MCM2	16
3.3 Phosphoproteome of MCM2 overexpression in A549 cells and silencing MCM2 in H1299 cells	16
3.4 Identification of differentially regulated phosphoproteins in response to MCM2	18
3.5 Overlap between phosphoproteome of MCM2 overexpression and silencing MCM2.....	18
3.6 Functional annotation of MCM2-regulated phosphoproteins.....	19



3.7 Overexpression of MCM2 in A549 increased cell migration while silencing MCM2 in H1299 cells decreased cell migration	20
3.8 Silencing MCM2 in H1299 cells induced cell cycle arrest.....	20
3.9 Phosphorylation of HMGA1 at Ser99 is essential for viability	21
Chapter 4 DISCUSSION	23
Chapter 5 CONCLUSION	28
Chapter 6 FUTURE WORK	29
ABBREVIATION	30
REFERENCES	32
FIGURES	41
TABLES	61



LIST OF FIGURES



- Figure 1. Schematic illustration of the experimental design of this study.
- Figure 2. Schematic workflow of phosphoproteomics.
- Figure 3. Endogenous expression of MCM2 in lung cancer cells.
- Figure 4. Overexpression of MCM2 in A549 increased cell growth in lung cancer cells.
- Figure 5. Silencing MCM2 in H1299 cells decreased cell proliferation.
- Figure 6. The relationship between P53 and MCM2.
- Figure 7. Confirmation of the MCM2 protein expression upon MCM2 overexpression in A549 cells and silencing MCM2 in H1299 cells.
- Figure 8. Distribution of single, doubly, triply and quadruply phosphorylated peptides.
- Figure 9. Distribution of phosphorylated serine, threonine, and tyrosine sites.
- Figure 10. Phosphoproteome of MCM2 in lung cancer cells.
- Figure 11. List of GO-term of regulated phosphoproteins in phosphoproteome of MCM2 overexpression in A549 cells.
- Figure 12. List of GO-term of regulated phosphoproteins in phosphoproteome of silencing MCM2 in H1299 cells.
- Figure 13. Protein enrichment analysis.
- Figure 14. Overexpression of MCM2 in A549 increased cell migration.
- Figure 15. Silencing MCM2 in H1299 cells decreased cell migration.
- Figure 16. Silencing MCM2 in H1299 cells induced cell cycle arrest.
- Figure 17. The MS/MS spectrum of the phosphopeptide KLEKEEEEGISQESSEEEQ from HMGA1 (high mobility group protein HMG-I/HMG-Y).

Figure 18. Phosphorylation of HMGA1 at S99 is essential for viability.



LIST OF TABLES



Table 1. PCR primer sequences for plasmid construction.

Table 2. Number of phosphopeptides, phosphosites and phosphoproteins.

Table 3. List of all common differentially regulated phosphosites.

Table 4. List of all differentially regulated phosphosites.

Table 5. List of GO-term of regulated phosphoproteins in phosphoproteome of MCM2 overexpression in A549 cells.

Table 6. List of GO-term of regulated phosphoproteins in phosphoproteome of silencing MCM2 in H1299 cells.

Table 7. The phosphosites on MCM2 identified in the phosphoproteome data.

Table 8. The phosphosites on high mobility group (HMG) proteins identified in the phosphoproteome data.

Chapter 1 INTRODUCTION



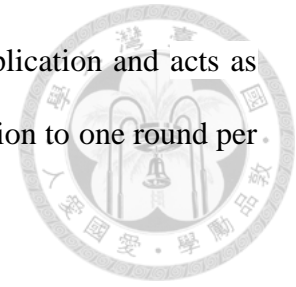
1.1 Lung cancer

Lung cancer is the most common cancers in the world. Due to lacking of advances in diagnostic and therapeutic techniques, the overall 5-year survival rate of lung cancer remains low, which is less than 18%.¹ In Taiwan, lung cancer remains the leading cause of cancer death which recorded the 5-year survival rate of 15.9%, with a median survival of 13.2 months.² In general, there are two major types of lung cancer: small cell lung cancer (SCLC) and non-small cell lung cancer (NSCLC). NSCLC is further categorized into subgroups including adenocarcinomas, squamous cell and large cell carcinomas. NSCLC accounts for approximately 80–85% of lung cancer cases, with squamous cell carcinoma and adenocarcinoma being the most common histological subtypes.³

1.2 Minichromosome maintenance protein 2 (MCM2)

Mcm2-7 is a helicase complex which consists of six different subunits (historically numbered from 2 to 7). MCM2 is also called as DNA replication licensing factor, is one of six members of the minichromosome maintenance (MCM) protein family. Briefly, replication initiation starts with licensing process, which involved the assembly of pre-replicative complexes (pre-RCs) at replication origins. The six subunit origin recognition complex (ORC; subunits Orc1-6), Cdc6 and Cdt1 cooperate to load the hexameric MCM2-7 complex onto double-stranded DNA as an inactive double hexamer.^{4,5} At the G1/S transition, two kinases, CDK and Dbf4-dependent kinase (DDK), activate the MCM helicase, which involves the recruitment of Cdc45 and the heterotetrameric GINS complex to form the CMG complex.⁶⁻⁸ MCM complex forms the

part of the pre-replication complex (pre-RC) at origins of DNA replication and acts as of "licensing factor" to initiate DNA replication and to limit replication to one round per cell cycle.^{9,10}

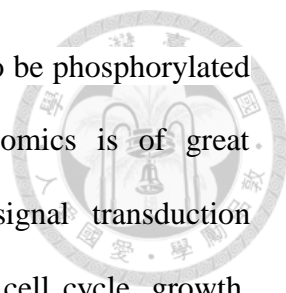


1.3 The MCM2 and cancer

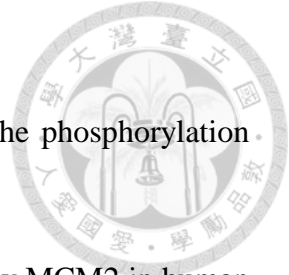
MCM2 have been proposed as an excellent proliferation marker to evaluate the proliferation state in many types of cancer including colon cancer, gastric cancer, breast cancer and prostate cancer.¹¹⁻¹⁴ Previous studies reported that MCM2 is a promising marker in premalignant lung cells and non-small cell cancer.^{15,16} *MCM* genes are associated with lung cancer as evidenced by a study of 178 tumor genomes revealed that 10% of lung squamous cell carcinomas were found to contain amplifications and 12% of lung squamous cell carcinomas contained point mutations in at least one of the six *MCM* genes.¹⁷ In *in-vivo* animal studies, an experimental reduction of MCM2 expression in transgenic mice caused lymphomas, implied that reductions in MCM2 expression levels are linked to human cancer.^{18,19} Recent studies revealed the role of MCM2 as a novel therapeutic target of anti-cancer drugs such as TSA in colon cancer cells and lovastatin in NSCLCs, suggested that MCM2 might play an important role in cancer treatment.^{20,21} The molecular regulation of MCM2 in lung cancer has not been fully elucidated and the MCM2 offers a novel target for drug development to block uncontrolled cancer proliferation.

1.4 Phosphoproteomics

Recently, phosphoproteomic technologies which primarily focusing on post-translation modifications have emerged as useful tools for large-scale study of phosphorylated proteins and contributed to the development of cancer biomarkers and drug targets. Protein phosphorylation is the most frequent reversible post-translation modifications.



In eukaryotic proteome, upwards of 30% of the proteins are prone to be phosphorylated at some point during their existence.²² Study of phosphoproteomics is of great importance as protein phosphorylation governs most of the signal transduction processes and regulates a number of cellular processes, including cell cycle, growth, apoptosis, and differentiation. In phosphoproteomic experiments, the problem of low abundant phosphorylated proteins needed to be tackled. To date, there are various methods developed to enrich the low abundant phosphorylated proteins or peptides prior to MS analysis. The common approaches for serine/threonine and tyrosine phosphopeptide enrichment included the immobilized metal affinity chromatography (IMAC), IMAC with methyl esterification, strong cation exchange chromatography and metal oxide chromatography (MOC) using titania, zirconia and alumina.²³⁻³² A more popular phosphopeptides enrichment method using MOC modified with aliphatic hydroxy acids named as Hydroxy Acid-modified Metal Oxide chromatography (HAMMOC) has proven to be successful in large scale phosphoproteomic studies with advantage of reducing non-specific binding of the acidic amino acid residues.³³ In this study, we applied mass spectrometry-based phosphoproteomics using HAMMOC phosphopeptides enrichment method to characterize the phosphorylation events of MCM2 in NSCLC. We analyzed and interpreted the phosphoproteome data of NSCLC in response to MCM2 in order to identify the reliable candidate proteins for subsequent experimental studies or downstream analysis, to discover protein-protein interactions and to infer about the regulatory network. Here, we obtained a global view of protein phosphorylation events that occur downstream of MCM2 in lung cancer cells.



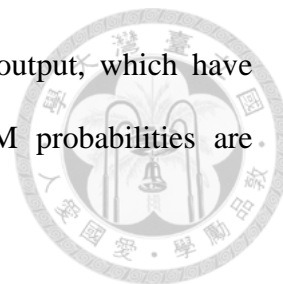
1.5 Aim of the study

1. To acquire the phosphoproteomic profile and characterize the phosphorylation events upon MCM2 overexpression and silencing MCM2.
2. To investigate and validate the biological process regulated by MCM2 in human lung cancer cells.
3. To identify the key phosphoproteins regulated by MCM2 and study its phosphoregulation function.

1.6 Experimental Design

The experimental design of this study is illustrated in Figure 1. We first compared the endogenous MCM2 protein expression level in two lung carcinoma cell lines A549 and H1299. Next, we optimized the transfection condition for MCM2 overexpression and silencing MCM2. For MCM2 overexpression in A549 cells, we transfect cells using 1 ug of MCM2-overexpressing plasmid and harvest cells after 24 hours. For silencing MCM2 in H1299 cells, we transfect cells using siRNA at final concentration of 10 nmol and harvest cells after 48 hours. Protein was extracted from cell lysates, subjected to the phosphoproteomics workflow (as shown in Figure 2) including reduction, alkylation and protein digestion, dimethyl labelling, phosphopeptide enrichment and nanoLC-MS/MS analysis. The raw LC-MS/MS data were analyzed by MaxQuant version 1.5.0.30 using the Andromeda Search engine and searched against the human Swiss-Prot database (reviewed, without isoforms) September 2014 release. We compared the overlap in phosphosites and phosphoproteins from phosphoproteome of MCM2 overexpression in A549 cells versus silencing MCM2 in H1299 cells. Phosphoproteins that change phosphorylation level significantly are selected by ratio H/L normalized ≤ 0.67 (1.5-fold reduced) or ≥ 1.5 (1.5-fold increased). Ratio H/L

normalized represents peptide ratios provided by the MaxQuant output, which have been normalized for each LC-MS/MS run. Localization of PTM probabilities are required to be at least of 0.75.



Chapter 2 EXPERIMENTAL PROCESSES



2.1 Cell Culture human lung epithelial cells

Human lung epithelial cells A549 (ATCC, CCL-185) and H1299 (ATCC, CRL-5803) were obtained from American Type Culture Collection (Manassas, VA, USA). The A549 cells were cultured in Dulbecco's modified Eagle's medium (DMEM, Gibco, Grand Island, NY, USA) while the H1299 cells were cultured in RPMI 1640 medium (Gibco, Grand Island, NY, USA), both are supplemented with 10% fetal bovine serum (FBS, Biological Industries, Beit Haemek, Israel). The cell lines were maintained at 37°C in a controlled humidified atmosphere in an incubator containing 5% CO₂.

2.2 Protein extraction

Cells were washed twice with PBS and trypsinized. Cell pellet was collected by centrifugation at 1000 ×g for 5 min and resuspended in PTS buffer (with aid of Phase-Transfer Surfactants) containing 12 mM sodium deoxycholate (SDC, Sigma-Aldrich, St. Louis, MO, USA) and 12 mM sodium lauroyl sarcosine (SLS, MP Biomedicals, Santa Ana, CA, USA) in triethyl ammonium bicarbonate (TEABC, Sigma-Aldrich). Protease inhibitor cocktail (Bioshop, Burlington, Ontario, Canada), Tyrosine and Serine/Threonine phosphatase inhibitors cocktail (Bionovas, Bremerton WA, USA) were added before sonication. The cells were sonicated on ice using a homogenizer (LABSONIC® M ultrasonic homogenizer, Sartorius AG, Goettingen, Germany) with 60% amplitude and 0.6 cycle duration for 1 minute. The supernatant containing the protein extract was collected by centrifugation at 12000×g for 20 min and the protein concentration was measured using a Pierce™ BCA Protein Assay Kit (Thermo Fisher Scientific, Waltham, MA, USA) according to the user manual.

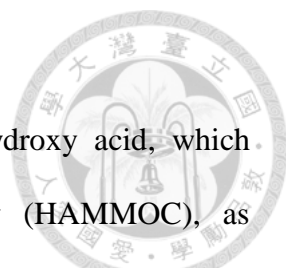
2.3 Reduction, Alkylation and Protein Digestion

Protein extract was reduced with 10 mM dithiothreitol (DTT, WAKO, Osaka, Japan) at room temperature for 30 min, and carbamidomethylated with 55 mM iodoacetamide (IAA, Sigma-Aldrich) at room temperature in darkness for 30 min. Alkylated protein was digested with endopeptidase Lys-C (1:100 w/w) (WAKO) for 2 h followed by sequencing grade modified trypsin (1:100 w/w) (Promega, Mannheim, Germany) for overnight at room temperature. The resulting peptide mixture was acidified with TFA to pH < 3, desalted using StageTips with SDB-XC Empore disc membranes (SDB-XC StageTip) (3M, Neuss, Germany) and eluted in a buffer containing 0.1% TFA and 80% acetonitrile. The digested peptides solution is vacuum dried prior to dimethyl labeling.

2.4 Dimethyl labelling

The stable isotope dimethyl labelling involves the formation of a Schiff base via the reaction of formaldehyde with the primary amines, which is then reduced by cyanoborohydride.³⁴ The digested peptides from the control and treatment samples were reconstituted separately with 100uL of 0.1M TEABC. 4uL of 4% CH₂O (37% Formaldehyde solution, Sigma-Aldrich) for light or 4% ¹³CD₂O (20% Formaldehyde-¹³C, d₂ solution, Sigma-Aldrich) for heavy together with 4 μL of 0.6 M sodium cyanoborohydride (NaBH₃CN, Sigma-Aldrich) was added to the digested peptides from the control and treated samples, respectively and incubated for 1 h at room temperature, with shaking. The reaction was quenched by adding 16 uL ammonia solution (WAKO) to the samples on ice and subsequently added 25 μl of 10% formic acid (WAKO) to the samples. The light-labelled and heavy-labelled samples were mixed and acidified with 10 μL of TFA before proceed to stage-tip desalting.

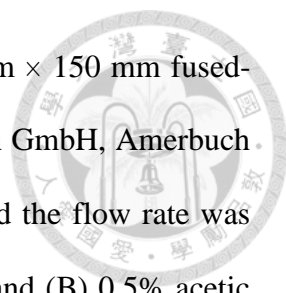
2.5 Phosphopeptide Enrichment



The phosphopeptides were enriched with the aid of aliphatic hydroxy acid, which named as hydroxy acid-modified metal oxide chromatography (HAMMOC), as previously described.³³ TiO₂ has higher affinity toward phosphate groups followed by lactic acid, with weaker affinity to the carboxylic groups of acidic amino acid residues, i.e., aspartic and glutamic acid. To efficiently reduce the non-specific binding of acidic non-phosphorylated peptides to TiO₂, the TiO₂ beads are blocked with lactic acid first, phosphopeptides in successive loading step compete out lactic acid for TiO₂ binding, whereas acidic non-phosphopeptides remain unbound due to the weaker affinity than lactic acid to TiO₂.³⁵ Briefly, custom-made HAMMOC tips were prepared by packing 0.5-mg TiO₂ beads (10 μm, GL Sciences, Tokyo, Japan) into 10-μL C8 StageTips. Prior to sample loading, the HAMMOC tips were equilibrated with solution A containing 0.1% TFA, 80% acetonitrile, and 300 mg/ mL of lactic acid. About 100 ug of the desalted peptide mixture was mixed with an equal volume of solution A and loaded onto the HAMMOC tips (100 μg of mixed peptides per tip). After successive washing with solution A and solution B (0.1% TFA and 80% acetonitrile), the resulting phosphopeptides were eluted by 0.5 and 5% piperidine (WAKO). The eluent was acidified with TFA and desalted with SDB-XC StageTip. After desalting with SDB-XC StageTip, the phosphopeptides were resuspended in 0.5% TFA and subjected to nanoliquid chromatography (nanoLC)–MS/MS analysis.

2.6 NanoLC–MS/MS Analysis

LTQ-Orbitrap XL hybrid mass spectrometer (Thermo Fisher Scientific, Bremen, Germany) was used in this study. MS system was coupled with a Dionex Ultimate3000 LC system (Thermo Fisher Scientific) with an HTC-PAL autosampler (CTC Analytics,

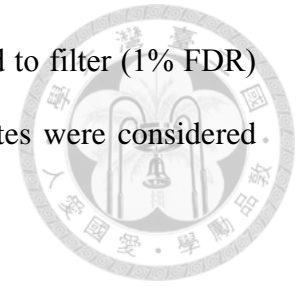


Zwingen, Switzerland). Peptide mixtures were loaded onto a 100 μm \times 150 mm fused-silica capillary column packed with C18 material (3 μm , Dr. Maisch GmbH, Amerbuch, Germany). The injection volume for peptide samples was 5 μL , and the flow rate was 500 nL/min. The mobile phases consisted of (A) 0.5% acetic acid and (B) 0.5% acetic acid and 80% acetonitrile. A three-step linear gradient of 5–10% B in 5 min, 10–40% B in 60 min, 40–100% B in 5 min, and 100% B for 10 min was employed throughout this study. For LTQ-Orbitrap XL, the instrument was operated in the positive ion mode, and data was acquired as follows: a full MS scan (m/z 300–1500) was recorded, and the top 10 precursor ions were selected in the MS scan by the Orbitrap detector for subsequent MS/MS scans by ion trap in the automated gain control mode and the automated gain control values of 5.0×10^5 and 1.0×10^4 were set for full MS and MS/MS, respectively. All the measurements in the LTQ Orbitrap XL were performed with a lock mass.³⁶ For each sample, duplicate nanoLC–MS/MS analyses were performed.

2.7 Data Processing and Analyses

All raw LC-MS/MS data were analyzed by MaxQuant version 1.5.0.30 using the Andromeda Search engine and searched against the human Swiss-Prot database, the reviewed part of Uniprot, without isoforms (September 2014 release). Enzyme specificity was set to trypsin, allowing for cleavage N-terminal to proline and between aspartic acid and proline. The search included carbamidomethylation of cysteine as a fixed modification and N-acetylation and oxidation of methionine (and phosphorylation of serine, threonine, or tyrosine for phosphoproteins) as variable modifications. Up to two missed cleavages were allowed for protease digestion, and enzyme specificity was set to trypsin, defined as C-terminal to arginine and lysine excluding proline. The match between run feature and the second peptide option was disabled and everything else set

to the default values. The “identify” module in MaxQuant was used to filter (1% FDR) identifications at the peptide and protein level. Phosphorylation sites were considered localized at a site localization probability above 75%.



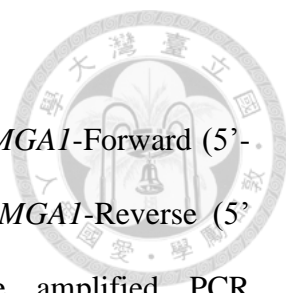
2.8 Plasmid construction and transfection

To construct Mcm2 expressing plasmid, a full-length sequence of MCM2 was amplified by PCR using the primer pair *MCM2-Forward* (5'-GCTAGCGCCACCATGGCGGAATCATCGGAA 3') and *MCM2-Reverse* (5'-CGCACGCGTACAAGCTTTCAGAACTGCTGCAGGAT 3'). The amplified PCR products was inserted into the *NheI/HindIII* sites of pcDNA3.1(+)(Invitrogen, Burlington,ON,USA). The p53 expressing plasmid pcDNA3.1(-)/TP53 was kindly provided by Dr. Hsin-Yi Chang (our laboratory). The shRNA targeting p53 and luciferase were obtained from the National RNAiCore, Academia Sinica, Taiwan. All sequence of insert was confirmed by sequencing result. Prior to plasmid transfection into cells, 2×10^5 of A549 cells or 5×10^4 of H1299 cells were seeded on 6-well plates per well and allowed to attach overnight. Cells at 70-80% confluence were transfected with plasmid or shRNA (sh-TP53 in H1299 cells) using Lipofectamine 2000 or Lipofectamine 3000 (Invitrogen, Burlington, IA, USA) according to the manufacturer's instructions.

2.9 siRNA transfection

H1299 cells were transfected with three different siRNA duplexes against MCM2 or control siRNA (Cat # SR302835, Origene, Rockville, MD, USA) using Lipofectamine 3000 (Invitrogen, Burlington,IA, USA) according to the manufacturer instructions. At 48 hours after transfection, cells were harvested and used for Western blotting.

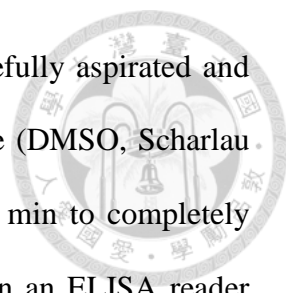
2.10 Site-directed mutagenesis



The HMGA1 gene was amplified by PCR using the primer pair *HMGA1*-Forward (5'-AAAGGATCCGCCACCATGAGTGAGTCGAGCTCG 3') and *HMGA1*-Reverse (5'-AAATTGGGCCCTCACTGCTCCTCCTCCGAGGACT 3'). The amplified PCR products was inserted into the *Apal/BamHI* sites of pcDNA3.1(+)(Invitrogen, Burlington,ON,USA). Primers containing the desired mutation, are listed below: *HMGA1*-S99A (5' GGAGGGCATCGCGCAGGAGTC 3'); *HMGA1*-S99E (5' GGAGGGCATCCAGCAGGAGTCC 3'). Synthesis of the mutant strand was performed by PCR using the plasmid pcDNA3.1(+)/HMGA1-WT as template in the presence of Phusion high-fidelity DNA polymerase (Finnzymes, Espoo, Finland). Suitable cycling parameters were chosen according to the QuikChange site-directed mutagenesis kit (Stratagene, La Jolla, CA, USA). At the end of the PCR, 1 μ L of the restriction enzyme DpnI (Merck) was added directly to each amplified product, and the reaction was incubated at 37°C for 1 h. Finally, 1 μ L of the *DpnI*-treated DNA from each amplification reaction was transformed into the E. coli strain DH5-alpha. The plasmid DNA was sequenced at the DNA Sequencing Facility (Genomics BioSci & Tech.).

2.11 MTT and MTS cell viability assay

The MTT powder (3-(4,5-dimethylthiazol-2-yl)-2,5-diphenyltetrazolium bromide Sigma-Aldrich) were prepared as stock in PBS at the concentration of 5 mg/ml and filtered. The MTS reagent powder (3-(4,5-dimethylthiazol-2-yl)-5-(3-carboxymethoxyphenyl)-2-(4-sulfophenyl)-2H-tetrazolium, inner salt, Promega) were prepared as stock in PBS at the concentration of 20 mg/ml and filtered. At 24 hours post-transfection, 5000 cells were reseeded in 96-well plate and incubate for 24 and 48 hours. 20 μ l MTT solution was added to each well at each time point and followed by incubation for 3 hours at



37°C with 5% CO₂ until the violate crystal formed. MTT was carefully aspirated and the formazan crystals were dissolved with 50 ul dimethyl sulfoxide (DMSO, Scharlau Chemie, Barcelona, Spain) and agitated avoided from light for 15 min to completely solubilize the crystals. The absorbance was measured at 570 nm on an ELISA reader (BioRad Laboratories, Hercules, CA, USA). For MTS assay, 20 ul mixture of MTS solution and PMS (phenazine methosulfate) at ratio 1:20 were added to each well at each time point and followed by incubation for 1 hours at 37°C with 5% CO₂. The absorbance was measured at 490 nm.

2.12 Colony formation assay

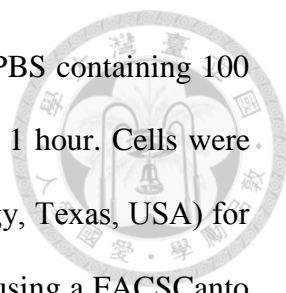
At 24 hours post-transfection, 500 cells were seeded into 6-well plates. Colonies were allowed to form for 8 days. The colonies were washed with 1xPBS. The cells were fixed with methanol and stained with crystal violet (0.2mg/ml) for 15 minutes at room temperature.

2.13 Cell migration assay

A migration assay was performed using 8-µm pore size transwell plates (Corning, MA, USA). At 48 hours post-transfection, 3x10⁴ cells with serum-free medium were loaded into the inserts and medium containing 10% FBS was loaded into the lower compartments. The cells were incubated at 37°C for six hours. The cells were fixed for 30 minutes using 100% methanol and stained with 0.1% crystal violet for 30 minutes. Cotton swabs were used to remove cells from the upper site of the inserts. Images of five different fields of each insert were captured and the number of cells was counted.

2.14 Cell cycle analysis using flow cytometry

Cells were collected, fixed in 70% ethanol (Sigma-Aldrich) and stored at -20°C for



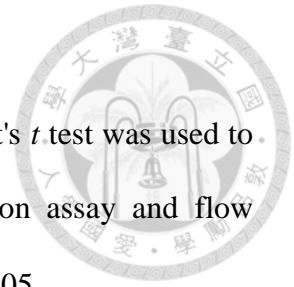
overnight. Then, the cells were washed using PBS, resuspended in PBS containing 100 µg/ml RNase A and 0.1% Triton X-100 and incubated at 37°C for 1 hour. Cells were stained with 5 µg/ml propidium iodide (PI, Santa Cruz Biotechnology, Texas, USA) for 15 minutes in the dark. The DNA content of the cells was analyzed using a FACSCanto instrument (BD Biosciences Immunocytometry Systems, San Jose, CA, USA). At least 10,000 cells were collected for each measurement in a triplicate experiment. The percentage of cells in different phases of the cell cycle was analyzed using ModFit LT (Verity Software House, USA).

2.15 Western blot

Samples (30 µg) were mixed with sodium dodecyl sulfate polyacrylamide gel electrophoresis (SDS-PAGE) sample buffer, boiled for 5 minutes, electrophoresed on a 10% SDS polyacrylamide gel, and transferred onto polyvinylidene difluoride (PVDF) membrane (Millipore). The membrane was blocked in 5% non-fat milk in TBST for 1 hour with gentle agitation. The membrane was incubated with the following primary antibody diluted in blocking buffer at 4°C overnight: rabbit anti-MCM2 (GeneTex, San Antonio, TX, USA; 1:1000), mouse anti-P53 (Santa Cruz, CA, USA; 1:1000), rabbit anti-HMGA1 (abcam, Cambridge, MA, USA; 1:1000) and mouse anti-Actin (Millipore; 1:5000). After washing, the membrane was incubated with appropriate horseradish peroxidase-labelled secondary antibody (Sigma-Aldrich; 1:100000) for 2 hours at room temperature. Signal was developed with Clarity Western ECL Substrate Kit (BioRad Laboratories, Hercules, CA, USA).

2.16 Statistics analysis

Results are expressed as the mean \pm standard deviation. The Student's *t* test was used to analyze the cell viability assay, colony formation assay, migration assay and flow cytometry. The statistical significance in this study was set at $P < 0.05$.



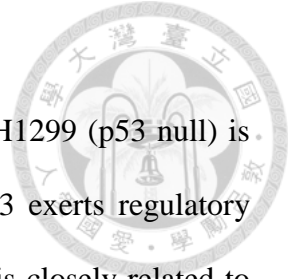
Chapter3 RESULTS



3.1 Overexpression of MCM2 in A549 increased cell proliferation and silencing

MCM2 in H1299 cells decreased cell proliferation

As described previously, MCM2 is known as good proliferation marker in various cancer cells. To investigate the role of MCM2 in lung cancer cells, we performed functional analysis of MCM2 overexpression and silencing MCM2 using A549 and H1299 cells. Both A549 and H1299 cells are lung carcinoma where A549 cells express p53 while H1299 do not. The H1299 cells have a homozygous partial deletion of the p53 protein and lack expression of p53 protein. We first compared the endogenous expression of MCM2 in two types of lung cancer cells, A549 and H1299 cells. Western blot analysis (Figure 3) showed that the endogenous expression of MCM2 in H1299 (p53 null) is higher if compared to A549 (p53 wild-type). Due to the significant different in endogenous MCM2 expression between these two cell lines, we performed MCM2 overexpression using A549 cells and silencing MCM2 using H1299 cells. MTT or MTS proliferation assay and colony formation assay were performed to evaluate the cell proliferation of A549 and H1299 cells in response to MCM2 overexpression and silencing MCM2 respectively. MCM2-overexpressed A549 cells exhibited a significant increase in cell proliferation (increased 65.0% and 38.2% of cell viability at 24 and 48 hours) and higher number of colonies formed as compared to control vector (Figure 4). In contrary, MCM2-silenced H1299 cells (both si-2 and si-3) showed a significant decrease in cell proliferation and lower number of colonies formed as compared to control siRNA. As shown in Figure 5, si-2 reduced 18.8% and 14.2% of cell viability while si-3 reduced 20.7% and 16.6% of cell viability at 24 and 48 hours.

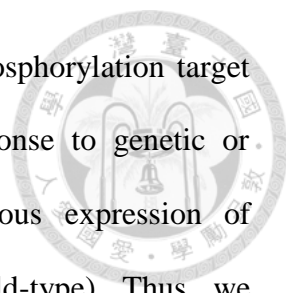


3.2 P53 might be the up-regulator of MCM2

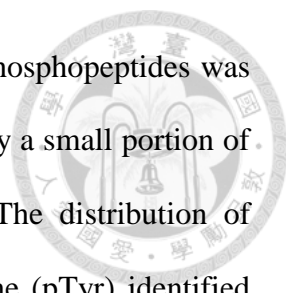
As described previously, the endogenous expression of MCM2 in H1299 (p53 null) is higher if compared to A549 (p53 wild-type). We wondered if p53 exerts regulatory effect on MCM2 in lung cancer. Increased susceptibility to cancer is closely related to loss or mutation of p53.³⁷ In lung cancer, TP53 gene abnormalities such as mutation or other alterations are frequently occur in both SCLC and NSCLC types.³⁸ However, the relationship between MCM2 and p53 has not been studied. In looking for a possible correlation between MCM2 and p53, we analyzed their protein expression level in lung cancer cells. To examine the effect of p53 overexpression in H1299 cells (p53 null), cells were transfected with either control plasmid or pcDNA3.1(-)/TP53 for 48 hrs. Figure 6A and 6B showed that overexpression of p53 in H1299 resulted in downregulation of MCM2 expression. To further support the causal correlation between p53 and MCM2, we knockdown p53 expression in A549 cells using plasmid shRNA-TP53 (knockdown efficiency= 44%). Figure 6C and 6D showed that MCM2 protein expression was increased in p53-silencing cells. These results support that p53 could be the upregulator of MCM2 in lung cancer cells. Here, we established a basic regulatory relationship between p53 and MCM2 but their detailed regulation mechanism remains unclear. Since the data indicated that p53 might control the upstream regulation of MCM2, the p53 status in A549 cells and H1299 cells would not affect the downstream study of MCM2.

3.3 Phosphoproteome of MCM2 overexpression in A549 cells and silencing MCM2 in H1299 cells

In order to reveal the regulatory networks of MCM2 in lung cancer cells, we performed quantitative MS analysis of phosphorylated proteins in A549 cells and H1299 cells.



Quantitative phosphoproteomics provide information about the phosphorylation target sites and the quantitative phosphorylation level changes in response to genetic or environmental perturbations. As described previously, endogenous expression of MCM2 in H1299 (p53 null) is higher than in A549 (p53 wild-type). Thus, we performed MCM2 overexpression in A549 cells and silencing MCM2 in H1299 cells in order to detect the phosphorylation events induced by MCM2. For MCM2 overexpression, A549 cells were transfected with either control vector or MCM2 expressing plasmid (pcDNA3.1+/MCM2) and were cultured for 24 hours. This time point was selected because the overexpression level of MCM2 was highest at 24 hours post-transfection as shown in Figure 7A. For silencing MCM2, H1299 cells were transfected with either non-target siRNA or siRNA for MCM2 and were cultured for 48 hours. Two siRNAs for MCM2 (si-1 and si-2) which showed high knockdown efficiency at 48 hours post-transfection (as shown in Figure 7B and 7C) were used in this phosphoproteomics experiment. In total, we performed phosphoproteomics experiments of MCM overexpression, silencing MCM2-si-1 and silencing MCM2-si-2 with two biological replicates and two LC-MS/MS measurements in each biological replicate. MaxQuant is a software platform that has been widely used for the analysis of shotgun proteomics data.^{39,40} As shown in Table 2, using MaxQuant software, we identified over 1409 phosphopeptides that mapped to 1494 phosphorylation sites on 594 phosphoproteins in MCM2-overexpressed A549 cells. In MCM2-silenced H1299 cells, we identified over 1347 phosphopeptides that mapped to 1599 phosphorylation sites on 588 phosphoproteins. In the phosphoproteome of MCM2 overexpression, a majority of phosphopeptides was either single (48.3%) or doubly (45.1%) phosphorylated, followed by a small portion of triply (6.2%) and quadruply (0.4%) phosphorylated (Figure 8)



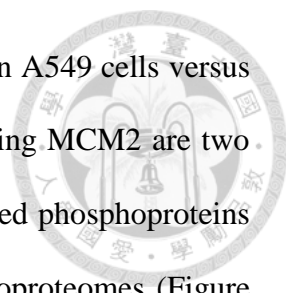
while in the phosphoproteome of silencing MCM2, a majority of phosphopeptides was either single (41.6%) or doubly (48.2%) phosphorylated, followed by a small portion of triply (9.5%) and quadruply (0.7%) phosphorylated (Figure 8). The distribution of phosphoserine (pSer), phosphothreonine (pThr) and phosphotyrosine (pTyr) identified in phosphoproteome of MCM2 overexpression was 85%, 14% and 1% respectively (Figure 9A) while in phosphoproteome of silencing MCM2 was 84%, 15% and 1% respectively (Figure 9B). The percentages of serine, threonine and tyrosine phosphorylation sites identified in both phosphoproteome of MCM2 overexpression and silencing MCM2 are close to that observed in the most common forms of protein phosphorylation, including O-phosphorylations on serine (~90%), threonine (~10%) and tyrosine (~<1%).⁴¹

3.4 Identification of differentially regulated phosphoproteins in response to MCM2

Phosphorylation level of each phosphopeptide is represented as peptide ratios (Ratio H/L normalized) provided by the MaxQuant output, which have been normalized for each LC-MS/MS run. Phosphoproteins that change phosphorylation level significantly are selected by ratio H/L normalized ≤ 0.67 (1.5-fold reduced) or ≥ 1.5 (1.5-fold increased). Localization of PTM probabilities are required to be at least of 0.75. In A549 cells, a total of 105 phosphoproteins were significantly changed in response to MCM2 overexpression. In H1299 cells, a total of 54 phosphoproteins were significantly changed in response to MCM2 silencing (Table 4).

3.5 Overlap between phosphoproteome of MCM2 overexpression and silencing MCM2

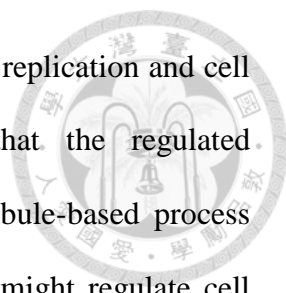
Our goal is to sort out the key phosphoproteins that are likely regulated by MCM2 regardless of types of cell line. We examined the overlap in phosphosites and



phosphoproteins from phosphoproteome of MCM2 overexpression in A549 cells versus silencing MCM2 in H1299 cells. MCM2 overexpression and silencing MCM2 are two contrast perturbations, thus we only considered the common regulated phosphoproteins with opposing phosphorylation change pattern in these two phosphoproteomes (Figure 10). The common differentially regulated phosphoproteins identified in both MCM2 overexpression and silencing MCM2 are HIV Tat-specific factor (Ser713), High mobility group protein HMG-I/HMG-Y(Ser99), Calnexin (Ser564), Protein DEK (Ser301, Ser302, Ser303, Ser304), DNA replication licensing factor MCM2 (Ser139, Ser27), Hsc70-interacting protein (Ser79); Putative protein FAM10A4 (Ser75), 28 kDa heat- and acid-stable phosphoprotein (Ser60, Ser63) and Membrane-associated progesterone receptor component 2 (Tyr211). Of these overlapping regulated phosphoproteins, there are only 8 phosphoproteins showed the opposing phosphorylation change pattern in phosphoproteome of MCM2 overexpression and silencing MCM2, which are HTSF1, F10A1/ST134, CALX, DEK, HMGA1, HAP28 and MCM2. PGRC2 showed decreased phosphorylation change in both phosphoproteomes (Table 3).

3.6 Functional annotation of MCM2-regulated phosphoproteins

To further elucidate the biological processes affected by MCM2, we used The Functional Annotation Tool on DAVID v6.7 to facilitate the annotation of up- and down-regulated phosphoproteins in each phosphoproteome. Functional annotation analysis showed that MCM2-overexpressed proteins were involved mainly in RNA splicing, protein folding, regulation of protein complex assembly, regulation of cytoskeleton organization, regulation of actin filament polymerization (Figure 11). MCM2-silenced proteins were mainly involved in macromolecular complex subunit



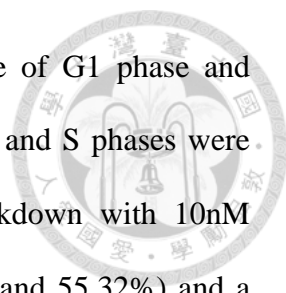
organization, RNA processing, microtubule-based movement, DNA replication and cell cycle (Figure 12). Functional enrichment analysis showed that the regulated phosphoproteins were enriched in mRNA processing and microtubule-based process (Figure 13). From these analysis results, we inferred that MCM2 might regulate cell cycle and affect cell migration.

3.7 Overexpression of MCM2 in A549 increased cell migration while silencing MCM2 in H1299 cells decreased cell migration

Cell migration ability is closely associated with cancer metastasis. The biological functions enriched in both MCM2 overexpression and silencing MCM2 were regulation of cytoskeleton organization, regulation of actin filament polymerization and microtubule-based movement. To explore the role of MCM2 in cell migration, we performed transwell migration assay to assess the migration ability of MCM2-overexpressed cells and MCM2-silenced cells. MCM2-overexpressed cells show significant ($p<0.05$) increase in migrated cells as shown in Figure 14 while MCM2-silenced cells show significant decrease ($p<0.05$) in migrated cells as shown in Figure 15. These results suggested that MCM2 play an important role in cell migration in human lung cancer.

3.8 Silencing MCM2 in H1299 cells induced cell cycle arrest

Based on the results of functional annotation analysis, the differentially regulated phosphoproteins of MCM2 silenced H1299 cells were involved in cell cycle. To investigate whether the effect of cell growth inhibition induced by silencing MCM2 was caused by cell cycle regulations, we used propidium iodide staining and flow cytometry to evaluate whether MCM2 knockdown can interrupt the cell cycle progression in H1299 cells. The G1/S cell cycle arrest means the cell cycle arrests in G1 phase and



does not proceed to S phase, resulting increase in the percentage of G1 phase and decrease in percentage of S phase. As shown in Figure 16, the G1 and S phases were 46.46% and 49.47% in control cells, respectively. MCM2 knockdown with 10nM siRNA (si-2 and si-3) resulted in a increase in G1 phase (54.46% and 55.32%) and a decrease in S phase (38.13% and 36.55%) at 48 hours siRNA post-transfection, indicating a G1/S arrest and a DNA synthetic inhibition existed in H1299 cells. The accumulation of cells in G2/M phase was also observed in MCM2-silenced cells (5.41% and 6.9%) as compared to control cells (3.13%).

3.9 Phosphorylation of HMGA1 at Ser99 is essential for viability

Previous studies showed that the high mobility group protein HMG-I/HMG-Y (HMGA1) is subjected to a number of post-translational modifications. By using mass spectrometry, we observed a common phosphorylation change at Ser99 on HMGA1 in both phosphoproteome of MCM2 overexpression and silencing. The MS/MS spectrum of the phosphopeptide KLEKEEEEGISQESSEEEQ from HMGA1 was showed in Figure 17. The biological significances of this phosphorylation site in lung cancer cells have not been investigated. We performed experiment to see if this phosphorylation site on HMGA1 is important for cell viability. Using the method of site-directed mutagenesis, we constructed two mutants of HMGA1 by substituting serine to non-phosphorylatable alanine (S99A) and phosphomimetic glutamic acid (S99E). The amino acid sequences showing the position to be mutated by substitution was illustrated in Figure 18A. The overexpression level of HMGA1 mutants was assessed by measuring the total HMGA1 protein. Western blot analysis (Figure 18B) showed the HMGA1 wild type and HMGA1 mutants (S99E and S99A) have similar total HMGA1 protein level, indicating that their overexpression efficiency are of the same magnitude. As illustrated

in Figure 18C, result revealed that mutation of Ser99 to alanine significantly reduced ($P<0.05$) the cell viability of A549 cells indicating the importance of this residue.

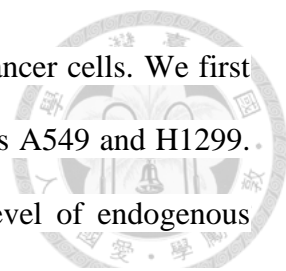


Chapter 4 DISCUSSION



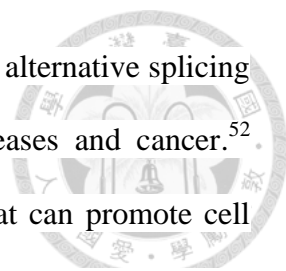
Cancer is tightly associated with abnormal uncontrolled proliferation. A new perspective of cancer progression proposes that DNA replication stress is induced by sustained proliferation, subsequently causing two other cancer hallmarks, escape from apoptosis and genomic instability.⁴² Small molecule inhibitors that block uncontrolled cancer proliferation by targeting leading or lagging strand synthesis have been used in cancer therapy, such as topoisomerases, DNA polymerases, DNA ligase, proliferating cell nuclear antigen (PCNA), ribonucleotide reductase, and telomerase.⁴³⁻⁴⁷ Eukaryotic replication factors are emerged as potential chemotherapeutic targets in cancer treatment but to date, little is known about the inhibitors targeting MCM proteins, which serve as a licensing factor in replication initiation. MCM2 is well-known for its good association with cell proliferation but its precise functional role in lung cancer cells has not been reported. Understanding the molecular basis of MCM2 in lung cancer cells enables us to discover alternative target for lung cancer therapy.

ZNF322 (Zinc finger protein 322) was isolated from an early human embryo heart cDNA library which encodes a zinc-finger protein containing 9 tandem repeated C2H2 type zinc fingers. Overexpression of ZNF322 increase transcription activities of SRE and AP-1, suggested the role of ZNF322 as transcriptional activator in MAPK signaling pathways.⁴⁸ From our previous studies, proteomics analysis of ZNF322A in human lung adenocarcinoma cells A549 using *Isobaric tags for relative and absolute quantitation* (iTRAQ) identified several candidate proteins that are regulated by ZNF322A.⁴⁹ MCM2 is one of the candidate proteins that are up-regulated by ZNF322A and their regulation relationship was validated by western blot analysis.



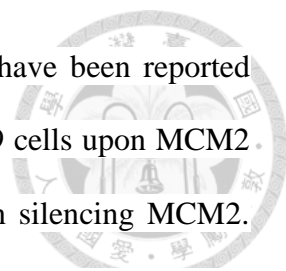
In the present study, we explored the role of MCM2 in lung cancer cells. We first evaluated the endogenous expression of MCM2 in NSCLC cell lines A549 and H1299. Western blotting demonstrated that H1299 cells showed higher level of endogenous MCM2 protein as compared to A549 cells. Cell viability analysis showed that MCM2 overexpression promotes cell proliferation in A549 cells and silencing MCM2 inhibits cell proliferation in H1299 cells. This is consistent with the essential role of MCM2 in cellular proliferation. Aberrant protein phosphorylation is often correlated with diseases.^{50,51} To better elucidate the post-translational events and to reveal the regulatory networks behind these effects, we set up a large-scale mass spectrometry-based quantitative phosphoproteomics study of MCM2 using HAMMOC-TiO₂ phosphopeptide enrichment strategies. We compared the differential regulation of phosphorylated proteins in the NSCLC cell lines A549 and H1299 cells in response to MCM2 overexpression and silencing MCM2 respectively. Phosphoproteomic analysis using two different cell lines would provide a more comprehensive profiling of MCM2 downstream events. Surprisingly, our results show that nearly all phosphosites are uniquely response to MCM2 overexpression or silencing MCM2, respectively. There is only a small overlap in differentially regulated phosphosites between the two phosphoproteomes, suggesting that MCM2 downstream regulations are cell-type dependent.

Bioinformatic analysis showed that the regulated phosphoproteins from both phosphoproteome are enriched most in biological functions such as RNA splicing, protein folding, regulation of protein complex assembly, regulation of cytoskeleton organization, regulation of actin filament polymerization, macromolecular complex subunit organization, microtubule-based movement, DNA replication and cell cycle.



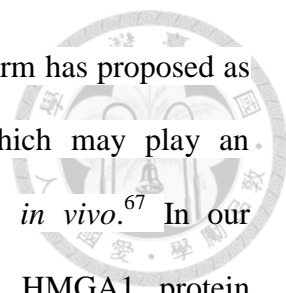
RNA has been linked to cancer-related functions in which defects in alternative splicing lead to various human diseases, primarily neurodegenerative diseases and cancer.⁵² Cancer cells with aberrant splicing profiles expressing isoforms that can promote cell proliferation, survival, migration and invasion, affect metabolism and in general involved in any aspect of tumor progression and maintenance.⁵³ It has been also reported that MCM2 involved in regulation of cell migration and invasion in medulloblastoma.⁵⁴ Not surprisingly, increased cell migration ability induced by MCM2 overexpression in A549 cells and reduced cell migration ability upon MCM2 knockdown in H1299 cells were observed in our study. Previous studies demonstrated that knockdown of MCM2 led to cell cycle arrest and cell apoptosis in colon cancer cells (HCT116) and NSCLCs (A549 and GLC-82).^{20,21} Our data from flow cytometric analysis indicated that silencing MCM2 in p53 null cell line H1299 induces cell cycle arrest in G1/S phase may result from a p53-independent pathway.

Phosphorylation of MCM2 occurs at multiple sites which resulted in a conformational change of the complex and activation of the helicase activity is essential for the initiation of DNA replication in human. Previous studies reported that three sites Ser40, Ser53 and Ser108 on MCM2 have been identified as Cdc7/Dbf4 phosphorylation sites in HeLa cells.⁵⁵ The Ser108 site was found to be the site of phosphorylation by ATR in the presence of DNA damage.⁵⁶ Furthermore, the Ser27, Ser41 and Ser139 sites have been identified as major Cdc7 phosphorylation sites in vitro and in HeLa cells confirming Ser139 as a Cdc7 phosphorylation site.⁵⁷ Perturbations of MCM2 protein in cancer cells by overexpression or suppression would probably induce changes in phosphorylation level of MCM2, thereby alter the process of initiation of DNA replication. Our data identified four sites (Ser26, Ser27, Ser108 and Ser 139) on MCM2



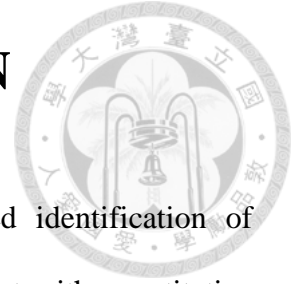
itself to be differentially phospho-regulated and all of these sites have been reported previously. Of these phosphosites, Ser108 is identified only in A549 cells upon MCM2 overexpression while Ser26 is identified only in H1299 cells upon silencing MCM2. The discrepancies of MCM2 phosphorylation sites between the two phosphoproteomes may due to the differences of cell lines used and the differences of perturbation to cell lines.

High mobility group (HMG) proteins are the most abundant non-histone chromatin associated proteins. The HMG proteins are categorized into three families based on their DNA binding domains: HMGA (containing AT-hooks), HMGB (containing HMG-boxes) and HMGN (containing nucleosomal binding domains).^{58,59} High mobility group A (HMGA) proteins bind the minor groove of AT-rich DNA sequences through three N-terminal basic domains called “AT-hooks”. The HMGA family consists of four members: HMGA1a, HMGA1b and HMGA1c (which are encoded through alternative splicing by the *HMGA1* gene) and HMGA2 (encoded by the *HMGA2* gene).^{60,61} Recent study reported that elevated expression of HMGA1 correlates with the malignant status and prognosis of non-small cell lung cancer.⁶² HMGA1 protein is highly regulated by post-translational modifications, such as acetylation, methylation and phosphorylation. Nearly all of HMGA1a and HMGA1b proteins are constitutively phosphorylated at the two or three serine occurred predominantly at the residues of the C-terminal peptide 88-106, a region known to be critical for HMGA1-DNA contact.^{63,64} HMGA1 phosphorylation reduced DNA-binding activity of HMGA1 whereas protein dephosphorylation increases HMGA1-DNA binding affinity, resulted in gene repression or activation.^{65,66} Constitutive and inducible phosphorylation at serine residues Ser98, Ser101 and Ser102 has been reported to be dependent on PI-3K via a casein kinase 2



(CK2)-like specificity.^{64,66} HMGA1, specifically the HMGA1a isoform has proposed as a novel downstream target of the INSR signaling pathway, which may play an important role in the regulation of insulin signaling and action *in vivo*.⁶⁷ In our phosphoproteome of MCM2 overexpression, tri-phosphorylated HMGA1 protein (Ser99, Ser102 and Ser103) was detected in A549 cells after 24 hours MCM2 overexpression but only the phosphosite of Ser99 show the significant increase in phosphorylation level. In phosphoproteome of silencing MCM2, a significant decrease of the tri-phosphorylated HMGA1 protein (Ser99, Ser102 and Ser103) was detectable in H1299 cells at 48 hours siMCM2 post-transfection. Interestingly, phosphorylated HMGN1 protein (Non-histone chromosomal protein HMG-14) at phosphosites of Ser86 and Ser89 was detected upon MCM2 overexpression but not in silencing MCM2. The phosphosite of Ser99 on HMGA1 was found to be differentially up-regulated upon MCM2 overexpression and differentially down-regulated upon silencing MCM2, thus is presented as a novel candidate for phosphoproteomics analysis. To further investigate the biological significances of HMGA1 phosphorylation at Ser99, we examined the cell viability of HMGA1 phosphorylation site mutants expressed in A549 cells. Our study showed that mutation of Ser99 to alanine significantly decreased cell viability of A549 cells, suggesting that phosphorylation of Ser99 of HMGA1 may play important roles in cancer proliferation. The function of this phosphorylation site is yet clearly understood. Future studies are needed to clarify the importance of HMGA1 phosphorylation in lung cancer study which might result in a profound impact on lung cancer treatment.

Chapter 5 CONCLUSION



Mass spectrometry-based quantitative phosphoproteomics allowed identification of hundreds or thousands of phosphorylation sites in single experiment with quantitative information of phosphorylation sites. We investigated the phosphorylation events regulated by MCM2 in response to MCM2 overexpression and silencing MCM2 in human lung cancer cells. We evaluated the phosphoproteome data, inferred the gene ontology biological processes, identified key phosphoproteins for downstream analysis and performed functional analysis. We identified 1484 phosphorylation sites in 593 phosphoproteins of MCM2-overexpressed A549 cells and 1599 phosphorylation sites in 592 phosphoproteins of MCM2-silenced H1299 cells. Bioinformatics analysis demonstrated that the differentially regulated phosphoproteins were enriched in RNA splicing, cell cycle and cytoskeleton regulation. Functional analysis showed that MCM2 regulated several biological processes such as cell proliferation, cell migration and cell cycle. Furthermore, we found that phosphorylation site of Ser99 on HMGA1 is important for cell viability in lung cancer cells. This study helps to elucidate the role of MCM2 in regulation of biological processes in lung cancer cells which may contribute to cancer therapy development.

Chapter 6 FUTURE WORK



First, we attempt to validate the phosphorylation status of HMGA1 induced by MCM2 in lung cancer cells. Since the phospho-specific antibody for HMGA1 are not available in market so far, we could not detect the phosphorylation of HMGA1 by western blot. Both the MCM2-overexpressed A549 cells and MCM2-silenced H1299 cells showed the differential phosphorylation level of the phosphosites of Ser99 on HMGA1, indicating the important link between MCM2 and HMGA1 phosphorylation. Phosphorylation of HMGA1 and its relevance to MCM2 needs substantial evidences and should be investigated in detail.

Second, it is still unclear that which specific pathway is induced by MCM2 to affect the biological processes such as cell proliferation, cell migration and cell cycle in human lung cancer cells. Future studies are needed to elucidate the molecular pathway regulating these biological processes in order to clarify the role of MCM2 in lung cancer cells.

Third, the western blot analysis showed that p53 is correlated with MCM2 but we did not know how exactly the p53 regulates MCM2. More experimental validations are needed to prove the relationship between p53 and MCM2 at transcriptional level.

ABBREVIATION



$^{13}\text{CD}_2\text{O}$ 20% formaldehyde- ^{13}C , d_2 solution

ACN acetonitrile

CH_2O 37% formaldehyde solution

DMSO dimethyl sulfoxide

DTT dithiothreitol

FDR false discovery rate

FDR false discovery rate

GO gene ontology

GO gene ontology

HAMMOC hydroxy acid-modified metal oxide chromatography

IAM iodoacetamide

iTRAQ isobaric tags for relative and absolute quantitation

LC-MS/MS liquid chromatography-tandem mass spectrometry

LTQ linear Trap Quadrupole

LysC Lysyl endopeptidase

MTS 3-(4,5-dimethylthiazol-2-yl)-5-(3-carboxymethoxyphenyl)-2-(4-sulfophenyl)-2H-tetrazolium, inner salt

MTT 3-(4,5-dimethylthiazol-2-yl)-2,5-diphenyltetrazolium bromide

NaBH_3CN sodium cyanoborohydride

PBS phosphate-buffered saline

PI propidium iodide

PMS phenazine methosulfate

PTS phase-transfer surfactants

PVDF polyvinylidene difluoride

SCX strong cation exchange chromatography

SDB-XC polyStyrenedivinyl- benzene

SDC sodium deoxycholate

SDS-PAGE sodium dodecyl sulfatepolyacrylamide gel electrophoresis

Ser serine

shRNA short hairpin RNA

siRNA small interfering RNA

SLS sodium lauroyl sarcosine

StageTip Stop-and-go-extraction tip

TEABC triethylammonium bicarbonate

TFA trifluoroacetic Acid

Thr threonine

TiO₂ titanium dioxide

Tyr tyrosine



REFERENCES



- (1) Siegel, R.; Ma, J.; Zou, Z.; Jemal, A., Cancer statistics, 2014. *CA Cancer J. Clin.* **2014**, 64 (1), 9-29.
- (2) Wang, B. Y.; Huang, J. Y.; Cheng, C. Y.; Lin, C. H.; Ko, J. L.; Liaw, Y. P., Lung Cancer and Prognosis in Taiwan: A Population-Based Cancer Registry. *J. Thorac. Oncol.* **2013**, 8 (9), 1128-1135.
- (3) Minna, J. D.; Roth, J. A.; Gazdar, A. F., Focus on lung cancer. *Cancer Cell* **2002**, 1 (1), 49-52.
- (4) Evrin, C.; Clarke, P.; Zech, J.; Lurz, R.; Sun, J.; Uhle, S.; Li, H.; Stillman, B.; Speck, C., A double-hexameric MCM2-7 complex is loaded onto origin DNA during licensing of eukaryotic DNA replication. *Proc. Natl. Acad. Sci. U S A* **2009**, 106 (48), 20240-20245.
- (5) Remus, D.; Beuron, F.; Tolun, G.; Griffith, J. D.; Morris, E. P.; Diffley, J. F., Concerted loading of Mcm2-7 double hexamers around DNA during DNA replication origin licensing. *Cell* **2009**, 139 (4), 719-730.
- (6) Gambus, A.; Jones, R. C.; Sanchez-Diaz, A.; Kanemaki, M.; van Deursen, F.; Edmondson, R. D.; Labib, K., GINS maintains association of Cdc45 with MCM in replisome progression complexes at eukaryotic DNA replication forks. *Nat. Cell Biol.* **2006**, 8 (4), 358-366.
- (7) Ilves, I.; Petojevic, T.; Pesavento, J. J.; Botchan, M. R., Activation of the MCM2-7 helicase by association with Cdc45 and GINS proteins. *Mol. Cell* **2010**, 37 (2), 247-258.

(8) Moyer, S. E.; Lewis, P. W.; Botchan, M. R., Isolation of the Cdc45/Mcm2-7/GINS (CMG) complex, a candidate for the eukaryotic DNA replication fork helicase. *Proc. Natl. Acad. Sci. U S A* **2006**, 103 (27), 10236-10241.

(9) Lei, M.; Tye, B. K., Initiating DNA synthesis: from recruiting to activating the MCM complex. *J. Cell Sci.* **2001**, 114 (8), 1447-1454.

(10) Kearsey, S. E.; Maiorano, D.; Holmes, E. C.; Todorov, I. T., The role of MCM proteins in the cell cycle control of genome duplication. *Bioessays* **1996**, 18 (3), 183-190.

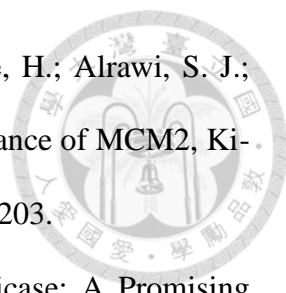
(11) Burger, M., MCM2 and MCM5 as Prognostic Markers in Colon Cancer: A Worthwhile Approach. *Dig. Dis. Sci.* **2009**, 54 (2), 197-198.

(12) Liu, M.; Li, J. S.; Tian, D. P.; Huang, B.; Rosqvist, S.; Su, M., MCM2 expression levels predict diagnosis and prognosis in gastric cardiac cancer. *Histol. Histopathol.* **2013**, 28 (4), 481-492.

(13) Wojnar, A.; Kobierzycki, C.; Krolicka, A.; Pula, B.; Podhorska-Okolow, M.; Dziegiel, P., Correlation of Ki-67 and MCM-2 proliferative marker expression with grade of histological malignancy (G) in ductal breast cancers. *Folia Histochem. Cytobiol.* **2010**, 48 (3), 442-446.

(14) Meng, M. V.; Grossfeld, G. D.; Williams, G. H.; Dilworth, S.; Stoeber, K.; Mulley, T. W.; Weinberg, V.; Carroll, P. R.; Tlsty, T. D., Minichromosome maintenance protein 2 expression in prostate: Characterization and association with outcome after therapy for cancer. *Clin. Cancer Res.* **2001**, 7 (9), 2712-2718.

(15) Tan, D. F.; Huberman, J. A.; Hyland, A.; Loewen, G. M.; Brooks, J. S.; Beck, A. F.; Todorov, I. T.; Bepler, G., MCM2--a promising marker for premalignant lesions of the lung: a cohort study. *BMC Cancer* **2001**, 1, 6.

- 
- (16) Yang, J.; Ramnath, N.; Moysich, K. B.; Asch, H. L.; Swede, H.; Alrawi, S. J.; Huberman, J.; Geradts, J.; Brooks, J. S.; Tan, D., Prognostic significance of MCM2, Ki-67 and gelsolin in non-small cell lung cancer. *BMC Cancer* **2006**, 6, 203.
- (17) Simon, N. E.; Schwacha, A., The Mcm2-7 Replicative Helicase: A Promising Chemotherapeutic Target. *BioMed Res. Int.* **2014**, 2014, 549719.
- (18) Kunnev, D.; Rusiniak, M. E.; Kudla, A.; Freeland, A.; Cady, G. K.; Pruitt, S. C., DNA damage response and tumorigenesis in Mcm2-deficient mice. *Oncogene* **2010**, 29 (25), 3630-3638.
- (19) Pruitt, S. C.; Bailey, K. J.; Freeland, A., Reduced Mcm2 expression results in severe stem/progenitor cell deficiency and cancer. *Stem Cells* **2007**, 25 (12), 3121-3132.
- (20) Liu, Y.; He, G.; Wang, Y.; Guan, X.; Pang, X.; Zhang, B., MCM-2 is a therapeutic target of Trichostatin A in colon cancer cells. *Toxicol. Lett.* **2013**, 221 (1), 23-30.
- (21) Zhang, X.; Teng, Y.; Yang, F.; Wang, M.; Hong, X.; Ye, L. G.; Gao, Y. N.; Chen, G. Y., MCM2 is a therapeutic target of lovastatin in human non-small cell lung carcinomas. *Oncol. Rep.* **2015**, 33 (5), 2599-2605.
- (22) Hubbard, M. J.; Cohen, P., On target with a new mechanism for the regulation of protein phosphorylation. *Trends Biochem. Sci.* **1993**, 18 (5), 172-177.
- (23) Sano, A.; Nakamura, H., Chemo-affinity of titania for the column-switching HPLC analysis of phosphopeptides. *Anal. Sci.* **2004**, 20 (3), 565-566.
- (24) Haydon, C. E.; Eyers, P. A.; Aveline-Wolf, L. D.; Resing, K. A.; Maller, J. L.; Ahn, N. G., Identification of novel phosphorylation sites on *Xenopus laevis* Aurora A and analysis of phosphopeptide enrichment by immobilized metal-affinity chromatography. *Mol. Cell Proteomics* **2003**, 2 (10), 1055-1067.

(25) Ficarro, S. B.; McClelland, M. L.; Stukenberg, P. T.; Burke, D. J.; Ross, M. M.; Shabanowitz, J.; Hunt, D. F.; White, F. M., Phosphoproteome analysis by mass spectrometry and its application to *Saccharomyces cerevisiae*. *Nat. Biotechnol.* **2002**, 20 (3), 301-305.

(26) Ndassa, Y. M.; Orsi, C.; Marto, J. A.; Chen, S.; Ross, M. M., Improved immobilized metal affinity chromatography for large-scale phosphoproteomics applications. *J. Proteome Res.* **2006**, 5 (10), 2789-2799.

(27) Ballif, B. A.; Villen, J.; Beausoleil, S. A.; Schwartz, D.; Gygi, S. P., Phosphoproteomic analysis of the developing mouse brain. *Mol. Cell. Proteomics* **2004**, 3 (11), 1093-1101.

(28) Beausoleil, S. A.; Jedrychowski, M.; Schwartz, D.; Elias, J. E.; Villen, J.; Li, J.; Cohn, M. A.; Cantley, L. C.; Gygi, S. P., Large-scale characterization of HeLa cell nuclear phosphoproteins. *Proc. Natl. Acad. Sci. U S A* **2004**, 101 (33), 12130-12135.

(29) Kokubu, M.; Ishihama, Y.; Sato, T.; Nagasu, T.; Oda, Y., Specificity of immobilized metal affinity-based IMAC/C18 tip enrichment of phosphopeptides for protein phosphorylation analysis. *Anal. Chem.* **2005**, 77 (16), 5144-5154.

(30) Larsen, M. R.; Thingholm, T. E.; Jensen, O. N.; Roepstorff, P.; Jorgensen, T. J. D., Highly selective enrichment of phosphorylated peptides from peptide mixtures using titanium dioxide microcolumns. *Mol. Cell. Proteomics* **2005**, 4 (7), 873-886.

(31) Kweon, H. K.; Hakansson, K., Selective zirconium dioxide-based enrichment of phosphorylated peptides for mass spectrometric analysis. *Anal. Chem.* **2006**, 78 (6), 1743-1749.

(32) Wolschin, F.; Wienkoop, S.; Weckwerth, W., Enrichment of phosphorylated proteins and peptides from complex mixtures using metal oxide/hydroxide affinity chromatography (MOAC). *Proteomics* **2005**, 5 (17), 4389-4397.

(33) Sugiyama, N.; Masuda, T.; Shinoda, K.; Nakamura, A.; Tomita, M.; Ishihama, Y., Phosphopeptide enrichment by aliphatic hydroxy acid-modified metal oxide chromatography for nano-LC-MS/MS in proteomics applications. *Mol. Cell. Proteomics* **2007**, 6 (6), 1103-1109.

(34) Hsu, J. L.; Huang, S. Y.; Chow, N. H.; Chen, S. H., Stable-isotope dimethyl labeling for quantitative proteomics. *Anal. Chem.* **2003**, 75 (24), 6843-6852.

(35) Ku, W.-C.; Sugiyama, N.; Ishihama, Y., Large-Scale Protein Phosphorylation Analysis by Mass Spectrometry-Based Phosphoproteomics. In *T Protein Kinase Technologies*, 2012; Vol. 68, pp 35-46.

(36) Olsen, J. V.; de Godoy, L. M.; Li, G.; Macek, B.; Mortensen, P.; Pesch, R.; Makarov, A.; Lange, O.; Horning, S.; Mann, M., Parts per million mass accuracy on an Orbitrap mass spectrometer via lock mass injection into a C-trap. *Mol. Cell. Proteomics* **2005**, 4 (12), 2010-2021.

(37) Vogelstein, B.; Lane, D.; Levine, A. J., Surfing the p53 network. *Nature* **2000**, 408 (6810), 307-310.

(38) Bougeard, G.; Hadj-Rabia, S.; Faivre, L.; Sarafan-Vasseur, N.; Frebourg, T., The Rapp-Hodgkin syndrome results from mutations of the TP63 gene. *Eur. J. Hum. Genet.* **2003**, 11 (9), 700-704.

(39) Cox, J.; Mann, M., MaxQuant enables high peptide identification rates, individualized p.p.b.-range mass accuracies and proteome-wide protein quantification. *Nat. Biotechnol.* **2008**, 26 (12), 1367-1372.

(40) Cox, J.; Neuhauser, N.; Michalski, A.; Scheltema, R. A.; Olsen, J. V.; Mann, M., Andromeda: a peptide search engine integrated into the MaxQuant environment. *J. Proteome Res.* **2011**, 10 (4), 1794-1805.

(41) Seet, B. T.; Dikic, I.; Zhou, M. M.; Pawson, T., Reading protein modifications with interaction domains. *Nat. Rev. Mol. Cell Biol.* **2006**, 7 (7), 473-483.

(42) Macheret, M.; Halazonetis, T. D., DNA replication stress as a hallmark of cancer. *Annu. Rev. Pathol.* **2015**, 10, 425-448.

(43) Pogorelcnik, B.; Perdih, A.; Solmajer, T., Recent developments of DNA poisons--human DNA topoisomerase IIalpha inhibitors--as anticancer agents. *Curr. Pharm. Des.* **2013**, 19 (13), 2474-2488.

(44) Keating, M. J.; Kantarjian, H.; Talpaz, M.; Redman, J.; Koller, C.; Barlogie, B.; Velasquez, W.; Plunkett, W.; Freireich, E. J.; McCredie, K. B., Fludarabine: a new agent with major activity against chronic lymphocytic leukemia. *Blood* **1989**, 74 (1), 19-25.

(45) Singh, D. K.; Krishna, S.; Chandra, S.; Shameem, M.; Deshmukh, A. L.; Banerjee, D., Human DNA ligases: a comprehensive new look for cancer therapy. *Med. Res. Rev.* **2014**, 34 (3), 567-595.

(46) Tan, Z.; Wortman, M.; Dillehay, K. L.; Seibel, W. L.; Evelyn, C. R.; Smith, S. J.; Malkas, L. H.; Zheng, Y.; Lu, S.; Dong, Z., Small-molecule targeting of proliferating cell nuclear antigen chromatin association inhibits tumor cell growth. *Mol. Pharmacol.* **2012**, 81 (6), 811-819.

(47) Aye, Y.; Li, M.; Long, M. J.; Weiss, R. S., Ribonucleotide reductase and cancer: biological mechanisms and targeted therapies. *Oncogene* **2015**, 34 (16), 2011-2021.

(48) Li, Y. Q.; Wang, Y. Q.; Zhang, C. B.; Yuan, W. Z.; Wang, J.; Zhu, C. B.; Chen, L.; Huang, W.; Zeng, W. Q.; Wu, X. S.; Liu, M. Y., ZNF322, a novel human C2H2 Kriippel-like zinc-finger protein, regulates transcriptional activation in MAPK signaling pathways. *Biochem. Biophys. Res. Commun.* **2004**, 325 (4), 1383-1392.

(49) Jen, J. L., L. L.; Chen, H. T.; Liao, S. Y.; Lo, F. Y.; Tang, Y. A.; Hsu, H. S.; Salgia, R.; Hsu, C. L.; Huang, H. C.; Juan, H. F.; Wang, Y. C., Oncoprotein ZNF322A transcriptionally deregulates alpha-adducin, cyclin D1 and p53 to promote tumor growth and metastasis in lung cancer. *Oncogene* (in press)

(50) Harsha, H. C.; Pandey, A., Phosphoproteomics in cancer. *Mol. Oncol.* **2010**, 4 (6), 482-495.

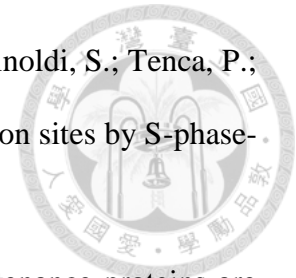
(51) Brognard, J.; Hunter, T., Protein kinase signaling networks in cancer. *Curr. Opin. Genet. Dev.* **2011**, 21 (1), 4-11.

(52) Cooper, T. A.; Wan, L. L.; Dreyfuss, G., RNA and Disease. *Cell* **2009**, 136 (4), 777-793.

(53) Venables, J. P.; Klinck, R.; Koh, C.; Gervais-Bird, J.; Bramard, A.; Inkel, L.; Durand, M.; Couture, S.; Froehlich, U.; Lapointe, E.; Lucier, J. F.; Thibault, P.; Rancourt, C.; Tremblay, K.; Prinos, P.; Chabot, B.; Elela, S. A., Cancer-associated regulation of alternative splicing. *Nat. Struct. Mol. Biol.* **2009**, 16 (6), 670-676.

(54) Lau, K. M.; Chan, Q. K. Y.; Pang, J. C. S.; Li, K. K. W.; Yeung, W. W.; Chung, N. Y. F.; Lui, P. C.; Tam, Y. S.; Li, H. M.; Zhou, L.; Wang, Y.; Mao, Y.; Ng, H. K., Minichromosome maintenance proteins 2, 3 and 7 in medulloblastoma: overexpression and involvement in regulation of cell migration and invasion. *Oncogene* **2010**, 29 (40), 5475-5489.

(55) Montagnoli, A.; Valsasina, B.; Brotherton, D.; Troiani, S.; Rainoldi, S.; Tenca, P.; Molinari, A.; Santocanale, C., Identification of Mcm2 phosphorylation sites by S-phase-regulating kinases. *J. Biol. Chem.* **2006**, 281 (15), 10281-10290.



(56) Cortez, D.; Glick, G.; Elledge, S. J., Minichromosome maintenance proteins are direct targets of the ATM and ATR checkpoint kinases. *Proc. Natl. Acad. Sci. U S A* **2004**, 101 (27), 10078-10083.

(57) Tsuji, T.; Ficarro, S. B.; Jiang, W., Essential role of phosphorylation of MCM2 by Cdc7/Dbf4 in the initiation of DNA replication in mammalian cells. *Mol. Biol. Cell* **2006**, 17 (10), 4459-4472.

(58) Bustin, M., Revised nomenclature for high mobility group (HMG) chromosomal proteins. *Trends Biochem. Sci.* **2001**, 26 (3), 152-153.

(59) Catez, F.; Hock, R., Binding and interplay of HMG proteins on chromatin: Lessons from live cell imaging. *Biochim. Biophys. Acta, Gene Regul. Mech.* **2010**, 1799 (1-2), 15-27.

(60) Fusco, A.; Fedele, M., Roles of HMGA proteins in cancer. *Nat. Rev. Cancer* **2007**, 7 (12), 899-910.

(61) Fedele, M.; Fusco, A., HMGA and cancer. *Biochim. Biophys. Acta* **2010**, 1799 (1-2), 48-54.

(62) Zhang, Z.; Wang, Q.; Chen, F.; Liu, J., Elevated expression of HMGA1 correlates with the malignant status and prognosis of non-small cell lung cancer. *Tumour Biol.* **2015**, 36 (2), 1213-1219.

(63) Piekietko, A.; Drung, A.; Rogalla, P.; Schwanbeck, R.; Heyduk, T.; Gerharz, M.; Bullerdiek, J.; Wisniewski, J. R., Distinct organization of DNA complexes of various

HMGI/Y family proteins and their modulation upon mitotic phosphorylation. *J. Biol. Chem.* **2001**, 276 (3), 1984-1992.

(64) Wang, D. Z.; Ray, P.; Boothby, M., Interleukin 4-Inducible Phosphorylation of Hmg-I(Y) Is Inhibited by Rapamycin. *J. Biol. Chem.* **1995**, 270 (39), 22924-22932.

(65) Edberg, D. D.; Bruce, J. E.; Siems, W. F.; Reeves, R., In vivo posttranslational modifications of the high mobility group A1a proteins in breast cancer cells of differing metastatic potential. *Biochemistry* **2004**, 43 (36), 11500-11515.

(66) Sgarra, R.; Rustighi, A.; Tessari, M. A.; Di Bernardo, J.; Altamura, S.; Fusco, A.; Manfioletti, G.; Giancotti, V., Nuclear phosphoproteins HMGA and their relationship with chromatin structure and cancer. *FEBS Lett.* **2004**, 574 (1-3), 1-8.

(67) Chiefari, E.; Nevolo, M. T.; Arcidiacono, B.; Maurizio, E.; Nocera, A.; Iiritano, S.; Sgarra, R.; Possidente, K.; Palmieri, C.; Paonessa, F.; Brunetti, G.; Manfioletti, G.; Foti, D.; Brunetti, A., HMGA1 is a novel downstream nuclear target of the insulin receptor signaling pathway. *Sci. Rep.* **2012**, 2.

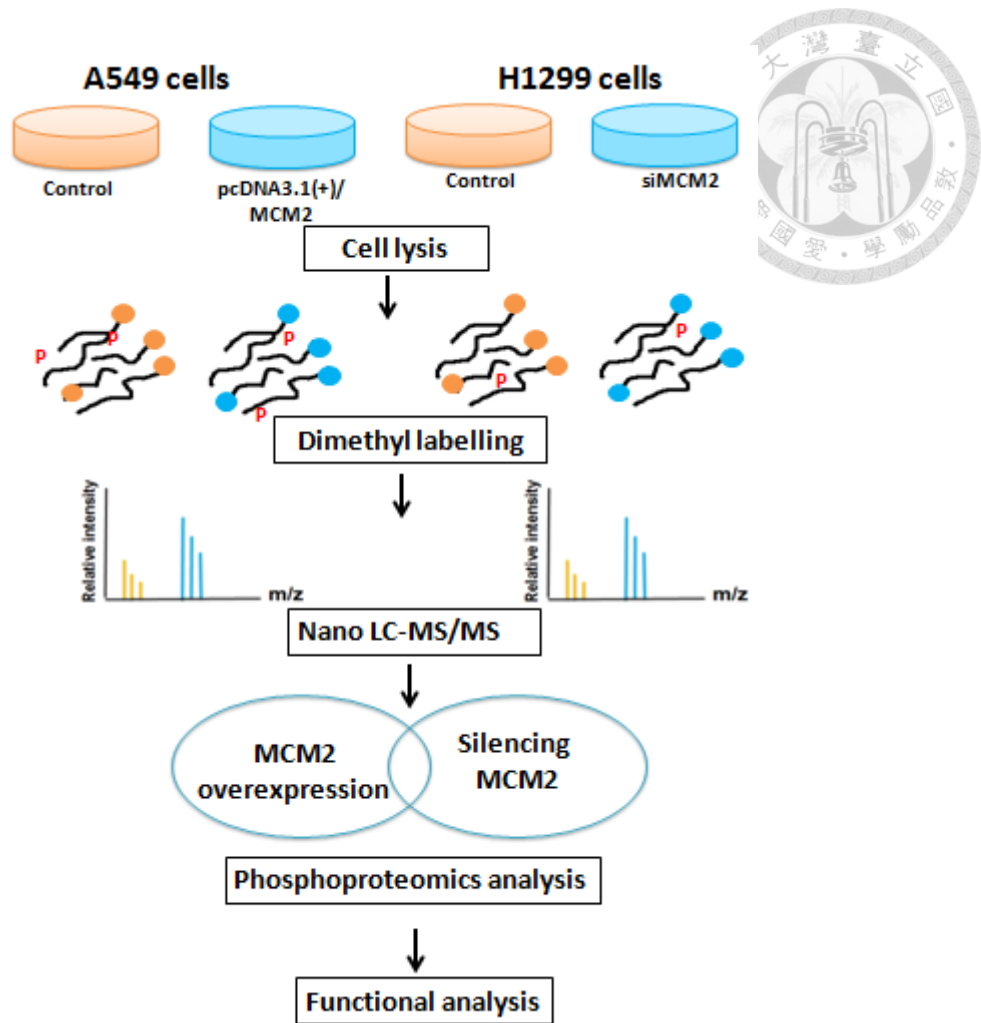


Figure 1. Schematic illustration of the experimental design of this study. For MCM2 overexpression in A549 cells, the cells were transfected with 1 ug of MCM2-overexpressing plasmid and harvested after 24 hours. For silencing MCM2 in H1299 cells, the cells were transfected with siRNA at final concentration of 10 nmol and harvested after 48 hours. The extracted protein was subjected to the phosphoproteomics workflow and nanoLC–MS/MS analysis. The differential regulation of phosphorylated proteins in these two phosphoproteomes was compared and the results were validated.

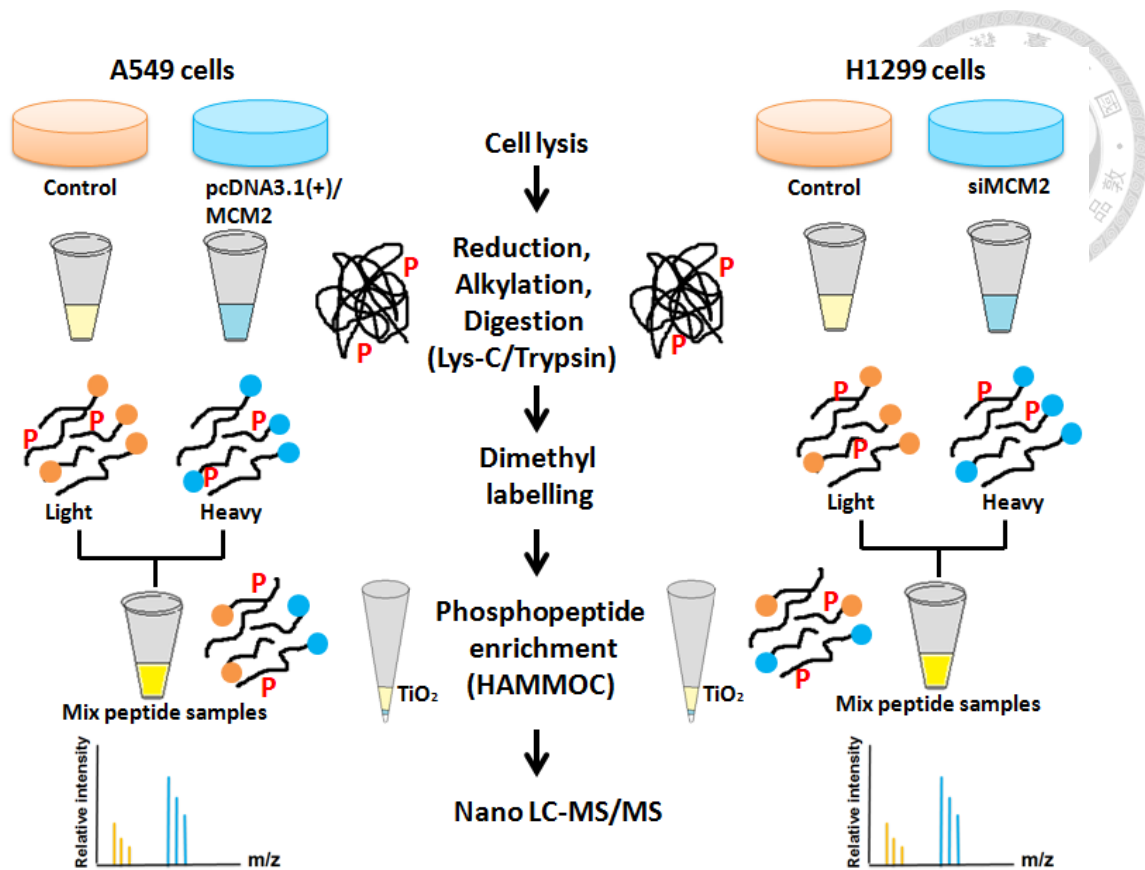


Figure 2. Schematic workflow of phosphoproteomics. Protein was extracted from cell lysates. The protein was then subjected to reduction, alkylation and protein digestion for overnight. The digested peptides from the control and treatment samples were subjected to dimethyl labelling, CH₂O (light) for control samples and ¹³CD₂O (heavy) for treated samples. The light-labeled and heavy-labeled samples were mixed and proceed to HAMMOC-TiO₂ phosphopeptide enrichment and finally nanoLC-MS/MS.

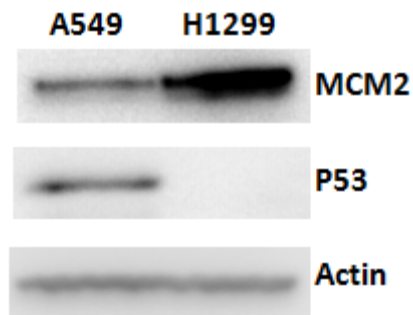


Figure 3. Endogenous expression of MCM2 in lung cancer cells. Protein samples (30 ug) were electrophoresed on a 10% SDS polyacrylamide gel. The membrane was incubated with the following primary antibody diluted in blocking buffer at 4°C overnight: rabbit anti-MCM2 (1:1000), mouse anti-P53 (1:1000) and mouse anti-Actin (1:5000) followed by incubation with appropriate horseradish peroxidase-labeled secondary antibody (1:100000) for 2 hours at room temperature. Signal was developed with Clarity Western ECL Substrate Kit. The result showed that H1299 (p53 null) show higher endogenous expression of MCM2 compared to A549 (p53 wild-type).

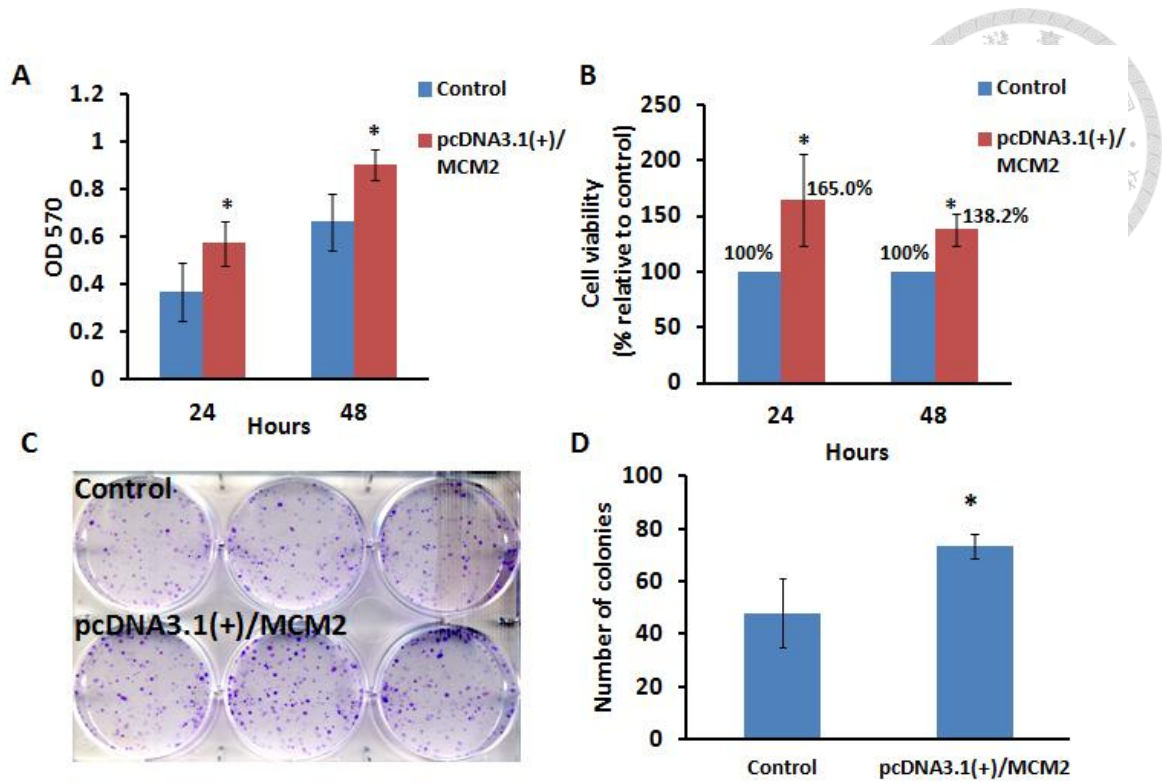


Figure 4. Overexpression of MCM2 in A549 increased cell growth in lung cancer cells. (A) and (B) The cell viability of MCM2-overexpressing cells. After 24 hours of post-transfection, 5000 cells were seeded onto the 96-well plate and incubated for 24 or 48 hours (C) and (D) The colony formation assay of MCM2-overexpressing cells. After 24 hours of post-transfection, 500 cells were seeded onto the 6-well plates and incubated for 8 days. The number of colonies in MCM2-overexpressing and control cells was counted manually. MCM2 overexpressed A549 cells exhibited a significant increase in cell proliferation (increased 65.0% and 38.2% of cell viability at 24 and 48 hours) and higher number of colonies formed as compared to control vector. (*, $P < 0.05$)

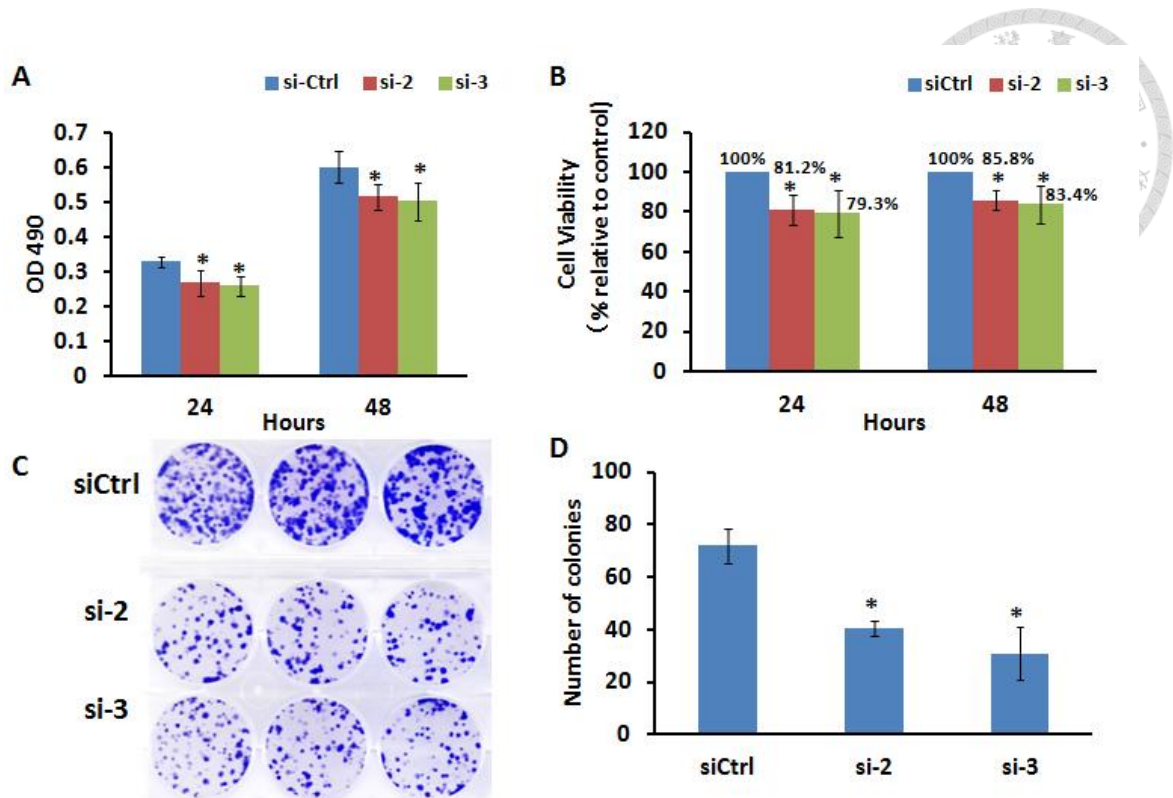


Figure 5. Silencing MCM2 in H1299 cells decreased cell proliferation. (A) and (B) The cell viability of MCM2-silenced cells. After 24 hours of post-transfection, 5000 cells were seeded onto the 96-well plate and incubated for 24 or 48 hours. The cell viability was determined using the MTS assay. (C) and (D) The colony formation assay of MCM2-silenced cells. After 24 hours of post-transfection, 500 cells were seeded onto the 6-well plates and incubated for 8 days. The number of colonies in MCM2-silenced and control cells was counted manually. MCM2 silenced H1299 cells (both si-2 and si-3) showed a significant decrease in cell proliferation and lower number of colonies formed as compared to control siRNA. Result showed that si-2 reduced 18.8% and 14.2% of cell viability while si-3 reduced 20.7% and 16.6% of cell viability at 24 and 48 hours. (*, $P < 0.05$)

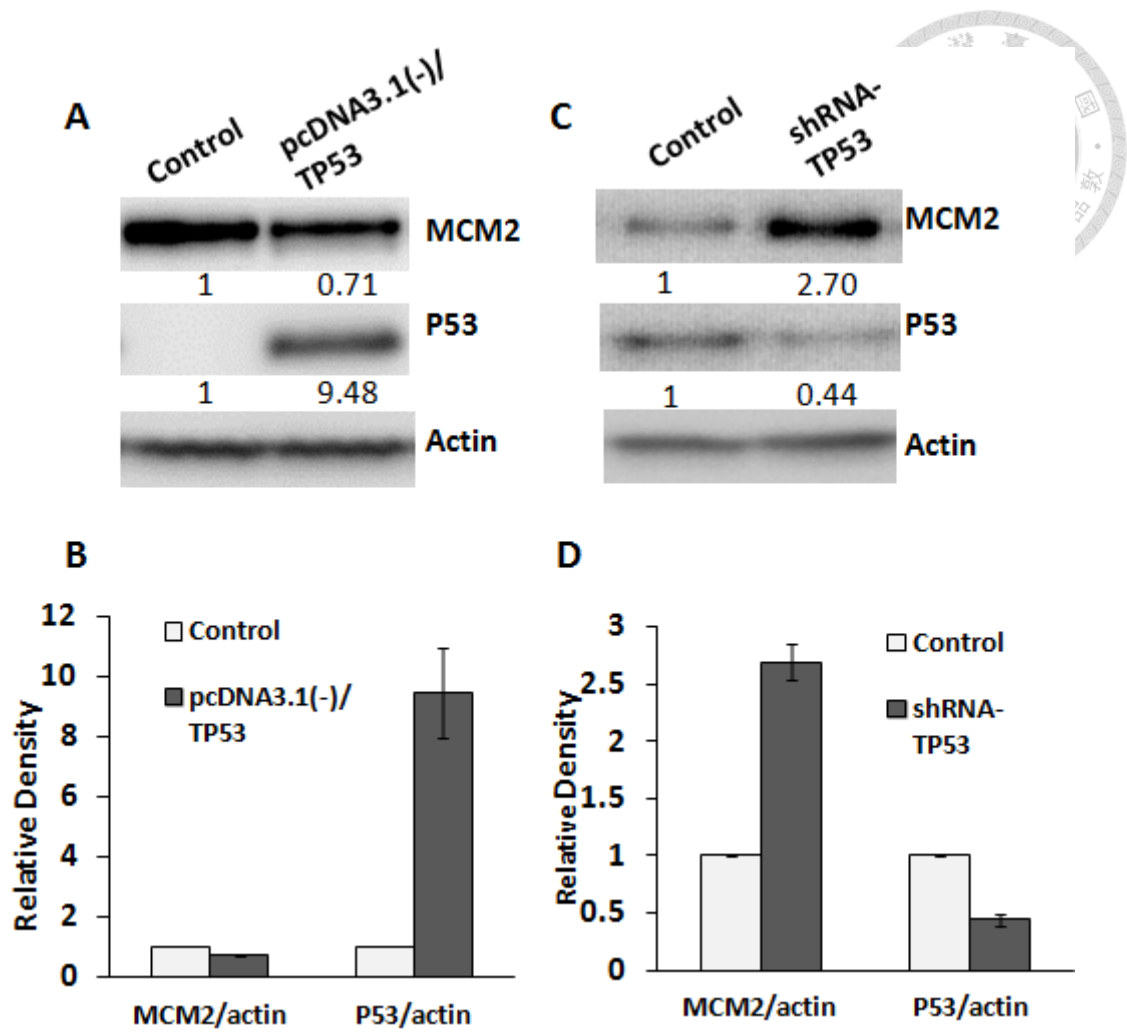


Figure 6. The relationship between P53 and MCM2. (A) and (B) P53 overexpression in H1299 cells. Cells were transfected with either control plasmid or pcDNA3.1(-)/TP53 for 24 hrs. Overexpression of P53 in H1299 resulted in downregulation of MCM2 expression. (C) and (D) P53 knockdown in A549 cells. Plasmid shRNA-TP53 was used to knockdown p53 expression in A549 cells (knockdown efficiency=44%). MCM2 protein expression was increased in p53-silencing cells.

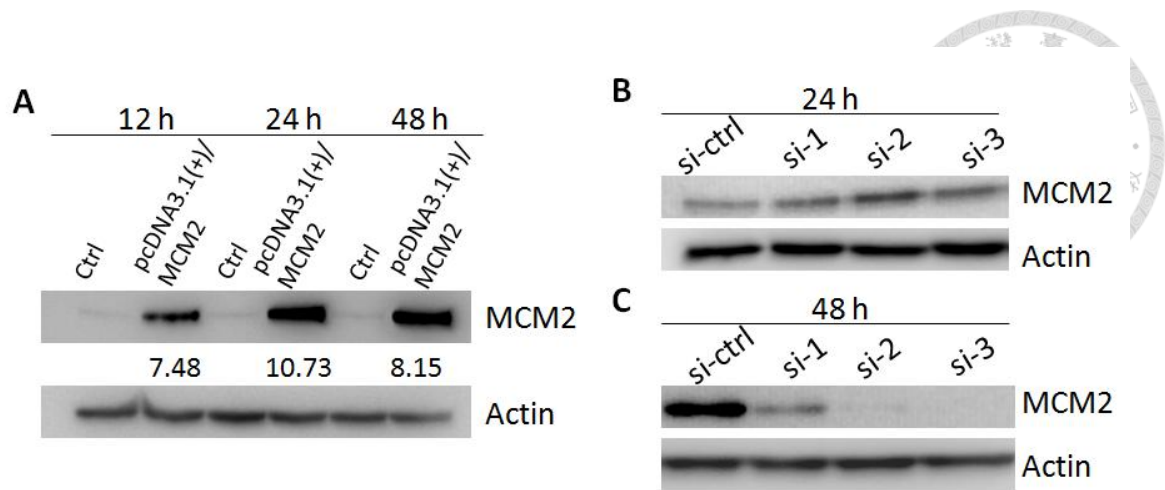


Figure 7. Confirmation of the MCM2 protein expression upon MCM2 overexpression in A549 cells and silencing MCM2 in H1299 cells. (A) A549 cells were transfected with 1 ug pcDNA3.1(+)/MCM2 or control vector. Cells were harvested at 12, 24 and 48 hours and the protein levels were analyzed by Western blotting. Overexpression level of MCM2 was highest at 24 hours post-transfection. (B) and (C) H1299 cells were treated with three siMCM2 (si-1,si-2 and si-3) or control siRNA at final concentration of 10nM. Cells were harvested at 24 and 48 hours and the protein levels were analyzed by Western blotting. Two siRNAs for MCM2 (si-1 and si-2) showed high knockdown efficiency at 48 hours.

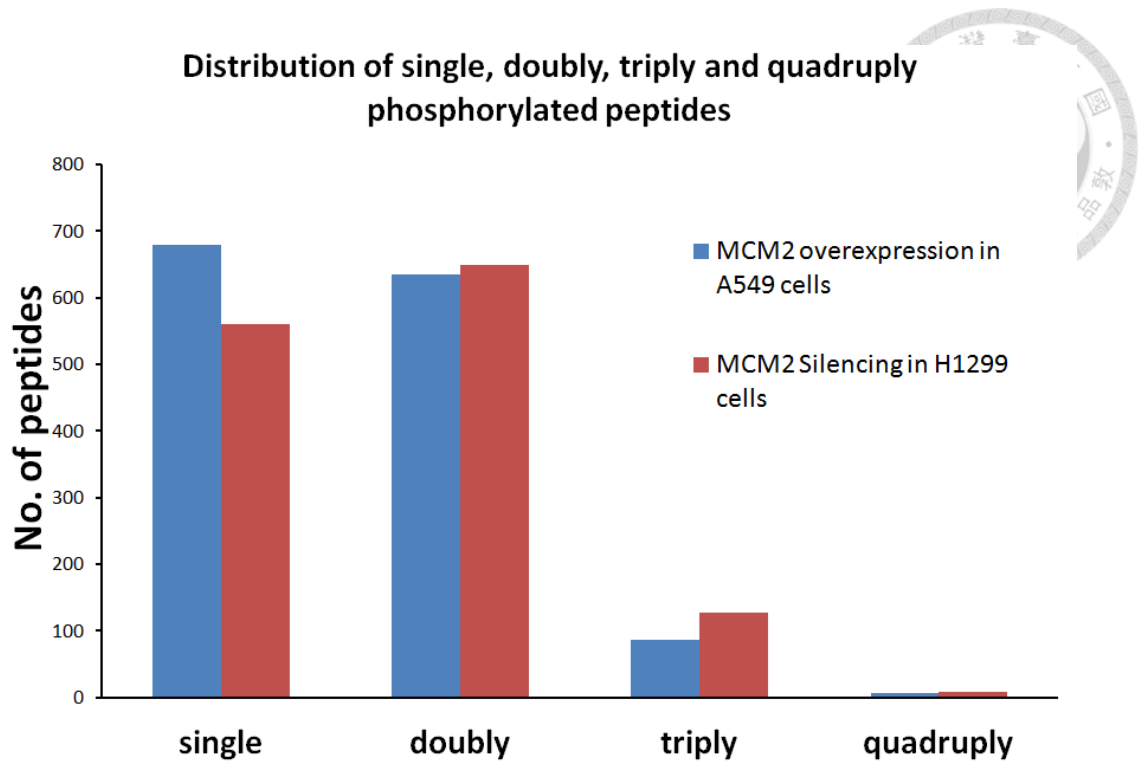


Figure 8. Distribution of single, doubly, triply and quadruply phosphorylated peptides. In the phosphoproteome of MCM2 overexpression, a majority of phosphopeptides was either single (48.3%) or doubly (45.1%) phosphorylated, followed by a small portion of triply (6.2%) and quadruply (0.4%) phosphorylated. In the phosphoproteome of silencing MCM2, a majority of phosphopeptides was either single (41.6%) or doubly (48.2%) phosphorylated, followed by a small portion of triply (9.5%) and quadruply (0.7%) phosphorylated.

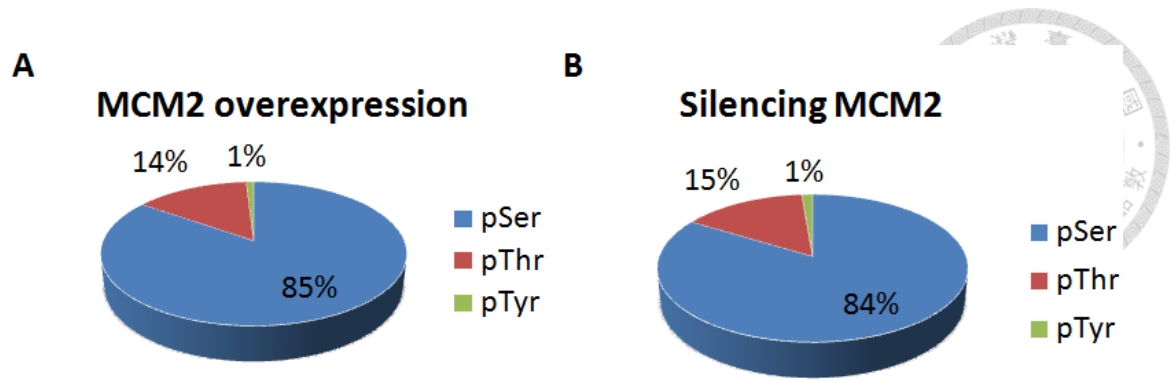


Figure 9. Distribution of phosphorylated serine, threonine, and tyrosine sites. Pie chart showed the percentages of serine, threonine and tyrosine phosphorylation sites identified in phosphoproteome of (A) MCM2 overexpression and (B) silencing MCM2. In the phosphoproteome of MCM2 overexpression, the distribution of phosphoserine (pSer), phosphothreonine (pThr) and phosphotyrosine (pTyr) was 85%, 14% and 1% respectively. In the phosphoproteome of silencing MCM2, The distribution of phosphoserine (pSer), phosphothreonine (pThr) and phosphotyrosine (pTyr) was 84%, 15% and 1% respectively.

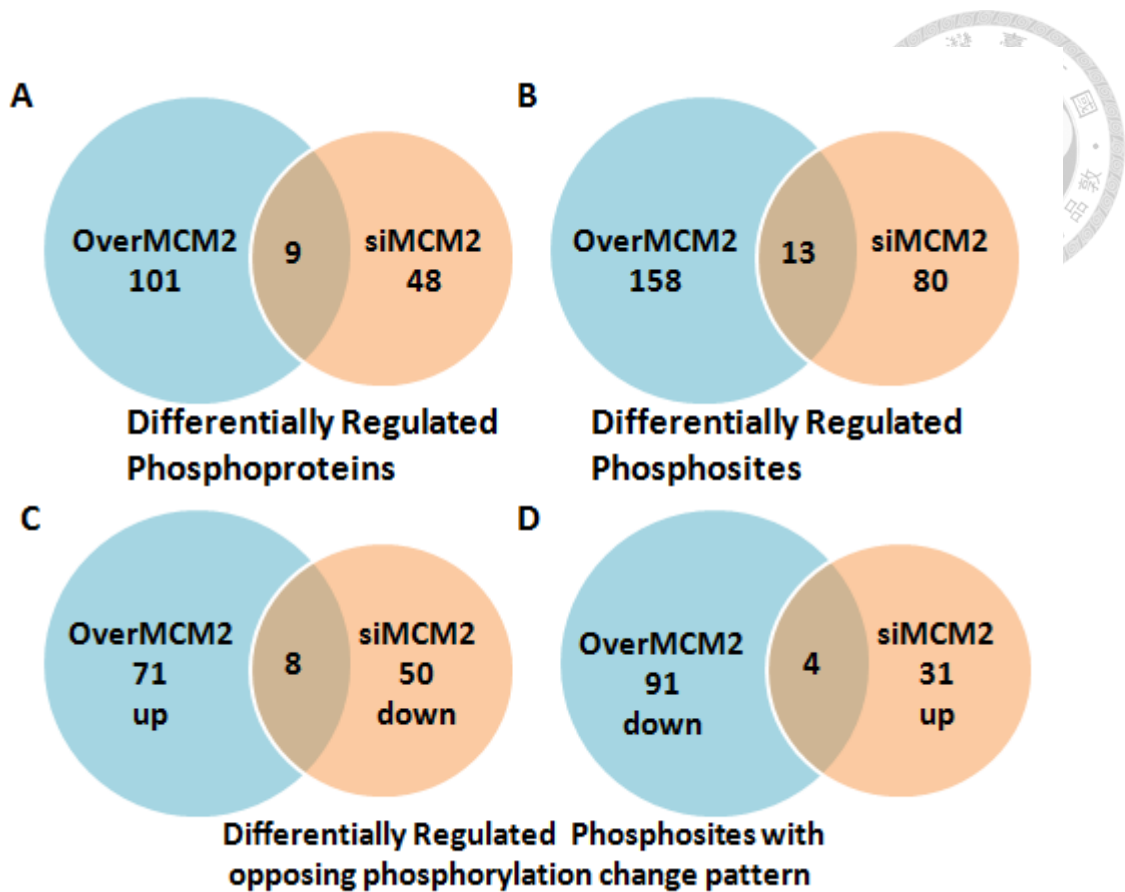


Figure 10. Phosphoproteome of MCM2 in lung cancer cells. (A) and (B) Venn diagram showed the overlap of differentially regulated phosphoproteins and phosphosites in MCM2 overexpression and silencing MCM2. (C) and (D) Overlap of phosphosites that showed the opposing phosphorylation change pattern in phosphoproteome of MCM2 overexpression and silencing MCM2. Phosphoproteins that change phosphorylation level significantly are selected by ratio H/L normalized ≤ 0.67 (1.5-fold reduced) or ≥ 1.5 (1.5-fold increased). Localization of PTM probabilities are required to be at least of 0.75.

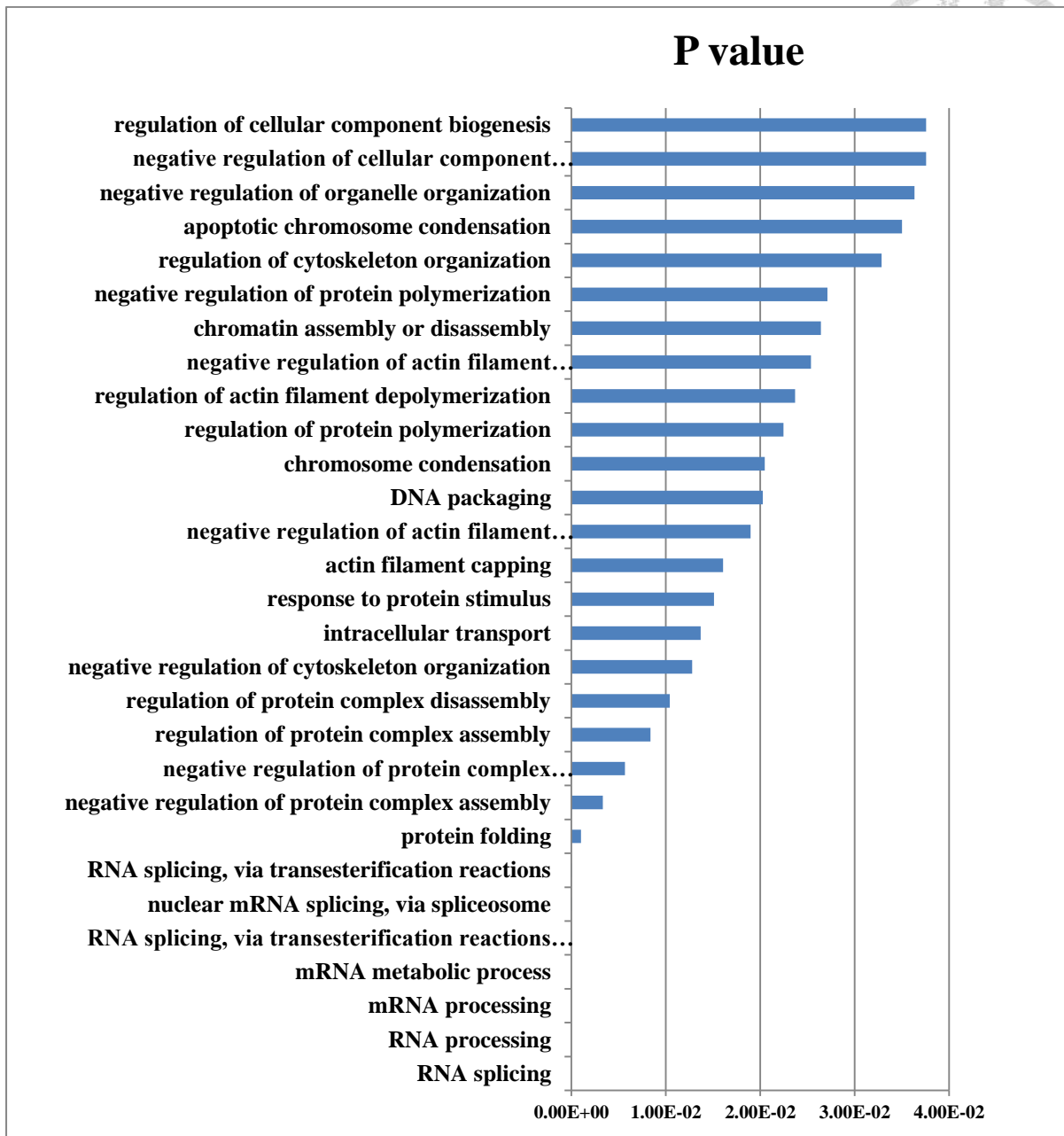


Figure 11. List of GO-term of regulated phosphoproteins in phosphoproteome of MCM2 overexpression in A549 cells. The Functional Annotation Tool on DAVID v6.7 was used to facilitate the annotation of up- (>1.5 fold) and down-regulated (>1.5 fold) phosphoproteins. MCM2-overexpressed proteins were involved in RNA splicing, protein folding, regulation of protein complex assembly, regulation of cytoskeleton organization, regulation of actin filament polymerization.

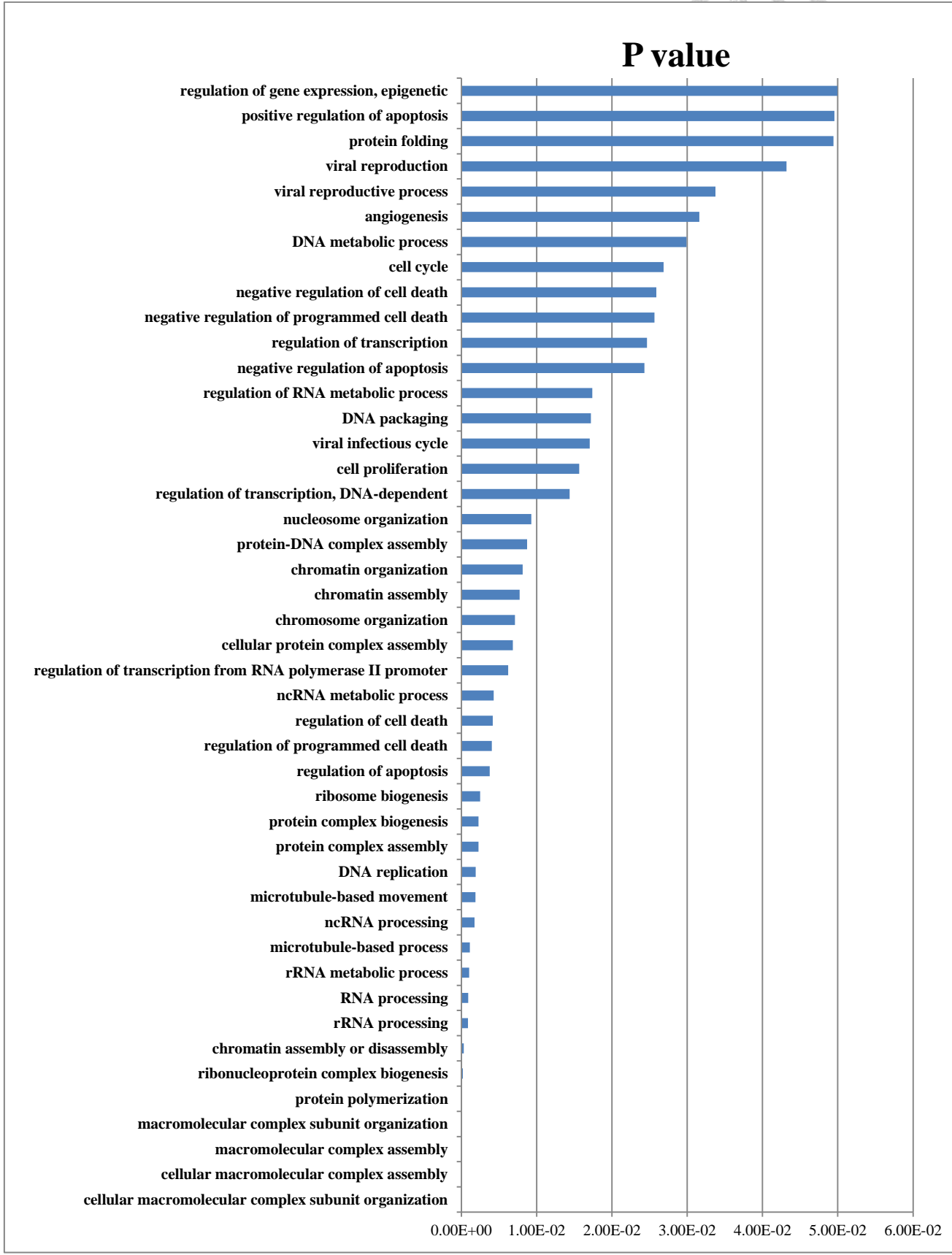


Figure 12. List of GO-term of regulated phosphoproteins in phosphoproteome of silencing MCM2 in H1299 cells. The Functional Annotation Tool on DAVID v6.7 was used to facilitate the annotation of up- (>1.5 fold) and down-regulated (>1.5 fold) phosphoproteins. MCM2-silenced proteins were mainly involved in macromolecular complex subunit organization, RNA processing, microtubule-based movement, DNA replication and cell cycle.

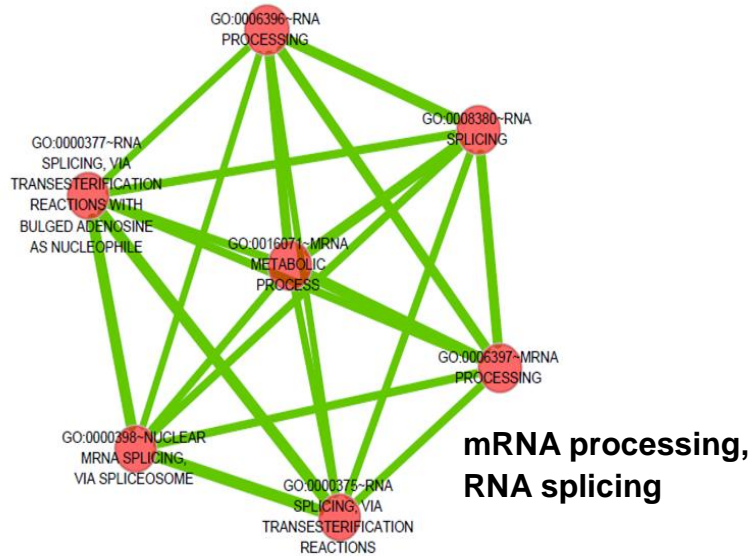
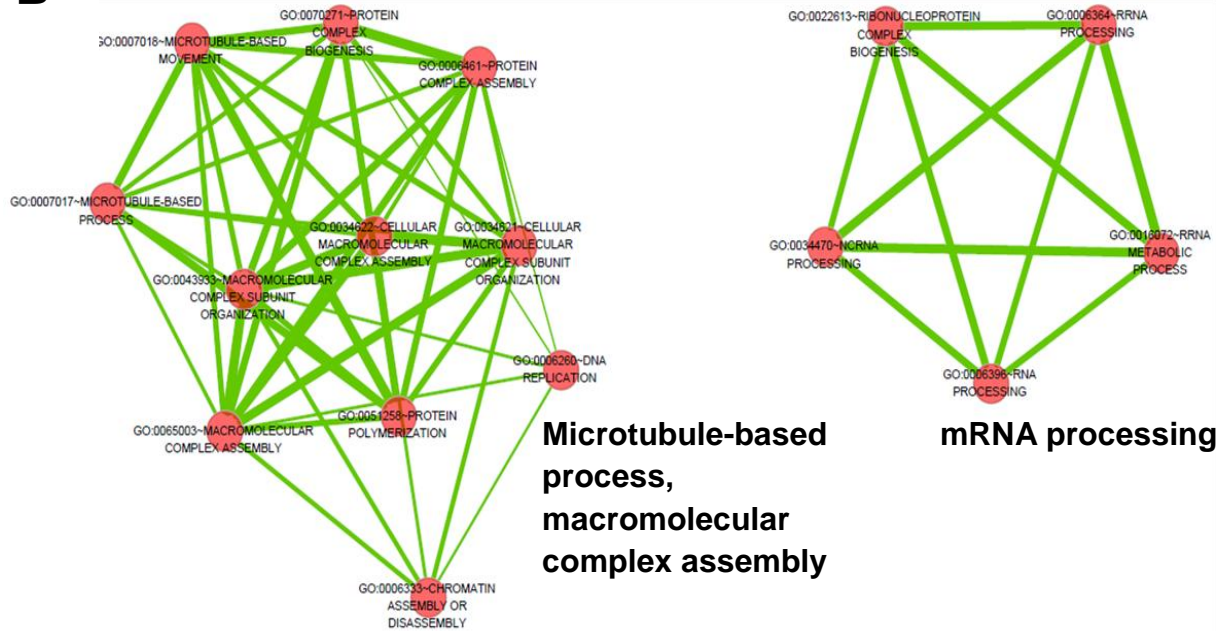
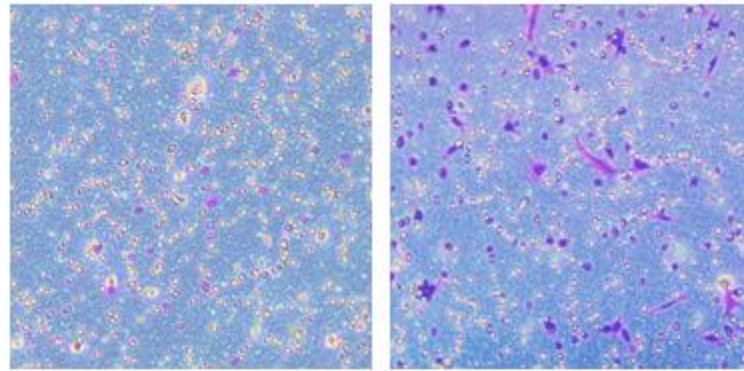
A**B**

Figure 13. Protein enrichment analysis. Visualization of enriched gene ontology term of (A) MCM2 overexpression and (B) silencing MCM2 phosphoproteome using Enrichment Map Cytoscape Plugin. Differentially up- and down-regulated phosphoproteins were analyzed for enrichment using DAVID database.

A



Control

pcDNA3.1(+)/MCM2

B

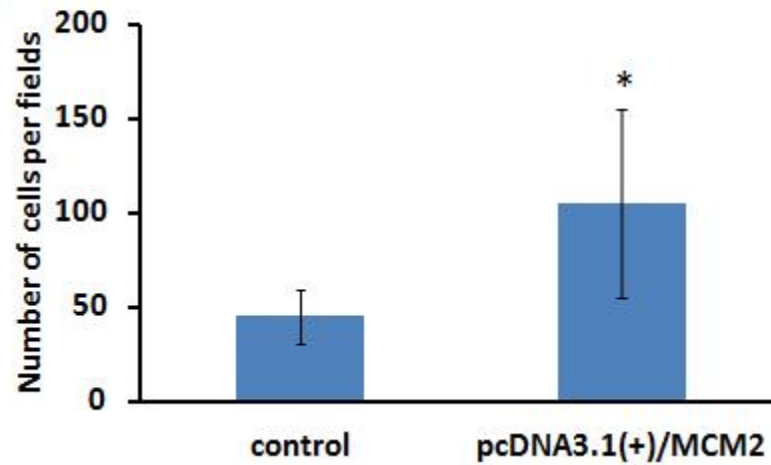


Figure 14. Overexpression of MCM2 in A549 increased cell migration. (A) The ability of cell migration was examined by transwell migration assay. 3×10^4 cells were seeded onto the upper chamber of a transwell and incubated for 6 hrs. (B) The number of migrated cells in MCM2-overexpressing and control cells. MCM2 overexpressed cells show significant increase in migrated cells. (*, $P < 0.05$)

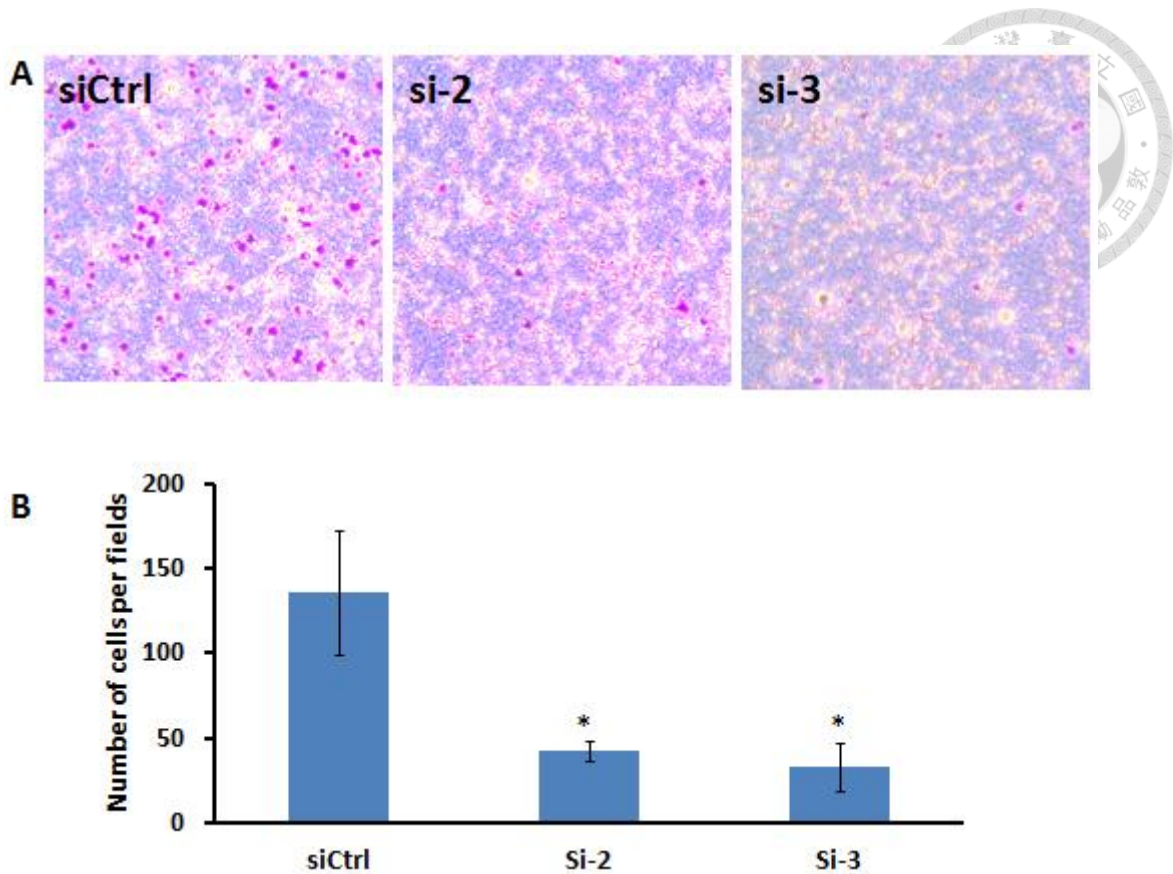


Figure 15. Silencing MCM2 in H1299 cells decreased cell migration. (A) The ability of cell migration was examined by transwell migration assay. 3×10^4 cells were seeded onto the upper chamber of a transwell and incubated for 6 hrs. (B) The number of migrated cells in MCM2-silenced and control cells. MCM2-silenced cells show significant decrease in migrated cells. (*, $P < 0.05$)

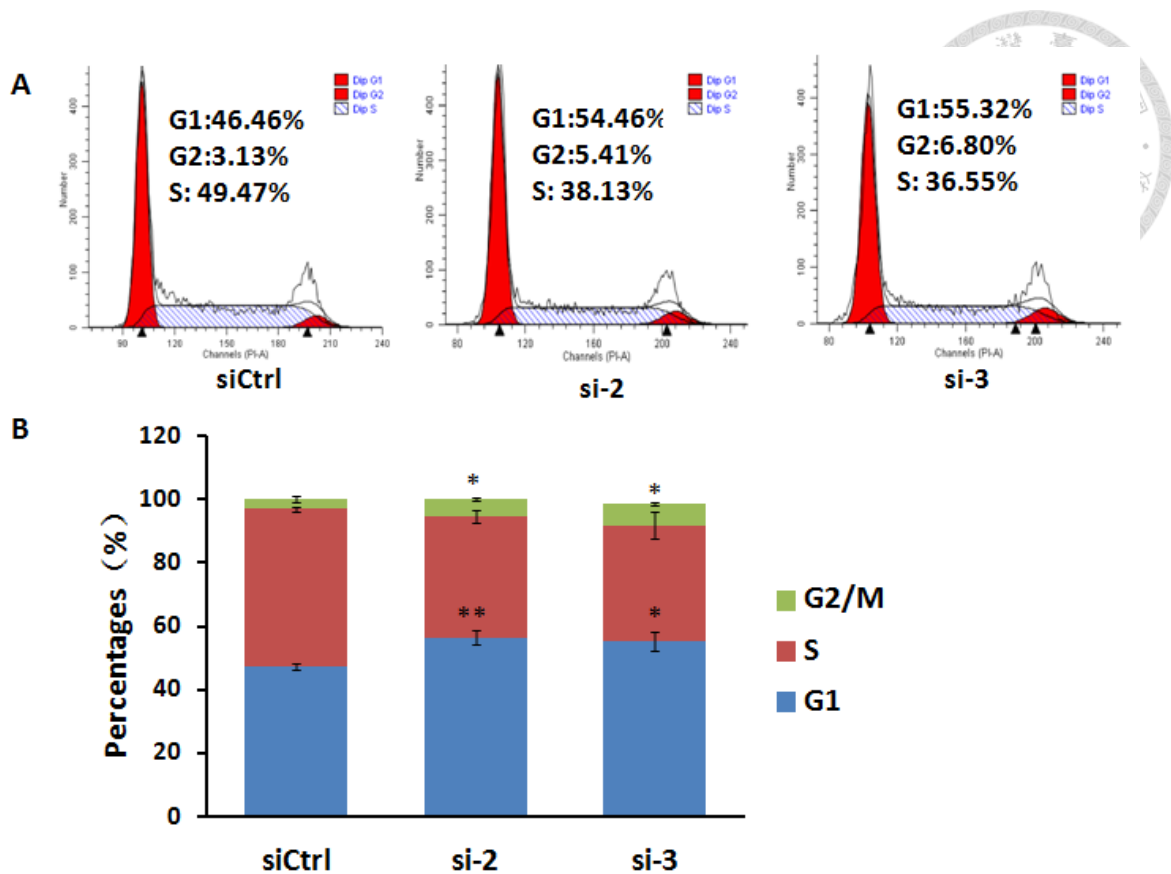


Figure 16. Silencing MCM2 in H1299 cells induced cell cycle arrest. Cells were stained with 5 $\mu\text{g/ml}$ propidium iodide for 15 minutes in the dark. The DNA content of the cells was analyzed using a FACSCanto instrument. At least 10,000 cells were collected for each measurement in a triplicate experiment. The percentage of cells in different phases of the cell cycle was analyzed using ModFit LT. MCM2 knockdown with 10nM siRNA (si-2 and si-3) resulted in a increase in G1 phase (54.46% and 55.32%) and a decrease in S phase (38.13% and 36.55%) at 48 hours siRNA post-transfection. The accumulation of cells in G2/M phase was also observed in MCM2-silenced cells (5.41% and 6.9%) as compared to control cells (3.13%). (*, $P < 0.05$; **, $P < 0.01$)

Uniprot: P17096 Symbol: HMGA1 Protein names: High mobility group protein HMG-I/HMG-Y Best score evidence ID: 4767 Best score MS/MS ID: 5684



Raw file Scan Method Score m/z
 141027-Si3-02 2713 ITMS; CID 176.17 860.7

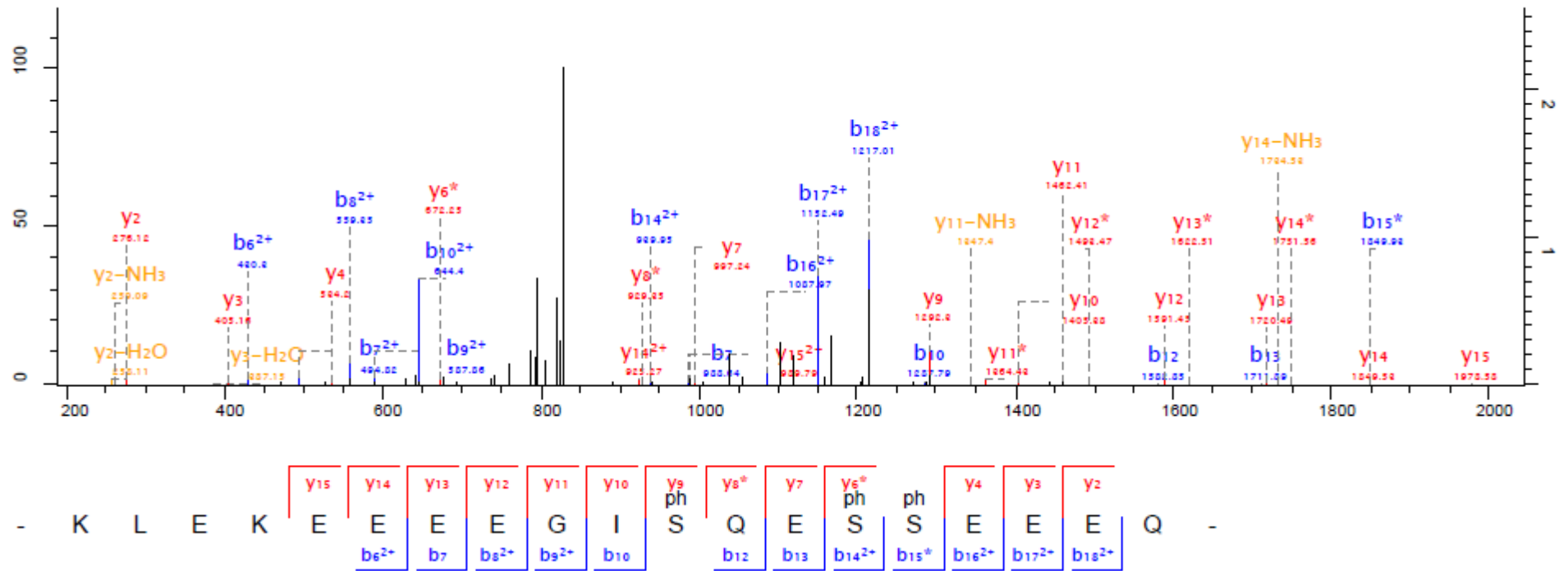


Figure 17. The MS/MS spectrum of the phosphopeptide KLEKEEEEGISQESSEEEQ from HMGA1 (high mobility group protein HMG-I/HMG-Y).

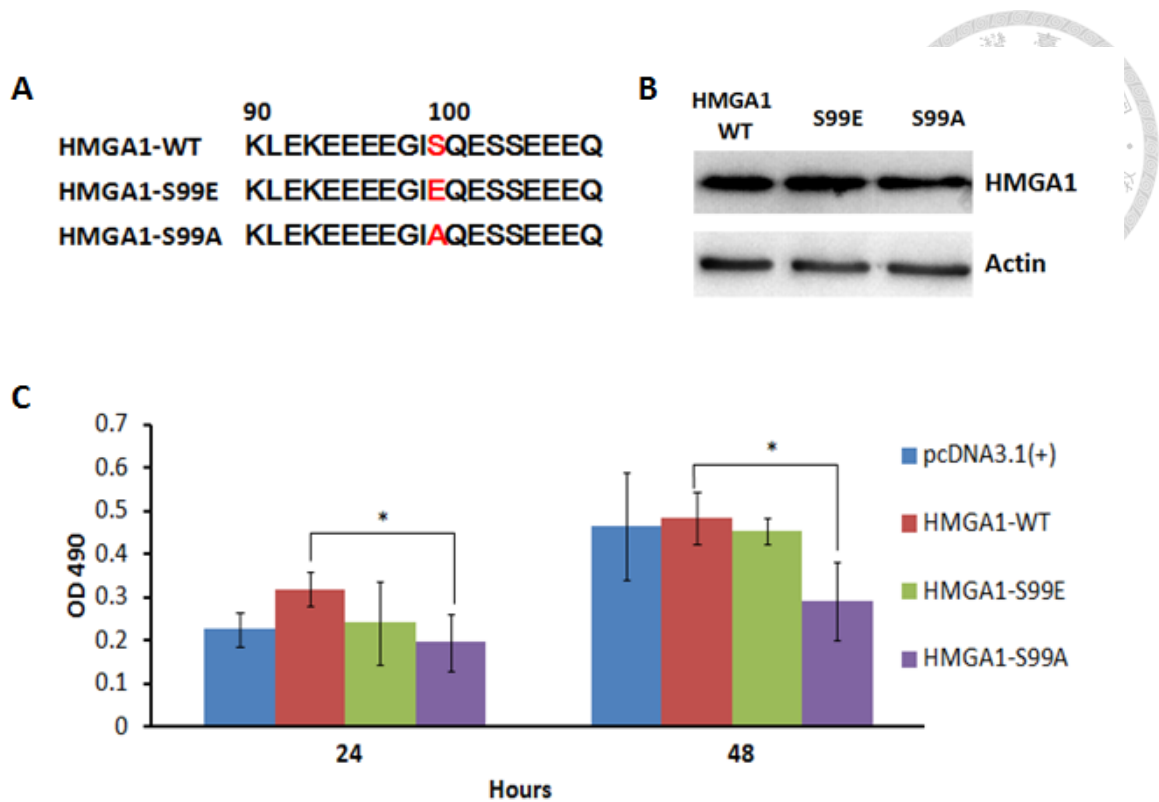


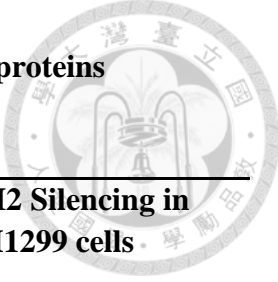
Figure 18. Phosphorylation of HMGA1 at S99 is essential for viability. (A) The amino acid sequences showing the position to be mutated by substitution. The Serine residues at position of 99 within HMGA1 protein were substituted with non-phosphorylatable alanine (Ala) and phosphomimetic glutamic acid (Glu) by site-directed mutagenesis. (B) The overexpression level of HMGA1 mutants was assessed by measuring the total HMGA1 protein. Western blot analysis showed the HMGA1 wild type and HMGA1 mutants (S99E and S99A) have similar total HMGA1 protein level, indicating that their overexpression efficiency are of the same magnitude. (C) A549 cells were transfected with pcDNA3.1(+) without insert, HMGA1 wild-type or HMGA1 mutants (S99E and S99A). At 24 hours of post-transfection, 5000 cells were seeded onto the 96-well plate and incubated for 24 or 48 hrs. Mutation of Ser99 to alanine significantly reduced (*, $P < 0.05$) the cell viability of A549 cell

Table 1. PCR primer sequences for plasmid construction



Gene	The sequence of primers
<i>MCM2</i> (Forward)	5'-GCTAGCGCCACCATGGCGGAATCATCGGAA 3'
<i>MCM2</i> (Reverse)	5' CGCACGCGTACAAGCTTTCAGAACTGCTGCAGGAT 3'
<i>HMGA1</i> (Forward)	5'- AAAGGATCCGCCACCATGAGTGAGTCGAGCTCG 3'
<i>HMGA1</i> (Reverse)	5' AAATTGGGCCCTCACTGCTCCTCCTCCGAGGACT 3'
<i>HMGA1-S99A</i> (Forward)	5' GGAGGGCATCGCGCAGGAGTC 3'
<i>HMGA1-S99A</i> (Reverse)	5' GACTCCTGCGCGATGCCCTCC 3'
<i>HMGA1-S99E</i> (Forward)	5' GGAGGGCATCCAGCAGGAGTCC 3'
<i>HMGA1-S99E</i> (Reverse)	5' GGACTCCTGCTGGATGCCCTCC 3'

Table 2. Number of phosphopeptides, phosphosites and phosphoproteins



Experiment	MCM2 overexpression in A549 cells	MCM2 Silencing in H1299 cells
No. of phosphopeptides	1409	1347
No. of phosphosites	1484	1599
No. of phosphoproteins	593	592

Spectra were analyzed using MaxQuant version 1.5.0.30 and searched against SwissProt Database (version 2014-09). In MCM2 overexpressing A549 cells, a total 1409 unique phosphopeptides on 593 phosphoproteins were identified. In MCM2 silencing H1299 cells, a total 1347 unique phosphopeptides on 592 phosphoproteins were identified.

Table 3. List of differentially regulated phosphosites that response to both MCM2 overexpression in A549 cells and silencing MCM2 in H1299 cells

No.	Uniprot ^a	Symbol ^b	Protein name ^c	Positions within proteins ^d	Amino acid ^e	Ratio H/L normalized MCM2 ^f	Ratio H/L normalized siMCM2 ^g	Localization prob MCM2 ^h	Localization prob siMCM2 ⁱ
1	O43719	HTSF1	HIV Tat-specific factor 1	713	S	0.249	1.546	0.999995	0.999636
2	P17096	HMGA1	High mobility group protein HMG-I/HMG-Y	99	S	2.793	0.211	1	1
3	P27824	CALX	Calnexin	564	S	0.493	1.638	1	0.999996
4	P35659	DEK	Protein DEK	301	S	2.212	0.394	1	1
5	P35659	DEK	Protein DEK	303	S	2.212	0.394	1	1
6	P35659	DEK	Protein DEK	306	S	2.212	0.394	1	1
7	P35659	DEK	Protein DEK	307	S	2.212	0.394	1	1
8	P49736	MCM2	DNA replication licensing factor MCM2	139	S	13.38	0.188	1	1
9	P49736	MCM2	DNA replication licensing factor MCM2	27	S	13.63	0.197	0.994583	0.999487
10	P50502; Q8IZP2	F10A1; ST134	Hsc70-interacting protein; Putative protein FAM10A4	79;75	S	0.316	1.506	1	1
11	Q13442	HAP28	28 kDa heat- and acid-stable phosphoprotein	60	S	3.147	0.637	0.999634	0.999994
12	Q13442	HAP28	28 kDa heat- and acid-stable phosphoprotein	63	S	3.147	0.633	1	1
13	O15173	PGRC2	Membrane-associated progesterone receptor component 2	211	T	0.637	0.543	0.999378	0.973173

^a The official protein Uniprot ID given to the identified protein.

^b The official gene symbol given to identified protein.

^c The official protein name obtained from Uniprot

^d The amino acid position sites to be phosphorylated within the identified phosphosites

^e The amino acid to be phosphorylated in the identified phosphosites

^f The normalized ratio between two medium and light label partners of the identified phosphosites in MCM2 overexpression experiment

^g The normalized ratio between two medium and light label partners of the identified phosphosites in silencing MCM2 experiment

^h The localization probability of the identified phosphosites in MCM2 overexpression experiment

ⁱ The localization probability of the identified phosphosites in silencing MCM2 experiment

Table 4. List of differentially regulated phosphosites

No.	Uniprot ^a	Symbol ^b	Protein names ^c	Sequence window ^d	Positions within proteins ^e	Amino acid ^f	Ratio H/L normalized ^g	Localization prob ^h	Phospho (STY) Probabilities ⁱ
Up-regulated phosphosites upon MCM2 overexpression in A549 cells									
1	Q07157	ZO1	Tight junction protein ZO-1	SRPDPEPVS DNEEDSYDEEIHDPGRSGRVV	132	Y	26.391	0.7808	VQIPVSRPDPEPVS(0.998)DNEEDS(0.221)Y(0.781)DEEIHDPGR
2	Q07157	ZO1	Tight junction protein ZO-1	KKVQIPVSRPDPEPVS DNEEDSYDEEIHDPGR	125	S	16.028	0.9992	VQIPVSRPDPEPVS(1)DNEEDS(0.553)Y(0.447)DEEIHDPGR
3	P49736	MCM2	DNA replication licensing factor MCM2	SSPAQRRRGNDPLTSSPGRSSRRTDALTSSP	27	S	13.627	0.9946	RGNDPLTS(0.001)S(0.999)PGR
4	P49736	MCM2	DNA replication licensing factor MCM2	AGRGLGRMRRLGLLYDSDEEDEERPARKRRQV	139	S	13.379	1	GLLYDS(1)DEEDEERPAR
5	Q8IZM8	ZN654	Zinc finger protein 654	SSSNEKQTISLPVSTSKSRKESTEPKTCIES	368	S	10.792	0.992	QT(0.422)IS(0.581)LPVS(0.842)T(0.163)S(0.992)K
6	P62995; Q13595	TRA2B; TRA2A	Transformer-2 protein homolog beta; Transformer-2 protein homolog alpha	DRDQIYRRRSPSPYYSRGGYRSRSRSYSP	270;266	S	10.792	0.9299	RRS(0.055)PS(0.719)PY(0.234)Y(0.062)S(0.93)R
7	Q8IZM8	ZN654	Zinc finger protein 654	KDSSSNEKQTISLPVSTSKSRKESTEPKTCI	366	S	10.792	0.8421	QT(0.422)IS(0.581)LPVS(0.842)T(0.163)S(0.992)K
8	Q15149	PLEC	Plectin	AQSTKGYYSYPVSGSGSTAGSRTGSRTGSR	4620	S	8.9892	0.9051	GYYSYPVSVS(0.006)GS(0.905)GS(0.136)T(0.464)AGS(0.072)RT(0.106)GS(0.31)R
9	P49736	MCM2	DNA replication licensing factor MCM2	EGLALDDEDVEELTASQREAAERAMRQRDRE	108	S	7.4536	0.9653	AIPELDAYEAEGALDDEDVEELT(0.035)AS(0.965)QR
10	Q96I25	SPF45	Splicing factor 45	DRHEASGFARRPDPDSDEDEDYERERRKRSM	155	S	5.6277	1	RPDPDS(1)DEDEDYERER
11	Q15149	PLEC	Plectin	STKGYYSYPVSGSGSTAGSRTGSRTGSRAG	4622	S	4.7957	0.9218	GYYSYPY(0.001)S(0.012)VS(0.012)GS(0.012)GS(0.922)T(0.765)AGS(0.276)R
12	Q9H7N4	SFR19	Splicing factor, arginine/serine-rich 19	RLDKSDPRGSPAPASSPKREVLYDSEGLSG	724	S	4.5167	0.8156	GPS(0.004)PAPAS(0.816)S(0.18)PKREVLY(0.269)DS(0.818)EGLS(0.914)GEER
13	Q9NYF8	BCLF1	Bcl-2-associated transcription factor 1	KESGKQKFNDSEGDDTEETEDYRQFRKSVLA	402	T	4.4777	1	QKFNDS(1)EGDDT(1)EETEDYR
14	Q92882	OSTF1	Osteoclast-stimulating factor 1	VRTLSNAEDYLDDSDS_____	213	S	3.8796	1	TLNSNAEDYLDDSDS(1)D
15	Q9NYF8	BCLF1	Bcl-2-associated transcription factor 1	DYFSDKESGKQKFNDSEGDDTEETEDYRQFR	397	S	3.768	1	QKFNDS(1)EGDDT(1)EETEDYR
16	P24534	EF1B	Elongation factor 1-beta	GPADVEDTTGSGATDSKDDDDIDLFGSDDEE	95	S	3.4117	0.8466	YGPADVEDT(0.006)T(0.019)GS(0.064)GAT(0.064)DS(0.847)KDDDDIDLFGS(0.963)DDEEES(0.037)EAKR
17	Q13442	HAP28	28 kDa heat- and acid-stable phosphoprotein	AGDPKKEKKSLSDESEDEEDDYQKCRKGVE	63	S	3.1474	1	SLDS(1)DES(1)EDEEDDYQK
18	Q13442	HAP28	28 kDa heat- and acid-stable phosphoprotein	DGAAGDPKKEKKSLSDESEDEEDDYQKCRK	60	S	3.1474	0.9996	SLDS(1)DES(1)EDEEDDYQK

Table 4. Continued

No.	Uniprot ^a	Symbol ^b	Protein names ^c	Sequence window ^d	Positions within proteins ^e	Amino acid ^f	Ratio H/L normalized ^g	Localization prob ^h	Phospho (STY) Probabilities ⁱ
19	P46821	MAP1B	Microtubule-associated protein 1B	TEPVEAYVIQKEREVTKGPAESPDEGITTE	885	T	2.8707	0.8142	EREVT(0.814)KGPAES(0.183)PDEGIT(0.001)T(0.001)T(0.001)EGEGECEQT(1)PELEPVEK
20	Q96SB4	SRPK1	SRSF protein kinase 1	HSESDLPEQEEEEILGSDDDEQEDPNDYCKGG	51	S	2.8304	1	GSAPHSESDLPEQEEEEILGS(1)DDDEQEDPNDYCK
21	P17096	HMGA1	High mobility group protein HMG-I/HMG-Y	RGRPCKLEKEEEEGISQESSEEEQ_____	99	S	2.7934	1	KLEKEEEEGIS(1)QES(1)S(1)EEEQ
22	Q5JSH3	WDR44	WD repeat-containing protein 44	IMRRTKEYVSNDAAQSDDEEKLQSQPTDTDG	403	S	2.6827	0.9134	EYVS(0.009)NDAAQ(0.913)DDEEKLQS(0.053)QPT(0.021)DT(0.004)DGGR
23	Q12789	TF3C1	General transcription factor 3C polypeptide 1	VRCPRVRKNSSTDQGSDEEGLSQKEQESAMD	1068	S	2.5159	0.981	VRKNS(0.427)S(0.427)T(0.145)DQGS(0.981)DEEGS(0.019)LQK
24	Q9H7N4	SFR19	Splicing factor, arginine/serine-rich 19	ASSPKREVLVDSEGLSGEERGGKSSQKDRRR	738	S	2.373	0.9135	REVLVD(1)EGLS(1)GEER
25	Q9H7N4	SFR19	Splicing factor, arginine/serine-rich 19	SPAPASSPKREVLVDSEGLSGEERGGKSSQK	734	S	2.373	0.818	REVLVD(1)EGLS(1)GEER
26	P04792	HSPB1	Heat shock protein beta-1	IESPAVAAPAYSRALSRQLSSGVSEIRHTAD	78	S	2.3684	1	ALS(1)RQLS(0.792)S(0.208)GVSEIR
27	P35659	DEK	Protein DEK	DSSTTKKNQNSKKKESESEDSSDDEPLIKKL	301	S	2.2119	1	KES(1)ES(1)EDS(1)S(1)DDEPLIKK
28	P35659	DEK	Protein DEK	STTKKNQNSKKKESESEDSSDDEPLIKKLK	303	S	2.2119	1	KES(1)ES(1)EDS(1)S(1)DDEPLIKK
29	P35659	DEK	Protein DEK	KKNQNSKKKESESEDSSDDEPLIKKLKPPPT	306	S	2.2119	1	KES(1)ES(1)EDS(1)S(1)DDEPLIKK
30	P35659	DEK	Protein DEK	KNQNSKKKESESEDSSDDEPLIKKLKPPPTD	307	S	2.2119	1	KES(1)ES(1)EDS(1)S(1)DDEPLIKK
31	Q9Y618	NCOR2	Nuclear receptor corepressor 2	GNTSQPPAFFSKLTESNSAMVKSKKQEINKK	2286	S	2.18	0.9761	LT(0.994)ES(0.976)NS(0.023)AMVKS(0.007)K
32	P13611	CSPG2	Versican core protein	QEVNPVRQEIESETTSEEQIQEEKSFESPQN	2116	S	2.1637	0.9643	QEIES(0.196)ET(0.876)T(0.964)S(0.964)EEQIQEEK
33	P13611	CSPG2	Versican core protein	RQEVNPVRQEIESETTSEEQIQEEKSFESPQ	2115	T	2.1637	0.9643	QEIES(0.196)ET(0.876)T(0.964)S(0.964)EEQIQEEK
34	P13611	CSPG2	Versican core protein	SRQEVNPVRQEIESETTSEEQIQEEKSFESP	2114	T	2.1637	0.8758	QEIES(0.196)ET(0.876)T(0.964)S(0.964)EEQIQEEK
35	Q9H1C4	UN93B	Protein unc-93 homolog B1	KVRGYRYLEEDNSDESDAEAGEHGDGAEAEAP	550	S	2.0949	0.9906	Y(0.067)LEEDNS(0.942)DES(0.991)DAEAGEHGDGAEEEEAPPAGPRGPEPAGLGR
36	Q9H1C4	UN93B	Protein unc-93 homolog B1	PQHKVRGYRYLEEDNSDESDAEAGEHGDGAEE	547	S	2.0949	0.9487	Y(0.072)LEEDNS(0.949)DES(0.979)DAEAGEHGDGAEEEEAPPAGPRGPEPAGLGR
37	Q9UJV9	DDX41	Probable ATP-dependent RNA helicase DDX41	RKRARTDEVPAAGSRSEAEDDEDYVPYVP	23	S	2.0691	0.9501	T(0.155)DEVPAAGGS(0.89)RS(0.95)EAEDDEDY(0.004)VPY(0.001)VPLR
38	Q9UJV9	DDX41	Probable ATP-dependent RNA helicase DDX41	PERKRARTDEVPAAGSRSEAEDDEDYVPY	21	S	2.0691	0.8902	T(0.146)DEVPAAGGS(0.97)RS(0.884)EAEDDEDYVPYVPLR
39	Q96TA1	NIBL1	Niban-like protein 1	VSVVQDEEVGLPFEASPESPPASPDPGVTEI	638	S	2.0111	0.9849	QVVS(0.002)VVQDEEVGLPFEAS(0.985)PES(0.993)PPPAS(0.898)PDGVT(0.122)EIR
40	Q8WX93	PALLD	Palladin	SPRSPSGHPHVRPRSRSDSGDENEPIQER	1116	S	1.9787	0.8393	S(0.839)RS(0.165)RDS(0.995)GDENEPIQER

Table 4. Continued

No.	Uniprot ^a	Symbol ^b	Protein names ^c	Sequence window ^d	Positions within proteins ^e	Amino acid ^f	Ratio H/L normalized ^g	Localization prob ^h	Phospho (STY) Probabilities ⁱ
41	Q9Y618	NCOR2	Nuclear receptor corepressor 2	SPGNTSQPPAFFSKLTESNSAMVSKKKQEIN	2284	T	1.9783	0.9942	LT(0.994)ES(0.976)NS(0.023)AMVKS(0.007)K
42	P46821	MAP1B	Microtubule-associated protein 1B	DEPVPDSESPIEKVLSPLRSPPLIGSESAYE	1396	S	1.9707	1	VLS(1)PLRS(1)PPLIGSESAYESFLSADDK
43	P46821	MAP1B	Microtubule-associated protein 1B	PDESPIEKVLSPLRSPPLIGSESAYESFLS	1400	S	1.9707	1	VLS(1)PLRS(1)PPLIGSESAYESFLSADDK
44	O15355	PPM1G	Protein phosphatase 1G	ELQPESGKRKLEEVVSTEGAEENGNSDKKKK	527	S	1.9574	0.8522	RKLEEVLS(0.852)T(0.148)EGAEENGNSDK
45	P11388	TOP2A	DNA topoisomerase 2-alpha	AKSVRAKKPIKYLEESDEDDLF_____	1525	S	1.934	0.8706	Y(0.093)LEES(0.907)DEDDLF
46	Q09666	AHNK	Neuroblast differentiation-associated protein AHNAK	SGSKGDLKSSKASLGSLEGEAEAEASSPKGK	5752	S	1.8235	0.9989	AS(1)LGS(1)LEGEAEAEASSPK
47	Q7Z4S6	KI21A	Kinesin-like protein KIF21A	ELSPPPGLPSKIGSISRQSSLEKKIPEPSP	1225	S	1.7943	0.9154	IGS(0.069)IS(0.915)RQS(0.386)S(0.629)LS(0.001)EK
48	O15027	SC16A	Protein transport protein Sec16A	PEDEASGSFFKQIDSSPVGGETDETTVSQNY	391	S	1.793	0.9505	QIDS(0.049)S(0.95)PVGGETDETTVSQNYR
49	Q4G0J3	LARP7	La-related protein 7	DTSNTSISKMKRSRPTSEGSDIESTEPQKQC	257	T	1.7554	0.7708	RSRPT(0.771)S(0.23)EGS(0.999)DIESTEPQK
50	Q13523	PRP4B	Serine/threonine-protein kinase PRP4 homolog	SEPSSPQSSTRTRSPSPDDILERVAADVKEY	580	S	1.7277	1	T(0.012)RS(0.988)PS(1)PDDILER
51	Q13523	PRP4B	Serine/threonine-protein kinase PRP4 homolog	VPSEPSSPQSSTRTRSPSPDDILERVAADVK	578	S	1.7277	0.9884	T(0.012)RS(0.988)PS(1)PDDILER
52	Q8N556	AFAP1	Actin filament-associated protein 1	PPSSPVHKAELEKLLSSERPSSDGEVGVVENG	277	S	1.7202	0.8213	KLS(0.821)S(0.446)ERPS(0.366)S(0.366)DGEGVV ENGITTCNGK
53	P15336	ATF2	Cyclic AMP-dependent transcription factor ATF-2	ARNDSVIVADQTPTPTRFLKNCEEVGLFNEL	73	T	1.7201	0.8146	NDSVIVADQT(0.998)PT(0.188)PT(0.815)R
54	Q9BQG0	MBB1A	Myb-binding protein 1A	QKKNQKPSQVNGAPGSPTEPAGQKQHQAALP	1267	S	1.7045	0.9717	NQKPSQVNGAPGS(0.972)PT(0.028)EPAGQK
55	Q9H1E3	NUCKS	Nuclear ubiquitous casein and cyclin-dependent kinase substrate 1	PVRNRKVVVDYSQFQESDDADEDYGRDSGPPT	19	S	1.69	1	VVDYSQFQES(1)DDADEDYGR
56	P29317	EPHA2	Ephrin type-A receptor 2	APDSLKTLADFDPRVSIIRLPSTSGSEGVVPR	892	S	1.663	0.9987	T(0.001)LADFDPRVS(0.999)IRLPS(0.422)T(0.422) S(0.422)GS(0.735)EGVPR
57	Q09666	AHNK	Neuroblast differentiation-associated protein AHNAK	SPEASISGSKGDLKSSKASLGSLEGEAEAEA	5746	S	1.6618	0.7886	S(0.789)S(0.789)KAS(0.312)LGS(0.11)LEGEAEAE AS(0.283)S(0.718)PK
58	Q09666	AHNK	Neuroblast differentiation-associated protein AHNAK	GSPEASISGSKGDLKSSKASLGSLEGEAEAEA	5745	S	1.6618	0.7886	S(0.789)S(0.789)KAS(0.312)LGS(0.11)LEGEAEAE AS(0.283)S(0.718)PK
59	O75369	FLNB	Filamin-B	VGSPPFKAKVTGQRLVSPGSANETSSILVESV	2478	S	1.6241	0.9892	LVS(0.989)PGS(0.011)ANETSSILVESVTR
60	Q8NHZ8	CDC26	Anaphase-promoting complex subunit CDC26	YKPQPKPNNRSSQFGSLEF_____	82	S	1.6222	0.9833	S(0.008)S(0.008)QFGS(0.983)LEF
61	Q02880	TOP2B	DNA topoisomerase 2-beta	GRKTSKTTSKPKKTSFDQDSDVDIFPSDFP	1576	S	1.6072	0.7511	KT(0.727)S(0.751)FDQDS(0.521)DVDIFPSDFPTEP PSLPR

Table 4. Continued

No.	Uniprot ^a	Symbol ^b	Protein names ^c	Sequence window ^d	Positions within proteins ^e	Amino acid ^f	Ratio H/L normalized ^g	Localization prob ^h	Phospho (STY) Probabilities ⁱ
62	Q13185	CBX3	Chromobox protein homolog 3	PQIVIAFYEERLTHWSCPEDEAQ_____	176	S	1.6048	0.9986	LT(0.001)WHS(0.999)CPEDEAQ
63	P35612	ADDB	Beta-adducin OS=Homo sapiens	GEKETAPEEPGSPAKSAPASPVQSPAKEAET	596	S	1.575	1	ETAPEEPGS(1)PAKS(1)APAS(0.999)PVQS(0.001)PAK
64	P35612	ADDB	Beta-adducin	LELDGEKETAPEEPGSPAKSAPASPVQSPAK	592	S	1.575	0.9999	ETAPEEPGS(1)PAKS(1)APAS(0.999)PVQS(0.001)PAK
65	P35612	ADDB	Beta-adducin	TAPEEPGSPAKSAPASPVQSPAKEAETKSPL	600	S	1.575	0.9993	ETAPEEPGS(1)PAKS(1)APAS(0.999)PVQS(0.001)PAK
66	Q01130	SRSF2	Serine/arginine-rich splicing factor 2	VEGMTSLKVDNLTyrTSPDTRLRRVFEKYGRV	25	T	1.5625	0.8121	VDNLT(0.038)Y(0.032)RT(0.812)S(0.116)PDT(0.002)LR
67	Q9UKV3	ACINU	Apoptotic chromatin condensation inducer in the nucleus	RVKPEEMMDERPKTRSQEVEVLERGGRFTRS	328	S	1.5588	0.9964	T(0.004)RS(0.996)QEVEVLER
68	Q8IYB3	SRRM1	Serine/arginine repetitive matrix protein 1	RLSPSASPPRRRHRPSPATPPPKTRHSPTP	402	S	1.5587	1	HRPS(1)PPAT(1)PPPK
69	Q9Y6G9	DC1L1	Cytoplasmic dynein 1 light intermediate chain 1	VHAELDRITRKPVTVSPTTPTSPTEGEAS__	510	S	1.5577	0.8742	KPVTVS(0.994)PT(0.673)T(0.241)PT(0.112)S(0.979)PT(0.001)EGEAS
70	P17544	ATF7	Cyclic AMP-dependent transcription factor ATF-7	KFGPARTDSVIIADQTPTPTRFLKNCEEVGL	51	T	1.5483	1	TDSVIIADQT(1)PT(0.985)PT(0.015)R
71	P17544	ATF7	Cyclic AMP-dependent transcription factor ATF-7	GPARTDSVIIADQTPTPTRFLKNCEEVGLFN	53	T	1.5483	0.9983	TDSVIIADQT(1)PT(0.998)PT(0.002)R
72	Q4G0J3	LARP7	La-related protein 7	KEASEASKENRDIEISTEEEEKDTGDLKDSSL	337	S	1.5421	1	DIEIS(1)T(1)EEEEK
73	Q4G0J3	LARP7	La-related protein 7	EASEASKENRDIEISTEEEEKDTGDLKDSSL	338	T	1.5421	1	DIEIS(1)T(1)EEEEK
74	Q9BX95	SGPP1	Sphingosine-1-phosphate phosphatase 1	PASPRRAGALRRNSLTGEEGQLARVSNWPLY	114	T	1.5336	0.8186	RNS(0.181)LT(0.819)GEEGQLAR
75	P63104	1433Z	14-3-3 protein zeta/delta	IMQLLRDNLTWTSQDQDEAEAGEGGEN__	232	T	1.5334	0.8382	DNLT(0.02)LWT(0.022)S(0.12)DT(0.838)QGDEAEAGEGGEN
76	Q9Y6E2	BZW2	Basic leucine zipper and W2 domain-containing protein 2	QMKKFVEWLQNAEEEESESEGEEN_____	412	S	1.5194	1	FVEWLQNAEEEEES(1)ES(1)EGEEN
77	Q9Y6E2	BZW2	Basic leucine zipper and W2 domain-containing protein 2	KKFVEWLQNAEEEESESEGEEN_____	414	S	1.5194	1	FVEWLQNAEEEEES(1)ES(1)EGEEN
78	Q02880	TOP2B	DNA topoisomerase 2-beta	KTTSKKPKKTSFDQSDVDIFPSPDFPTEPPS	1581	S	1.513	0.9419	KT(0.529)S(0.529)FDQSD(0.942)DVDIFPSPDFPTEP PSLPR
79	Q9Y6G9	DC1L1	Cytoplasmic dynein 1 light intermediate chain 1	AELDRITRKPVTVSPTTPTSPTEGEAS____	512	T	1.5023	0.8133	KPVT(0.087)VS(0.874)PT(0.813)T(0.089)PT(0.605)S(0.476)PT(0.054)EGEAS(0.002)

Table 4. Continued

No.	Uniprot ^a	Symbol ^b	Protein names ^c	Sequence window ^d	Positions within proteins ^e	Amino acid ^f	Ratio H/L normalized ^g	Localization prob ^h	Phospho (STY) Probabilities ⁱ
Down-regulated phosphosites upon MCM2 overexpression in A549 cells									
80	O75752	B3GL1	UDP-GalNAc:beta-1,3-N-acetylgalactosaminyltransferase 1	_____MASALWTVLPSRMSLRSL	3	S	0.0594	0.9993	MAS(0.999)ALWT(0.994)VLPS(0.004)RMS(0.002)LR
81	O75752	B3GL1	UDP-GalNAc:beta-1,3-N-acetylgalactosaminyltransferase 1	_____MASALWTVLPSRMSLRSLKWSL	7	T	0.0594	0.9943	MAS(0.999)ALWT(0.994)VLPS(0.004)RMS(0.002)LR
82	P40238	TPOR	Thrombopoietin receptor	PRACPLSSQSMPHFGTRYVCQFPDQEEVRLF	89	T	0.0898	0.9929	ACPLS(0.376)S(0.448)QS(0.184)MPHFGT(0.993)R
83	Q86UU0	BCL9L	B-cell CLL/lymphoma 9-like protein	GWVASPKTAMPSPGVSNKQPPLNMNSSTTL	1021	S	0.0933	0.9998	T(0.124)AMPS(0.876)PGVS(1)QNK
84	Q86UU0	BCL9L	B-cell CLL/lymphoma 9-like protein	VSPSPGWVASPKTAMPSPGVSNKQPPLNMNS	1017	S	0.0933	0.8763	T(0.124)AMPS(0.876)PGVS(1)QNK
85	O43719	HTSF1	HIV Tat-specific factor 1	EDDDSNKLFDEEEDSSEKLFDDSDERGTLG	713	S	0.2485	1	LFDEEEDS(1)S(1)EKLFDSDER
86	Q9H307	PININ	Pinin	EEAGEEEEEKEIAIVHSDAEKEQEEEEQKQEM	347	S	0.2875	1	EIAIVHS(1)DAEKEQEEEEQK
87	P50502; Q8IZP2	F10A1; ST134	Hsc70-interacting protein; Putative protein FAM10A4	KVEEDLKADEPSSEESDLEIDKEGVIEPDTD	79;75	S	0.3157	1	KVEEDLKADEPS(1)S(1)EES(1)DLEIDK
88	Q8ND56	LS14A	Protein LSM14 homolog A	QDTRSLKTQLSQGRSSPQLDPLRKSPTMEQA	183	S	0.3327	0.9138	T(0.078)QLS(0.777)QGRS(0.207)S(0.939)PQLDPLR
89	P50502; Q8IZP2	F10A1; ST134	Hsc70-interacting protein; Putative protein FAM10A4	DSKKVEEDLKADEPSSEESDLEIDKEGVIEP	76;72	S	0.3599	1	KVEEDLKADEPS(1)S(1)EES(1)DLEIDK
90	Q15019	SEPT2	Septin-2	IEEHNIKHYHLPDAESDEDEDFKEQTRLLKA	218	S	0.3973	1	IYHLPDAES(1)DEDEDFKEQTR
91	Q9Y2W1	TR150	Thyroid hormone receptor-associated protein 3	GQFDHGSGLSPSKKSPVKGKSPSTGTYGS	315	S	0.4038	0.9958	KS(1)PVGKS(0.979)PPS(0.009)T(0.008)GS(0.001)T(0.001)Y(0.001)GSS(0.001)QK
92	Q9Y2W1	TR150	Thyroid hormone receptor-associated protein 3	GSGSLSPSKKSPVKGKSPSTGTYGSSQKEE	320	S	0.4038	0.8677	KS(1)PVGKS(0.997)PPS(0.002)TGSTYGSSQK
93	Q86UE4	LYRIC	Protein LYRIC	SLLKSQEPDQKVSDDDDKEKGEALPTGK	426	S	0.4169	1	SQEPDQKVS(1)DDDK
94	Q09666	AHMK	Neuroblast differentiation-associated protein AHNAK	GGLGSKSKGHYEVGTGSDDETGKLGSGVSLA	5841	S	0.4301	0.9808	GHYEVGTGS(1)DDETGK
95	P17812	PYRG1	CTP synthase 1	QKGCRLSPRDYSDRSGSSPDSEITELKFP	571	S	0.4414	0.9636	DTYSDRS(0.975)GS(0.951)S(0.054)S(0.017)PDS(0.001)EITELK
96	Q9NR09	BIRC6	Baculoviral IAP repeat-containing protein 6	DIPKLEGSDDLLEDSDSEEHSRSDSVTGH	480	S	0.4419	0.9903	LEGSDDLLEDSDSEEHSR
97	P05114	HMG1	Non-histone chromosomal protein HMG-14	LPAENGETKTEESPASDEAGEKEAKSD____	89	S	0.4471	0.9955	EDLPAENGET(0.007)KT(0.026)EES(0.971)PAS(0.995)DEAGEK
98	P05114	HMG1	Non-histone chromosomal protein HMG-14	KEDLPAENGETKTEESPASDEAGEKEAKSD_	86	S	0.4471	0.9714	EDLPAENGET(0.007)KT(0.026)EES(0.971)PAS(0.995)DEAGEK
99	P21333	FLNA	Filamin-A	EGRVKESITRRRRAPSVANVGSHCDLSLKIP	2152	S	0.4503	1	RAPS(1)VANVGSHCDLSLK
100	P98175	RBM10	RNA-binding protein 10	RPSPPRGLVAAAYSGESDSEEEQERGGPEREE	736	S	0.4523	0.8475	GLVAAAYSGES(1)DS(1)EEEQER

Table 4. Continued

No.	Uniprot ^a	Symbol ^b	Protein names ^c	Sequence window ^d	Positions within proteins ^e	Amino acid ^f	Ratio H/L normalized ^g	Localization prob ^h	Phospho (STY) Probabilities ⁱ
101	P35606	COPB2	Coatomer subunit beta'	PSRSTAQQELDGKSPASPTPVIVASHTANKEE	859	S	0.4784	0.9399	STAQQELDGKSPAS(0.94)PT(0.06)PVIVASHTANK
102	P07900	HS90A	Heat shock protein HSP 90-alpha	YPITLTFVEKERDKEVSDDEAEKEDKEEEKE	231	S	0.4815	1	EVS(1)DDEAEKEDKEEEK
103	P27824	CALX	Calnexin	EEKQKSDAEEDGGTVSQEEDDRKPKAEDEI	564	S	0.4927	1	QKS(1)DAEEDGGTVS(1)QEEEDR
104	P08670	VIME	Vimentin	GSALRPSTSRSLYASSPGGVYATRSSAVRLR	56	S	0.4944	0.9712	SLYAS(0.001)S(0.999)PGGVYATR
105	Q9NYF8	BCLF1	Bcl-2-associated transcription factor 1	ERSGSGSVGNSSRYSPSQNSPIHHIPSRRS	285	S	0.498	0.8911	Y(0.005)S(0.913)PS(0.921)QNS(0.16)PIHHIPSR
106	P62753	RS6	40S ribosomal protein S6	RRRLSSLRASTSKSESSQK_____	246	S	0.5027	0.9152	LS(0.464)S(0.536)LRAS(0.926)T(0.316)S(0.215)KS(0.549)ES(0.939)S(0.054)QK
107	Q8NE71	ABCF1	ATP-binding cassette sub-family F member 1	KTKGGNVFAALIQQDQSEEEEEEEKHPPKPAK	140	S	0.5157	1	GGNVFAALIQQDS(1)EEEEEEK
108	Q6PKG0	LARP1	La-related protein 1	EPSTIARSLPTTVPEPNYRNRTRTPRTP	774	S	0.516	0.8629	SLPTTVPE(1)PNYR
109	Q9UK76	HN1	Hematological and neurological expressed 1 protein	GGREDLESSGLQRRNSSEASSGDFLDLKGEG	87	S	0.5171	0.9852	RNS(0.999)S(0.001)EASSGDFLDLK
110	Q7Z5L9	I2BP2	Interferon regulatory factor 2-binding protein 2	GSAQPTDLGAHKRPASVSSAAVEHEQREAA	240	S	0.519	0.7852	RPAS(0.785)VS(0.133)S(0.041)S(0.041)AAVEHEQR
111	Q01082	SPTB2	Spectrin beta chain, non-erythrocytic 1	ATEQRTSSKESPIPSPTSDRKAKTALPAQS	2169	S	0.5228	0.9918	ES(0.5)S(0.5)PIPS(0.996)PT(0.002)S(0.002)DRK
112	Q13523	PRP4B	Serine/threonine-protein kinase PRP4 homolog	PRDDILSRRERSKDasPINRWSPTRRRSRSP	431	S	0.5296	1	DAS(1)PINRWS(0.99)PT(0.01)R
113	Q13523	PRP4B	Serine/threonine-protein kinase PRP4 homolog	SRRERSKDasPINRWSPTRRRSRSP	437	S	0.5296	0.9905	DAS(1)PINRWS(0.99)PT(0.01)R
114	Q99543	DNJC2	DnaJ homolog subfamily C member 2	GRWFEAFVKRRNRNASASFQELEDKKELSEE	47	S	0.5299	1	NAS(1)AS(1)FQELEDKK
115	Q99543	DNJC2	DnaJ homolog subfamily C member 2	WFEAFVKRRNRNASASFQELEDKKELSEESE	49	S	0.5299	1	NAS(1)AS(1)FQELEDKK
116	O00567	NOP56	Nucleolar protein 56	SGSKKKRKFKEEPVSSGPEEAVGKSSSKKK	569	S	0.5375	1	EEPVS(1)S(1)GPEEAVGK
117	O75962	TRIO	Triple functional domain protein	SLGTLPLGKPRAGAASPLNSPLSSAVPSLGK	2455	S	0.5389	1	AGAAS(1)PLNS(0.999)PLS(0.001)SAVPSLGK
118	O75962	TRIO	Triple functional domain protein	LPLGKPRAGAASPLNSPLSSAVPSLGKPEFP	2459	S	0.5389	0.9986	AGAAS(1)PLNS(0.999)PLS(0.001)SAVPSLGK
119	Q5T200	ZC3HD	Zinc finger CCCH domain-containing protein 13	EVSPEVVRSLSPSPSLRKSSKSPKRKSSPK	211	S	0.5412	0.9223	S(0.022)KLS(0.804)PS(0.18)PS(0.994)LRK
120	P62753	RS6	40S ribosomal protein S6	RRRLSSLRASTSKSESSQK_____	247	S	0.5424	0.9889	LS(0.704)S(0.255)LRAS(0.341)T(0.385)S(0.267)KS(0.169)ES(0.89)S(0.989)QK
121	O00567	NOP56	Nucleolar protein 56	GSKKKRKFKEEPVSSGPEEAVGKSSSKKKK	570	S	0.5439	1	EEPVS(1)S(1)GPEEAVGK
122	Q86SQ0	PHLB2	Pleckstrin homology-like domain family B member 2	SGSYLTLSQPVPKRSPLGTSVRSPLA	71	S	0.5486	0.9467	RS(0.947)PS(0.913)PLGT(0.114)S(0.026)VR

Table 4. Continued

No.	Uniprot ^a	Symbol ^b	Protein names ^c	Sequence window ^d	Positions within proteins ^e	Amino acid ^f	Ratio H/L normalized ^g	Localization prob ^h	Phospho (STY) Probabilities ⁱ
123	Q86SQ0	PHLB2	Pleckstrin homology-like domain family B member 2	SYLTLSQPVPKRSPLGTSVRSSPSLAKI	73	S	0.5486	0.9132	RS(0.947)PS(0.913)PLGT(0.114)S(0.026)VR
124	Q9BPX3	CND3	Condensin complex subunit 3	TKKIKTLHCEGTEINSDDDEQESKEVEETATA	674	S	0.5487	1	TLHCEGTEINS(1)DDEQESK
125	O43719	HTSF1	HIV Tat-specific factor 1	KEVEDADEKLFEDDDSNKLFDEEEDSSEKL	702	S	0.5494	1	LFEDDD(1)NEK
126	P62995; Q13595	TRA2B; TRA2A	Transformer-2 protein homolog beta;Transformer-2 protein homolog alpha	GWRAAQDRDQIYRRRSPSPYYSRGGYRSRSR	264;260	S	0.5645	1	RS(1)PS(0.998)PY(0.002)YSR
127	Q9P1Y6	PHRF1	PHD and RING finger domain-containing protein 1	HLLRPDAAEKAEAPSSPDVAPAGKEDSPSAS	1360	S	0.5722	0.752	AEAPS(0.248)S(0.752)PDVAPAGKEDS(0.83)PS(0.069)AS(0.101)GR
128	Q5JTV8	TOIP1	Torsin-1A-interacting protein 1	PSPVMTRRGLRDSHSSEDEASSQTDLSTI	157	S	0.5736	0.9999	GLRDS(1)HS(1)S(1)EEDEASSQTDLSTISK
129	P62995; Q13595	TRA2B; TRA2A	Transformer-2 protein homolog beta;Transformer-2 protein homolog alpha	RAAQDRDQIYRRRSPSPYYSRGGYRSRSRSR	266;262	S	0.5759	0.9841	RS(0.995)PS(0.999)PY(0.006)YSR
130	P85037	FOXK1	Forkhead box protein K1	KIQFTSLYHKEEAPASPLRPLYPQISPLKIH	213	S	0.5885	0.9992	EEAPAS(1)PLRPLY(0.023)PQIS(0.977)PLK
131	P85037	FOXK1	Forkhead box protein K1	EEAPASPLRPLYPQISPLKIHPEPDLRSMV	223	S	0.5885	0.9971	EEAPAS(0.994)PLRPLY(0.006)PQIS(1)PLK
132	Q5JTV8	TOIP1	Torsin-1A-interacting protein 1	QPSVMTRRGLRDSHSSEDEASSQTDLSTI	156	S	0.5911	0.9999	GLRDS(1)HS(1)S(1)EEDEASSQTDLSTISK
133	P25054	APC	Adenomatous polyposis coli protein	GSESDRSERPVLVRQSTFIKEAPSPTLRRKL	2441	S	0.5967	1	QS(1)T(1)FIKEAPS(1)PT(1)LRR
134	P25054	APC	Adenomatous polyposis coli protein	RPVLVRQSTFIKEAPSPTLRRKLEESASFES	2449	S	0.5967	1	QS(1)T(1)FIKEAPS(1)PT(1)LRR
135	P25054	APC	Adenomatous polyposis coli protein	SESDRSERPVLVRQSTFIKEAPSPTLRRKLE	2442	T	0.5967	1	QS(1)T(1)FIKEAPS(1)PT(1)LRR
136	P25054	APC	Adenomatous polyposis coli protein	VLVRQSTFIKEAPSPTLRRKLEESASFESLS	2451	T	0.5967	1	QS(1)T(1)FIKEAPS(1)PT(1)LRR
137	Q9P1Y6	PHRF1	PHD and RING finger domain-containing protein 1	EAPSSPDVAPAGKEDSPSASGRVQEAAARPEE	1371	S	0.5994	0.9721	AEAPS(0.5)S(0.5)PDVAPAGKEDS(0.972)PS(0.027)AS(0.001)GR
138	P50502; Q8IZP2	F10A1; ST134	Hsc70-interacting protein; Putative protein FAM10A4	PDSKKVEEDLKADEPSSEESDLEIDKEGVIE	75;71	S	0.5998	1	KVEEDLKADEPS(1)S(1)EES(1)DLEIDK
139	O15446	RPA34	DNA-directed RNA polymerase I subunit RPA34	PQQSLSGSPLQIPASPPPQIPPGLRPRFCA	136	S	0.6106	0.9996	ILEGPQQS(0.093)LS(0.093)GS(0.814)PLQIPAS(1)PPPQIPPGLRPR
140	P49585	PCY1A	Choline-phosphate cytidylyltransferase A	PSFRWPFSGKTSPPCSPANLSRHKAAAYDIS	347	S	0.6167	1	T(0.172)S(0.828)PPCS(1)PANLSR
141	P49585	PCY1A	Choline-phosphate cytidylyltransferase A	RSPSPFRWPFSGKTSPPCSPANLSRHKAAA	343	S	0.6167	0.98	T(0.006)S(0.994)PPCS(1)PANLSR
142	Q9ULL5	PRR12	Proline-rich protein 12	ETAAVCGETDEEAGESGGEGIFRERDEFVIR	747	S	0.6175	1	KQET(0.089)AAVCGET(0.911)DEEAGES(1)GGEGIFR
143	Q86UU0	BCL9L	B-cell CLL/lymphoma 9-like protein	PLKSPQVLGSSLSVRSPTGSPSRLKSPSMAV	987	S	0.6195	0.9248	SPQVLGSS(0.001)LS(0.009)VRS(0.925)PT(0.089)GS(0.919)PS(0.057)R

Table 4. Continued

No.	Uniprot ^a	Symbol ^b	Protein names ^c	Sequence window ^d	Positions within proteins ^e	Amino acid ^f	Ratio H/L normalized ^g	Localization prob ^h	Phospho (STY) Probabilities ⁱ
144	Q86UU0	BCL9L	B-cell CLL/lymphoma 9-like protein	PQVLGSSLSVRSPTGSPSRLKSPSMAVPSPG	991	S	0.6195	0.9191	SPQVLGSS(0.001)LS(0.009)VRS(0.925)PT(0.089)GS(0.919)PS(0.057)R
145	Q86TB9	PATL1	Protein PAT1 homolog 1	DDRDLSERALPRRSTSPIIGSPPVRAVPIGT	179	S	0.6257	0.7812	RS(0.534)T(0.619)S(0.83)PIIGS(0.017)PPVR
146	Q86TB9	PATL1	Protein PAT1 homolog 1	EDDRDLSERALPRRSTSPIIGSPPVRAVPIG	178	T	0.6257	0.7812	RS(0.254)T(0.781)S(0.781)PIIGS(0.184)PPVR
147	O60763	USO1	General vesicular transport factor p115	LKDGLHPVEEEDLESGDQEDEDDESEDPGK	942	S	0.6258	1	DLGHPVEEEDLESGDQEDEDDESEDPGK
148	Q8IYB3	SRRM1	Serine/arginine repetitive matrix protein 1	RESPPAPKPRKVELSESEEDKGGKMAAADS	463	S	0.6266	1	KVELS(1)ES(1)EEDKGGK
149	Q8IYB3	SRRM1	Serine/arginine repetitive matrix protein 1	SPSPAPKPRKVELSESEEDKGGKMAAADSVQ	465	S	0.6266	1	KVELS(1)ES(1)EEDKGGK
150	P07910	HNRPC	Heterogeneous nuclear ribonucleoproteins C1/C2	DETNVMESEGGADDSAEEDLLDDDDNEDR	260	S	0.627	0.993	MESEGGADDS(1)AEEDLLDDDDNEDRGDDQL ELIK
151	P20700; Q03252	LMNB1; LMNB2	Lamin-B1; Lamin-B2	AYRKLEGEERLKLSPSPSSRVTVSRATSS	391;385	S	0.6279	0.9333	LKLS(1)PS(0.995)PS(0.004)S(0.001)R
152	P20700; Q03252	LMNB1; LMNB2	Lamin-B1; Lamin-B2	RKLEGEERLKLSPSPSSRVTVSRATSSRS;RKL LEGEERLKLSPSPSSRVTVSRATSSSS	393;387	S	0.6279	0.9261	LKLS(1)PS(0.998)PS(0.002)SR
153	Q9BU76	MMTA2	Multiple myeloma tumor-associated protein 2	EKKKKKDEHRRPAEATSSPTSPERPRHHHHD	215	T	0.6281	0.9827	RPAEAT(0.983)S(0.165)S(0.056)PT(0.754)S(0.042) PERPR
154	Q96T23	RSF1	Remodeling and spacing factor 1	PLDYSLVDLPSTNGQSPGKAIENLIGKPTEK	1375	S	0.6284	0.9873	VGS(0.183)PLDY(0.633)S(0.184)LVDLPS(0.007)T(0.007)NGQS(0.987)PGK
155	P62070	RRAS2	Ras-related protein R-Ras2	LVRVIRKFQEQECPSPPEPTRKEKDKKGCHC	186	S	0.6304	0.9999	FQEQECPSP(1)PEPTRK
156	Q8TF01	PNISR	Arginine/serine-rich protein PNISR	DSKKHSGSDSSGRSSSESPGSSKEKKAKKPK	762	S	0.6315	0.833	S(0.003)S(0.162)S(0.833)ES(0.084)PGS(0.459)S(0.459)KEKK
157	Q9H6F5	CCD86	Coiled-coil domain-containing protein 86	REPGSPPSVQRAGLGSPPERPPKTPSPGSRQLQ	58	S	0.6347	1	AGLGS(1)PERPPKT(0.38)S(0.633)PGS(0.987)PR
158	O15173	PGRC2	Membrane-associated progesterone receptor component 2	YVGRLLKPGEEPSEYTDEEDTKDHNKQD__	211	T	0.6366	0.9994	LLKPGEEPSEYT(0.999)DEEDTK
159	O43719	HTSF1	HIV Tat-specific factor 1	DDDSNEKLFDEEEDSSEKLFDDSDERGLGG	714	S	0.6391	1	LFDEEEDS(1)S(1)EKLFDSDER
160	P08238; Q58FF8	HS90B;H90B2	Heat shock protein HSP 90-beta; Putative heat shock protein HSP 90-beta 2	EDKDDEEKPKIEDVGSDEEDDSGKDKKKKTK	255;177	S	0.6405	1	IEDVGS(1)DEEDDS(1)GKDK
161	Q9UKM9	RALY	RNA-binding protein Raly	GEARTRDDGDEEGLLTHSEEELEHSQDTDAD	286	T	0.6454	0.7563	T(0.004)RDDGDDEEGLLT(0.756)HS(0.217)EEEELEHS(0.021)QDT(0.001)DADDGALQ
162	Q9NRL3	STRN4	Striatin-4	VLGQIPFLQNCEDSDDEDDELDSVQHKKQR	276	S	0.6471	0.9941	LGGSVLQIPFLQNCEDSDDEDDELDS(0.994)DEDEDLDS(0.006)VQHK
163	Q9UK58	CCNL1	Cyclin-L1	ALSTLGGFSPASKPSSPREVKAEKSPISIN	342	S	0.6531	0.778	GLNPDGTPALSTLGGFS(0.991)PAS(0.012)KPS(0.219)S(0.778)PR

Table 4. Continued

No.	Uniprot ^a	Symbol ^b	Protein names ^c	Sequence window ^d	Positions within proteins ^e	Amino acid ^f	Ratio H/L normalized ^g	Localization prob ^h	Phospho (STY) Probabilities ⁱ
164	Q9BVJ6	UT14A	U3 small nucleolar RNA-associated protein 14 homolog A	QEELADLPKDYLLSESEDEGDNDGERKHQKL	31	S	0.6545	1	DYLLS(1)ES(1)EDEGDNDGERK
165	Q9BVJ6	UT14A	U3 small nucleolar RNA-associated protein 14 homolog A	SQQEELADLPKDYLLSESEDEGDNDGERKHQ	29	S	0.6545	0.9999	DYLLS(1)ES(1)EDEGDNDGERK
166	Q6WCQ1	MPRIP	Myosin phosphatase Rho-interacting protein	RTKDQPDGSSLSPAQSPSQSPPAASSLREP	224	S	0.6546	0.9247	DQPDGS(0.112)S(0.305)LS(0.583)PAQS(0.925)PS(0.074)QS(0.001)QPPAASSLREPGLESK
167	O60841	IF2P	Eukaryotic translation initiation factor 5B	TSKDKKKKGGKQKGGKQSFDDNDSEELEDKDSK	107	S	0.6555	1	KQS(1)FDDNDS(1)EELEDKDSK
168	P42167; P42166	LAP2B; LAP2A	Lamina-associated polypeptide 2, isoforms beta/gamma; Lamina-associated polypeptide 2, isoform alpha	KLLKLREQGTESRSSTPLPTISSAENTRQN	160;160	T	0.6565	0.9684	EQGT(0.216)ES(0.597)RS(0.155)S(0.063)T(0.968)PLPTISSAENTR
169	Q9H6F5	CCD86	Coiled-coil domain-containing protein 86	TSPGSPRLQQGAGLESPOGQPEPGAASPQRQ	80	S	0.6566	1	LQQGAGLES(1)PQGQPEPGAAS(1)PQR
170	P46821	MAP1B	Microtubule-associated protein 1B	SAKAEADAYIREKRESVASGDDRAEEDMDEA	992	S	0.6606	1	RES(1)VAS(1)GDDRAEEDMDEAIEK
171	P46821	MAP1B	Microtubule-associated protein 1B	AADAYIREKRESVASGDDRAEEDMDEAIEK	995	S	0.6606	1	RES(1)VAS(1)GDDRAEEDMDEAIEK
172	Q9H694	BICC1	Protein bicaudal C homolog 1	NHGDPSIQTSGSEQTSPKSSPTEGCNDAFVE	612	S	0.6644	0.9845	VLSANHGDPSIQTSGSEQT(0.015)S(0.984)PK
173	Q66PJ3	AR6P4	ADP-ribosylation factor-like protein 6-interacting protein 4	QVEALPGPSLDQWHRSAEEEEEDGPVLTDEQK	332	S	0.666	1	S(1)AGEEEDGPVLTDEQK
174	Q9H6F5	CCD86	Coiled-coil domain-containing protein 86	TPLRRSRRLGGLRPESPELTSVSRTRRALV	18	S	0.6672	0.9498	LGGLRPES(0.992)PES(0.007)LT(0.001)SVSR
Up-regulated phosphosites upon silencing MCM2 in H1299 cells									
175	Q15691	MARE1	Microtubule-associated protein RP/EB family member 1	SLVAPALNPKPKPLTSSSAAPQRPISQRTA	155	S	3.3162	0.7832	KPLT(0.138)S(0.783)S(0.035)S(0.035)AAPQRPIS(0.004)T(0.004)QR
176	Q96MW1	CCD43	Coiled-coil domain-containing protein 43	EKQRKAALLAQYADVTDEEDEADEKDDSGAT	139	T	2.9779	0.9997	AALLAQYADVT(1)DEEDEADEK
177	P09601	HMOX1	Heme oxygenase 1	FEELQELLTHDTKDQSPSRAPGLRQRASNKV	229	S	2.6781	0.9613	DQS(0.961)PS(0.039)RAPGLR
178	Q9P2M7	CING	Cingulin	SDEEPGAYWNGKLLRSQSASLAGPGVDPS	129	S	1.9555	0.853	S(0.853)HS(0.326)QAS(0.821)LAGPGVDPSNR
179	Q16643	DREB	Drebrin	AGAIGQRLSNGLARLSSPVLHRLRLREDENA	141	S	1.864	0.8352	LS(0.835)S(0.165)PVLHR

Table 4. Continued

No.	Uniprot ^a	Symbol ^b	Protein names ^c	Sequence window ^d	Positions within proteins ^e	Amino acid ^f	Ratio H/L normalized ^g	Localization prob ^h	Phospho (STY) Probabilities ⁱ
180	Q9P2M7	CING	Cingulin	GAYWNGKLLRSHSQASLAGPGVPDPSNRSNS	134	S	1.8515	0.9808	S(0.226)HS(0.793)QAS(0.981)LAGPGVPDPSNR
181	Q13501	SQSTM	Sequestosome-1	EHGGKRSRLTPVSPSSSTEESKSSSQSSCC	275	S	1.8075	0.9352	S(0.162)RLT(0.838)PVS(0.98)PES(0.935)S(0.054)S(0.016)T(0.015)EEK
182	Q9P2M7	CING	Cingulin	EEPGAYWNGKLLRSHSQASLAGPGVPDPSNR	131	S	1.8073	0.8453	S(0.309)HS(0.845)QAS(0.845)LAGPGVPDPSNR
183	P30622	CLIP1	CAP-Gly domain-containing linker protein 1	TKTASESISNLSEAGSIKKGERELKIGDRVL	204	S	1.7733	1	TASESIS(0.011)NLS(0.989)EAGS(1)IK
184	P30622	CLIP1	CAP-Gly domain-containing linker protein 1	ISNLTKTASESISNLSEAGSIKKGERELKIG	200	S	1.7733	0.9994	TASESISNLS(1)EAGS(1)IK
185	Q1KMD3	HNRL2	Heterogeneous nuclear ribonucleoprotein U-like protein 2	GKREEDEPEERSGDETPGSEVPGDKAAEEQG	165	T	1.7624	1	REEDEPEERS(1)GDET(1)PGS(1)EVPGDK
186	Q6ZTI6	F101A	Protein FAM101A	LLDSPDGLPPSPSPPFYSLAPGILDARA	37	S	1.76	0.8969	EGLLDS(0.002)PDS(0.005)GLPPS(0.133)PS(0.854)PS(0.897)PPFY(0.051)S(0.058)LAPGILDAR
187	Q9BZW7	TSG10	Testis-specific gene 10 protein	ECTVHNLDDEMEQMSNMTLMKETISTVEKE	163	S	1.75	0.9659	MEQMS(0.966)NMT(0.066)LMKET(0.543)IS(0.543)T(0.881)VEK
188	Q9BZW7	TSG10	Testis-specific gene 10 protein	MEQMSNMTLMKETISTVEKEMKSLARKAMDT	174	T	1.75	0.8815	MEQMS(0.966)NMT(0.066)LMKET(0.543)IS(0.543)T(0.881)VEK
189	P48634	PRC2A	Protein PRC2A	NHPPAPRGRTASETRSEGSEYEEIPKRRRQR	1089	S	1.7253	0.9811	T(0.109)AS(0.455)ET(0.46)RS(0.981)EGS(0.933)EY(0.063)EEIPK
190	Q8NFC6	BD1L1	Biorientation of chromosomes in cell division protein 1-like 1	EERHMPKRKRKQHLYLSEDEPDDNPDVLDLR	2779	S	1.6563	0.9008	QHY(0.198)LS(0.901)S(0.901)EDEPDDNPDVLDLR
191	Q8NFC6	BD1L1	Biorientation of chromosomes in cell division protein 1-like 1	ERHMPKRKRKQHLYLSEDEPDDNPDVLDLR	2780	S	1.6563	0.9008	QHY(0.198)LS(0.901)S(0.901)EDEPDDNPDVLDLR
192	P27824	CALX	Calnexin OS=Homo sapiens	EEKQKSDAEEEDGGTVSQEEEDRKPKAEDEI	564	S	1.6382	1	QKS(1)DAEEDGGTVS(1)QEEEDR
193	Q92609	TBCD5	TBC1 domain family member 5	QLNKGLSSKNISSPSVESLPGGREFTGSPP	541	S	1.6371	0.997	NISS(0.002)S(0.004)PS(0.997)VES(0.997)LPGGR
194	Q92609	TBCD5	TBC1 domain family member 5	KGLSSKNISSPSVESLPGGREFTGSPPSSA	544	S	1.6371	0.9967	NISS(0.002)S(0.004)PS(0.997)VES(0.997)LPGGR
195	O94804	STK10	Serine/threonine-protein kinase 10	QVAQEQVAEQGGDLSPAANRSQKASQSRPN	438	S	1.6305	1	QVAEQGGDLS(1)PAANR
196	Q1KMD3	HNRL2	Heterogeneous nuclear ribonucleoprotein U-like protein 2	EQGLGKREEDEPEERSGDETPGSEVPGDKAA	161	S	1.6291	1	REEDEPEERS(1)GDET(1)PGS(1)EVPGDK
197	Q9NQC3	RTN4	Reticulon-4 OS=Homo sapiens	PPSTPAAPKRRGSSGSVDETLFALPAASEPV	184	S	1.6222	0.8467	RGS(0.539)S(0.526)GS(0.847)VDET(0.088)LFALPAASEPVIR
198	Q01082	SPTB2	Spectrin beta chain, non-erythrocytic 1	MVNGATEQRTSSKESPIPSPTSDRKAKTAL	2165	S	1.6206	0.8706	T(0.364)S(0.255)S(0.308)KES(0.099)S(0.973)PIPS(0.943)PT(0.043)S(0.015)DRK
199	Q01082	SPTB2	Spectrin beta chain, non-erythrocytic 1	EMVNGATEQRTSSKESPIPSPTSDRKAKTA	2164	S	1.5668	0.9793	ES(0.979)S(0.021)PIPS(0.443)PT(0.443)S(0.113)DRK

Table 4. Continued

No.	Uniprot ^a	Symbol ^b	Protein names ^c	Sequence window ^d	Positions within proteins ^e	Amino acid ^f	Ratio H/L normalized ^g	Localization prob ^h	Phospho (STY) Probabilities ⁱ
200	Q9C0C2	TB182	182 kDa tankyrase-1-binding protein	LSPSALKAKLRPRNRSAEEGELAESKSSQKE	1666	S	1.5546	1	NRS(1)AEEGELAESK
201	O43719	HTSF1	HIV Tat-specific factor 1	EDDDSNKLFDEEEDSSEKLFDDSDERGTG	713	S	1.5461	0.9996	LFDEEEDS(1)S(1)EKLFDSDDER
202	Q13501	SQSTM	Sequestosome-1	EVDIDVEHGGKRSRLTPVSPESSTEEKSSS	269	T	1.5456	1	SRLT(1)PVS(0.025)PES(0.913)S(0.051)S(0.01)TEEK
203	Q14684	RRP1B	Ribosomal RNA processing protein 1 homolog B	ETMEEQKTKVGDGDLSEAEIPENEVSLRRAV	245	S	1.5238	0.9873	VGDGDL(0.987)AEIPENEVS(0.013)LR
204	Q9HCK8	CHD8	Chromodomain-helicase-DNA-binding protein 8	TRHFSTLKDDDLVEFSDLESEDDERPRRRH	1420	S	1.5225	1	DDDLVEFS(1)DLES(1)EDDERPR
205	Q9HCK8	CHD8	Chromodomain-helicase-DNA-binding protein 8	STLKDDDLVEFSDLESEDDERPRRRHRRH	1424	S	1.5225	1	DDDLVEFS(1)DLES(1)EDDERPR
206	O94979	SC31A	Protein transport protein Sec31A	ALKDSDQVAQSDGEESPAEEQLLGEHIKEE	532	S	1.5207	1	DSDQVAQS(1)DGEES(1)PAEEQLLGEHIK
207	Q9Y2W1	TR150	Thyroid hormone receptor-associated protein 3	QTNTDKEKIKEKGSFSDTGLGDGKMKSDSFA	379	S	1.5169	0.9947	GS(0.001)FS(0.998)DT(0.001)GLGDGK
208	P50502; Q8IZP2	F10A1; ST134	Hsc70-interacting protein; Putative protein FAM10A4	KVEEDLKADEPSSEESDLEIDKEGVIEPDTD	79;75	S	1.5056	1	KVEEDLKADEPS(1)S(1)EES(1)DLEIDK
209	Q6ZT16	F101A	Protein FAM101A	EGLLDSPDSGLPPSPSPSPFFYSLAPGILDA	35	S	1.5004	0.8539	EGLLD(0.002)PDS(0.005)GLPPS(0.133)PS(0.854)PS(0.897)PPFY(0.051)S(0.058)LAPGILDAR
Down-regulated phosphosites upon silencing MCM2 in H1299 cells									
210	Q5VYK3	ECM29	Proteasome-associated protein ECM29 homolog	ALLSGLTDRNSVIQKSCAFAMGHLVVRTSRDS	1419	S	0.0426	1	S(1)CAFAMGHLVRT(0.005)S(0.165)RDS(0.277)S(0.277)T(0.277)EK
211	P17096	HMGA1	High mobility group protein HMG-I/HMG-Y	PKKLEKEEEEEGISQESSEEEQ_____	102	S	0.055	1	KLEKEEEEEGIS(1)QES(1)S(1)EEEQ
212	P17096	HMGA1	High mobility group protein HMG-I/HMG-Y	KKLEKEEEEEGISQESSEEEQ_____	103	S	0.055	1	KLEKEEEEEGIS(1)QES(1)S(1)EEEQ
213	O14974	MYPT1	Protein phosphatase 1 regulatory subunit 12A	RKDESPATWRLGLRKTGSYGALAEITASKEG	443	T	0.0959	0.9323	T(0.932)GS(0.067)Y(0.001)GALAEITASK
214	P51858	HDGF	Hepatoma-derived growth factor	EAAEGDGDKKGNAEGSSDEEGKLVIDEPAKE	132	S	0.1536	1	KGNAEGS(1)S(1)DEEGKLVIDEPAK
215	P51858	HDGF	Hepatoma-derived growth factor	AAEGDGDKKGNAEGSSDEEGKLVIDEPAKEK	133	S	0.1536	1	KGNAEGS(1)S(1)DEEGKLVIDEPAK
216	P49736	MCM2	DNA replication licensing factor MCM2	AGRGLGRMRRLLYDSDEEDEERPARRRQV	139	S	0.1885	1	GLLYDS(1)DEEDEERPAR
217	P49736	MCM2	DNA replication licensing factor MCM2	SSPAQRRRGNDPLTSSPGRSSRRTDALTSSP	27	S	0.1973	0.9995	RGNDPLTS(0.001)S(0.999)PGR
218	P17096	HMGA1	High mobility group protein HMG-I/HMG-Y	RGRPCKLEKEEEEEGISQESSEEEQ_____	99	S	0.2112	1	KLEKEEEEEGIS(1)QES(1)S(1)EEEQ

Table 4. Continued

No.	Uniprot ^a	Symbol ^b	Protein names ^c	Sequence window ^d	Positions within proteins ^e	Amino acid ^f	Ratio H/L normalized ^g	Localization prob ^h	Phospho (STY) Probabilities ⁱ
219	P49736	MCM2	DNA replication licensing factor MCM2	ASSPAQRRRGNDPLTSSPGRSSRRTDALTS	26	S	0.2171	0.8145	RGNDPLT(0.198)S(0.815)S(0.988)PGR
220	Q9BQG0	MBB1A	Myb-binding protein 1A	RPKLEKKDAKEIPSATQSPISKRRKKKGF	1161	T	0.2566	0.9564	EIPS(0.934)AT(0.956)QS(0.103)PIS(0.007)K
221	Q9BQG0	MBB1A	Myb-binding protein 1A	VQRPKLEKKDAKEIPSATQSPISKRRKKKGF	1159	S	0.2566	0.9344	EIPS(0.934)AT(0.956)QS(0.103)PIS(0.007)K
222	O14974	MYPT1	Protein phosphatase 1 regulatory subunit 12A	DESPATWRLGLRKTGSYGALAEITASKEGQK	445	S	0.3021	0.9084	T(0.061)GS(0.908)Y(0.03)GALAEITASK
223	Q9UQ35	SRRM2	Serine/arginine repetitive matrix protein 2	RKPIDSLRDSRSLSYSPVERRRSPQPSPRD	2694	S	0.3058	1	SLS(1)YS(1)PVER
224	Q9UQ35	SRRM2	Serine/arginine repetitive matrix protein 2	SPRKPIDSLRDSRSLSYSPVERRRSPQPSP	2692	S	0.3058	1	SLS(1)YS(1)PVER
225	Q14980	NUMA1	Nuclear mitotic apparatus protein 1	KAQVARGRQEAEKNSLISLSEEEVSILNRQ	1225	S	0.3347	0.9843	NS(0.984)LIS(0.03)S(0.155)LSEEEVS(0.831)ILNR
226	Q14980	NUMA1	Nuclear mitotic apparatus protein 1	AERKNSLISLSEEEVSILNRQVLEKEGESKE	1235	S	0.3347	0.8309	NS(0.984)LIS(0.03)S(0.155)LSEEEVS(0.831)ILNR
227	P35659	DEK	Protein DEK	DSSTTKKNQNSSKKESESEDSSDDEPLIKKL	301	S	0.3938	1	KES(1)ES(1)EDS(1)S(1)DDEPLIKK
228	P35659	DEK	Protein DEK	STTKKNQNSSKKESESEDSSDDEPLIKKLKK	303	S	0.3938	1	KES(1)ES(1)EDS(1)S(1)DDEPLIKK
229	P35659	DEK	Protein DEK	KKNQNSSKKESESEDSSDDEPLIKKLKPPPT	306	S	0.3938	1	KES(1)ES(1)EDS(1)S(1)DDEPLIKK
230	P35659	DEK	Protein DEK	KNQNSSKKESESEDSSDDEPLIKKLKPPPTD	307	S	0.3938	1	KES(1)ES(1)EDS(1)S(1)DDEPLIKK
231	Q9H093	NUAK2	NUAK family SNF1-like kinase 2	TLGKGTYGKVKKARESSGRLVAIKSIRKDKI	73	S	0.4064	1	ARES(1)S(1)GRLVAIK
232	Q9H093	NUAK2	NUAK family SNF1-like kinase 2	LGKGTYGKVKKARESSGRLVAIKSIRKDKIK	74	S	0.4064	1	ARES(1)S(1)GRLVAIK
233	P16401	H15	Histone H1.5	ETAPAETATPAPVEKSPAKKKATKKAAGAGA	18	S	0.4251	0.9999	SETAPAETATPAPVEKS(1)PAK
234	Q9UQ35	SRRM2	Serine/arginine repetitive matrix protein 2	EDKDKDKKEKSATRPSPPERSSTGPEPPAP	351	S	0.4479	0.9905	S(0.004)AT(0.004)RPS(0.991)PS(0.948)PERS(0.254)S(0.572)T(0.226)GPEPPAPTPLLAER
235	Q9Y5J1	UTP18	U3 small nucleolar RNA-associated protein 18 homolog	MGGVPAWAETTKRKTSSDDESEDEDDLLQR	205	S	0.4632	0.8782	RKT(0.126)S(0.878)S(0.996)DDES(1)EEDEDDLLQR
236	Q9H6F5	CCD86	Coiled-coil domain-containing protein 86	AGLGSPERPPKTSPPGSPRLQQGAGLESPQGQ	69	S	0.4725	0.9999	AGLGS(0.993)PERPPKT(0.204)S(0.803)PGS(1)PR
237	Q9UQ35	SRRM2	Serine/arginine repetitive matrix protein 2	KKEKSATRPSPPERSSTGPEPPAPTPLLAE	357	S	0.4924	0.8473	S(0.708)AT(0.708)RPS(0.259)PS(0.312)PERS(0.847)S(0.114)T(0.051)GPEPPAPTPLLAER
238	Q9H6F5	CCD86	Coiled-coil domain-containing protein 86	QQDLHLESPQRQPEYSPESPRCQPKPSEEAP	110	S	0.5087	0.9841	QQDLHLES(0.999)PQRQPEY(0.017)S(0.984)PES(1)PR
239	Q07955	SRSF1	Serine/arginine-rich splicing factor 1	IRVKVDGPRSPSYGRSRSRSRSRSRSRSRN	205	S	0.5157	0.9998	VDGPRS(0.98)PS(0.897)Y(0.123)GRS(1)R
240	Q07955	SRSF1	Serine/arginine-rich splicing factor 1	ETAYIRVKVDGPRSPSYGRSRSRSRSRSRSR	201	S	0.5157	0.897	VDGPRS(0.98)PS(0.897)Y(0.123)GRS(1)R
241	P27824	CALX	Calnexin	KLEEKQKSDAEEEDGGTVSQEEEDRKPKAEEED	562	T	0.5223	0.9739	QKS(1)DAEEDGGT(0.974)VS(0.026)QEEEDR

Table 4. Continued

No.	Uniprot ^a	Symbol ^b	Protein names ^c	Sequence window ^d	Positions within proteins ^e	Amino acid ^f	Ratio H/L normalized ^g	Localization prob ^h	Phospho (STY) Probabilities ⁱ
242	P19338	NUCL	Nucleolin	IEGRAIRLELQGPRGSPNARSQPSKTLFVKG	563	S	0.5251	1	LELQGPRGS(1)PNAR
243	Q99638	RAD9A	Cell cycle checkpoint control protein RAD9A	PVRSPQGPSPVLAEDSEGE_____	387	S	0.5354	0.9977	SPQGPSPVLAEDS(1)EGEG
244	O15173	PGRC2	Membrane-associated progesterone receptor component 2	YVGRLLKPGEEPSEYTDEEDTKDHNKQD__	211	T	0.5434	0.9732	LLKPGEEPSEYT(0.999)DEEDTK
245	P35579	MYH9	Myosin-9	FVVPRRMARKGAGDGSDEEVDGKADGAEAKP	1943	S	0.5471	1	GAGDGS(1)DEEVDGKADGAEAKPAE
246	Q9UQ35	SRRM2	Serine/arginine repetitive matrix protein 2	KDKDKKEKSATRPSPPERSSTGPEPPAFTP	353	S	0.5518	0.9936	S(0.008)AT(0.008)RPS(0.988)PS(0.996)PERSSTGP EPPAPTPLLAER
247	Q9H6F5	CCD86	Coiled-coil domain-containing protein 86	SVQRAGLGSPPERPPKTPSPGPRLLQGGAGLES	65	T	0.5568	0.915	AGLGS(0.001)PERPPKT(0.992)S(0.966)PGS(0.041)PR
248	Q9UK58	CCNL1	Cyclin-L1	LNPDPGTPALSTLGGFSPASKPSSPREVKAE	335	S	0.5638	0.9988	GLNPDGTPALST(0.001)LGGFS(0.999)PAS(0.968)KPS(0.603)S(0.428)PR
249	Q9Y5J1	UTP18	U3 small nucleolar RNA-associated protein 18 homolog	AWAETTKRKTSSDDESEDEEDDLLQRTGNFI	210	S	0.5915	1	T(0.001)S(0.056)S(0.943)DDES(1)EEDEDDLLQR
250	Q9Y3T9	NOC2L	Nucleolar complex protein 2 homolog	REAREAARSPDKPGGSPASRRKGRASEHKD	56	S	0.6007	0.909	EAARS(1)PDKPGGS(0.909)PS(0.054)AS(0.037)R
251	Q9Y3T9	NOC2L	Nucleolar complex protein 2 homolog	NSPQAETREAREAARSPDKPGGSPASRRKG	49	S	0.6049	1	EAARS(1)PDKPGGS(0.909)PS(0.054)AS(0.037)R
252	P62753	RS6	40S ribosomal protein S6	AKEKRQEQAIAKRRRLSRLASTSKSESSQK_	235	S	0.6094	1	RLS(1)S(1)LRAS(0.997)T(0.003)SK
253	Q9BQE3; Q6PEY2; Q13748	TBA1C; TBA3E; TBA3C	Tubulin alpha-1C chain; Tubulin alpha-3E chain; Tubulin alpha-3C/D chain	DGQMPSDKTIGGGDDSFNTFFSETGAGKHVP	48;48;48; 48;48	S	0.6094	0.9967	TIGGGDDS(0.997)FNT(0.003)FFSETGAGK
254	P31350	RIR2	Ribonucleoside-diphosphate reductase subunit M2	RVPLAPITDPQQLQLSPLKGLSLVDKENTPP	20	S	0.6128	1	VPLAPITDPQQLQLS(1)PLK
255	Q7Z5K2	WAPL	Wings apart-like protein homolog	NDTWNSQFGKRPEPSEISPIKGSVRTGLFE	223	S	0.6207	0.9299	RPES(0.003)PS(0.997)EIS(1)PIK
256	Q9UNE7	CHIP	E3 ubiquitin-protein ligase CHIP	KEEKEGGARLGAGGGSPEKSPSAQELKEQGN	19	S	0.6216	0.9987	LGAGGGS(1)PEKS(0.908)PS(0.092)AQELK
257	O14974	MYPT1	Protein phosphatase 1 regulatory subunit 12A	REKRRSTGVSFWTQDSDENEQEQQSDTEEGS	862	S	0.627	0.8805	ST(0.001)GVS(0.003)FWT(0.112)QDS(0.881)DENE QEQQS(0.722)DT(0.236)EEGS(0.045)NKK
258	Q96JG6	CC132	Coiled-coil domain-containing protein 132	YESDEQEKSAYQEYDSDSDVPEELKRDYVDE	559	S	0.6273	0.999	SAYQEY(0.004)DS(0.999)DS(0.997)DVPEELK
259	Q13442	HAP28	28 kDa heat- and acid-stable phosphoprotein	AGDPKKEKSLDSDESEDEEDDYQQRKRGVE	63	S	0.6328	1	SLDS(1)DES(1)EDEDYQQRK
260	O15061	SYNEM	Synemin OS=Homo sapiens	KAVESVVRESLSRQRSPAPGSPDEEGGAEAP	1044	S	0.6359	1	QRS(1)PAPGS(1)PDEEGGAEAPAAGIR
261	O15061	SYNEM	Synemin OS=Homo sapiens	VVRESLSRQRSPAPGSPDEEGGAEAPAAGIR	1049	S	0.6359	1	QRS(1)PAPGS(1)PDEEGGAEAPAAGIR

Table 4. Continued

No.	Uniprot ^a	Symbol ^b	Protein names ^c	Sequence window ^d	Positions within proteins ^e	Amino acid ^f	Ratio H/L normalized ^g	Localization prob ^h	Phospho (STY) Probabilities ⁱ
262	Q13442	HAP28	28 kDa heat- and acid-stable phosphoprotein	DGAAGDPKKEKKSLSDESEDEDDYQQRK	60	S	0.6366	1	SLDS(1)DES(1)EDEDDYQQRK
263	Q14137	BOP1	Ribosome biogenesis protein BOP1	TEMASARIGDEYAEDSSDEEDIRNTVGNVPL	126	S	0.6623	1	IGDEYAEDS(1)S(1)DEEDIR
264	Q14137	BOP1	Ribosome biogenesis protein BOP1	EMASARIGDEYAEDSSDEEDIRNTVGNVPLE	127	S	0.6623	1	IGDEYAEDS(1)S(1)DEEDIR
265	Q13112	CAF1B	Chromatin assembly factor 1 subunit B	RPVEGTPASRTQDPSSPGTTPPQARQAPAPT	429	S	0.663	0.9309	TQDPS(0.721)S(0.931)PGT(0.188)T(0.16)PPQAR
266	P48634	PRC2A	Protein PRRC2A	GSEYEEIPKRRRQRGSETGSETHESDLAPSD	1106	S	0.6645	0.7908	QRGS(0.791)ET(0.791)GS(0.319)ET(0.058)HES(0.041)DLAPSDK
267	P48634	PRC2A	Protein PRRC2A	EYEEIPKRRRQRGSETGSETHESDLAPSDKE	1108	T	0.6645	0.7908	QRGS(0.791)ET(0.791)GS(0.319)ET(0.058)HES(0.041)DLAPSDK

^a The official protein Uniprot ID given to the identified protein.

^b The official gene symbol given to identified protein.

^c The official protein name obtained from Uniprot

^d The amino acid sequence of the identified peptide.

^e The amino acid position sites to be phosphorylated within the identified peptides

^f The amino acid to be phosphorylated in the identified peptides

^g The normalized ratio between two medium and light label partners of the identified phosphosites in MCM2 overexpression or silencing MCM2 experiment.

^h The localization probability of the identified phosphosites in MCM2 overexpression experiment

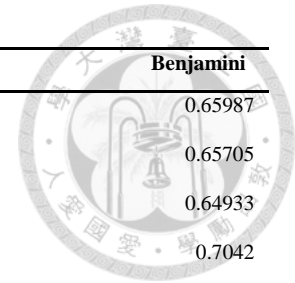
ⁱ The sequence representation of the peptide including PTM positioning probabilities ([0..1], where 1 is best match) for 'Phospho (STY)

Table 5. List of GO-term of regulated phosphoproteins in phosphoproteome of MCM2 overexpression in A549 cells

Category	Term	Count	%	PValue	Genes	Benjamini
GOTERM_BP_FAT	GO:0008380~RNA splicing	19	12.5	5.82E-11	SF1, TRA2B, PNN, SMN1, DDX41, TRA2A, RBM17, SF3B1, SRSF11, SCAF1, SRSF2, HNRNPC, RALY, PRPF4B, HNRNPK, RBM10, ARL6IP4, SRRM1, SRPK1	4.88E-08
GOTERM_BP_FAT	GO:0006396~RNA processing	24	15.8	3.92E-10	SF1, TRA2B, PNN, SMN1, 808508, DDX41, 781090, TRA2A, RBM17, SF3B1, 811974, SRSF11, SCAF1, SRSF2, HNRNPC, 804325, RALY, PRPF4B, HNRNPK, RBM10, ARL6IP4, SRRM1, SRPK1, NOP56	1.65E-07
GOTERM_BP_FAT	GO:0006397~mRNA processing	19	12.5	4.30E-10	SF1, TRA2B, PNN, SMN1, DDX41, TRA2A, RBM17, SF3B1, SRSF11, SCAF1, SRSF2, HNRNPC, 804325, RALY, PRPF4B, HNRNPK, RBM10, SRRM1, SRPK1	1.20E-07
GOTERM_BP_FAT	GO:0016071~mRNA metabolic process	20	13.2	5.93E-10	SF1, TRA2B, PNN, SMN1, DDX41, 781090, TRA2A, RBM17, SF3B1, SRSF11, SCAF1, SRSF2, HNRNPC, 804325, RALY, PRPF4B, HNRNPK, RBM10, SRRM1, SRPK1	1.24E-07
GOTERM_BP_FAT	GO:0000377~RNA splicing, via transesterification reactions with bulged adenosine as nucleophile	10	6.58	8.59E-06	SF1, TRA2B, SMN1, HNRNPK, TRA2A, SRRM1, SF3B1, SRSF11, SRSF2, HNRNPC	0.00144
GOTERM_BP_FAT	GO:0000398~nuclear mRNA splicing, via spliceosome	10	6.58	8.59E-06	SF1, TRA2B, SMN1, HNRNPK, TRA2A, SRRM1, SF3B1, SRSF11, SRSF2, HNRNPC	0.00144
GOTERM_BP_FAT	GO:0000375~RNA splicing, via transesterification reactions	10	6.58	8.59E-06	SF1, TRA2B, SMN1, HNRNPK, TRA2A, SRRM1, SF3B1, SRSF11, SRSF2, HNRNPC	0.00144
GOTERM_BP_FAT	GO:0006457~protein folding	8	5.26	0.001	CANX, ST13, DNAJC2, RANBP2, HSP90AA1, HSP90AB3P, HSP90AB1, HSP90AB2P	0.13086
GOTERM_BP_FAT	GO:0031333~negative regulation of protein complex assembly	4	2.63	0.00333	SPTBN1, SPTAN1, EIF4EBP1, ADD2	0.3298
GOTERM_BP_FAT	GO:0043242~negative regulation of protein complex disassembly	4	2.63	0.00568	SPTBN1, SPTAN1, MAP1B, ADD2	0.44957
GOTERM_BP_FAT	GO:0043254~regulation of protein complex assembly	5	3.29	0.00837	SPTBN1, SPTAN1, EIF4EBP1, MAP1B, ADD2	0.54341
GOTERM_BP_FAT	GO:0043244~regulation of protein complex disassembly	4	2.63	0.0104	SPTBN1, SPTAN1, MAP1B, ADD2	0.58412
GOTERM_BP_FAT	GO:0051494~negative regulation of cytoskeleton organization	4	2.63	0.01277	SPTBN1, SPTAN1, MAP1B, ADD2	0.62493
GOTERM_BP_FAT	GO:0046907~intracellular transport	13	8.55	0.01368	SPTBN1, RANBP2, HSP90AA1, FLNA, YWHAZ, USO1, KIF4A, MAPK1, AGFG1, MYBBP1A, COPB2, AP3B1, GBF1	0.61831
GOTERM_BP_FAT	GO:0051789~response to protein stimulus	5	3.29	0.01509	HSP90AA1, MAP1B, HSP90AB1, DEK, HSPB1	0.6251
GOTERM_BP_FAT	GO:0051693~actin filament capping	3	1.97	0.01605	SPTBN1, SPTAN1, ADD2	0.62087
GOTERM_BP_FAT	GO:0030835~negative regulation of actin filament depolymerization	3	1.97	0.01896	SPTBN1, SPTAN1, ADD2	0.65725
GOTERM_BP_FAT	GO:0006323~DNA packaging	5	3.29	0.02027	RSF1, TOP2A, MCM2, NCAPG, ACIN1	0.6583
GOTERM_BP_FAT	GO:0030261~chromosome condensation	3	1.97	0.02049	TOP2A, NCAPG, ACIN1	0.64007
GOTERM_BP_FAT	GO:0032271~regulation of protein polymerization	4	2.63	0.02247	SPTBN1, SPTAN1, MAP1B, ADD2	0.65325
GOTERM_BP_FAT	GO:0030834~regulation of actin filament depolymerization	3	1.97	0.0237	SPTBN1, SPTAN1, ADD2	0.65328

Table 5. Continued

Category	Term	Count	%	PValue	Genes	Benjamini
GOTERM_BP_FAT	GO:0030837~negative regulation of actin filament polymerization	3	1.97	0.02538	SPTBN1, SPTAN1, ADD2	0.65987
GOTERM_BP_FAT	GO:0006333~chromatin assembly or disassembly	5	3.29	0.02643	CBX3, RSF1, MCM2, HIRIP3, HMGA1	0.65705
GOTERM_BP_FAT	GO:0032272~negative regulation of protein polymerization	3	1.97	0.0271	SPTBN1, SPTAN1, ADD2	0.64933
GOTERM_BP_FAT	GO:0051493~regulation of cytoskeleton organization	5	3.29	0.03284	SPTBN1, SPTAN1, MAP1B, 787315, ADD2	0.7042
GOTERM_BP_FAT	GO:0030263~apoptotic chromosome condensation	2	1.32	0.03502	TOP2A, ACIN1	0.71237
GOTERM_BP_FAT	GO:0010639~negative regulation of organelle organization	4	2.63	0.03634	SPTBN1, SPTAN1, MAP1B, ADD2	0.71127
GOTERM_BP_FAT	GO:0051129~negative regulation of cellular component organization	5	3.29	0.03758	SPTBN1, SPTAN1, EIF4EBP1, MAP1B, ADD2	0.70945
GOTERM_BP_FAT	GO:0044087~regulation of cellular component biogenesis	5	3.29	0.03758	SPTBN1, SPTAN1, EIF4EBP1, MAP1B, ADD2	0.70945



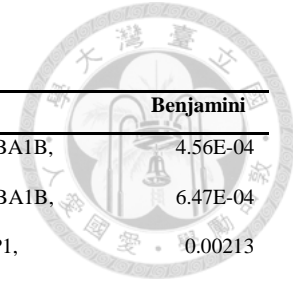


Table 6. List of GO-term of regulated phosphoproteins in phosphoproteome of silencing MCM2 in H1299 cells

Category	Term	Count	%	PValue	Genes	Benjamini
GOTERM_BP_FAT	GO:0034621~cellular macromolecular complex subunit organization	12	14.8	6.68E-07	TUBA3C, HIST1H1B, TUBA3E, CHAF1B, HELLS, MCM2, TUBA1A,TUBA1B, SRSF1, NUFIP1, TUBA1C, HMGA1	4.56E-04
GOTERM_BP_FAT	GO:0034622~cellular macromolecular complex assembly	11	13.6	1.89E-06	TUBA3C, HIST1H1B, TUBA3E, CHAF1B, HELLS, MCM2, TUBA1A,TUBA1B, SRSF1, NUFIP1, TUBA1C	6.47E-04
GOTERM_BP_FAT	GO:0065003~macromolecular complex assembly	14	17.3	9.36E-06	HIST1H1B, TUBA3C, TUBA3E, RRM2, MCM2, TUBA1A, SRSF1, NUFIP1, CHAF1B,THRAP3, HELLS,TUBA1B, TUBA1C, HMGA1	0.00213
GOTERM_BP_FAT	GO:0043933~macromolecular complex subunit organization	14	17.3	1.88E-05	HIST1H1B, TUBA3C, TUBA3E, RRM2, MCM2, TUBA1A, SRSF1, NUFIP1, CHAF1B,THRAP3, HELLS,TUBA1B, TUBA1C, HMGA1	0.00321
GOTERM_BP_FAT	GO:0051258~protein polymerization	5	6.17	7.73E-05	TUBA3C, TUBA3E, TUBA1A,TUBA1B, TUBA1C	0.01051
GOTERM_BP_FAT	GO:0022613~ribonucleoprotein complex biogenesis	7	8.64	1.85E-04	RPS6, UTP18,BOP1, SRSF1, NUFIP1, PA2G4, RRP1B	0.02084
GOTERM_BP_FAT	GO:0006333~chromatin assembly or disassembly	6	7.41	3.06E-04	HIST1H1B, CHAF1B, HELLS, MCM2, CHD8, HMGA1	0.02945
GOTERM_BP_FAT	GO:0006364~rRNA processing	5	6.17	8.78E-04	RPS6, UTP18,BOP1, PA2G4, RRP1B	0.07227
GOTERM_BP_FAT	GO:0006396~RNA processing	10	12.3	9.12E-04	RPS6, UTP18,BOP1, SSB, SRRM2, PRKRA, SRSF1, NUFIP1, PA2G4, RRP1B	0.06691
GOTERM_BP_FAT	GO:0016072~rRNA metabolic process	5	6.17	0.00103	RPS6, UTP18,BOP1, PA2G4, RRP1B	0.06795
GOTERM_BP_FAT	GO:0007017~microtubule-based process	7	8.64	0.00112	TUBA3C, TUBA3E, PCM1, TUBA1A,TUBA1B, MYH9, TUBA1C	0.06741
GOTERM_BP_FAT	GO:0034470~ncRNA processing	6	7.41	0.00176	RPS6, UTP18,BOP1, SSB, PA2G4, RRP1B	0.09529
GOTERM_BP_FAT	GO:0007018~microtubule-based movement	5	6.17	0.00188	TUBA3C, TUBA3E, TUBA1A,TUBA1B, TUBA1C	0.09422
GOTERM_BP_FAT	GO:0006260~DNA replication	6	7.41	0.00188	RAD9A, CHAF1B, RRM2, MCM2, TNKS1BP1, HMGA1	0.08793
GOTERM_BP_FAT	GO:0006461~protein complex assembly	9	11.1	0.00227	TUBA3C, TUBA3E, CHAF1B, RRM2,THRAP3, TUBA1A,TUBA1B, TUBA1C, HMGA1	0.09839
GOTERM_BP_FAT	GO:0070271~protein complex biogenesis	9	11.1	0.00227	TUBA3C, TUBA3E, CHAF1B, RRM2,THRAP3, TUBA1A,TUBA1B, TUBA1C, HMGA1	0.09839
GOTERM_BP_FAT	GO:0042254~ribosome biogenesis	5	6.17	0.00249	RPS6, UTP18,BOP1, PA2G4, RRP1B	0.10089
GOTERM_BP_FAT	GO:0042981~regulation of apoptosis	11	13.6	0.00377	FOSL1, RPS6, HMOX1, RAD9A, HELLS, PRKRA, SQSTM1, BNIP2, CHD8, YBX3,RTN4	0.14093
GOTERM_BP_FAT	GO:0043067~regulation of programmed cell death	11	13.6	0.00405	FOSL1, RPS6, HMOX1, RAD9A, HELLS, PRKRA, SQSTM1, BNIP2, CHD8, YBX3,RTN4	0.14268
GOTERM_BP_FAT	GO:0010941~regulation of cell death	11	13.6	0.00416	FOSL1, RPS6, HMOX1, RAD9A, HELLS, PRKRA, SQSTM1, BNIP2, CHD8, YBX3,RTN4	0.13904
GOTERM_BP_FAT	GO:0034660~ncRNA metabolic process	6	7.41	0.00429	RPS6, UTP18,BOP1, SSB, PA2G4, RRP1B	0.1366
GOTERM_BP_FAT	GO:0006357~regulation of transcription from RNA polymerase II promoter	10	12.3	0.00622	FOSL1, HMOX1,THRAP3, RBL1, HTATSF1, SQSTM1, NUFIP1, CHD8, DEK, YBX3	0.1837

Table 6. Continued

Category	Term	Count	%	PValue	Genes	Benjamini
GOTERM_BP_FAT	GO:0043623~cellular protein complex assembly	5	6.17	0.00682	TUBA3C, TUBA3E, TUBA1A,TUBA1B, TUBA1C	0.19147
GOTERM_BP_FAT	GO:0051276~chromosome organization	8	9.88	0.00712	HIST1H1B, CHAF1B, RBL1, HELLS, MCM2, CHD8, TNKS1BP1, HMGA1	0.19128
GOTERM_BP_FAT	GO:0031497~chromatin assembly	4	4.94	0.00773	HIST1H1B, CHAF1B, HELLS, MCM2	0.19809
GOTERM_BP_FAT	GO:0006325~chromatin organization	7	8.64	0.00813	HIST1H1B, CHAF1B, RBL1, HELLS, MCM2, CHD8, HMGA1	0.19998
GOTERM_BP_FAT	GO:0065004~protein-DNA complex assembly	4	4.94	0.00874	HIST1H1B, CHAF1B, HELLS, MCM2	0.20596
GOTERM_BP_FAT	GO:0034728~nucleosome organization	4	4.94	0.00928	HIST1H1B, CHAF1B, MCM2, HMGA1	0.21001
GOTERM_BP_FAT	GO:0006355~regulation of transcription, DNA-dependent	16	19.8	0.01438	HMOX1, HTATSF1, NUFIP1, PA2G4, FOSL1, ATF2,THRAP3, RBL1, HELLS, SQSTM1, CHD8, MYBBP1A, DEK, IRX5, YBX3, HMGA1	0.29768
GOTERM_BP_FAT	GO:0008283~cell proliferation	7	8.64	0.01564	MAPRE1, HMOX1, HDGF, PDAP1,BOP1, HELLS, PA2G4	0.3102
GOTERM_BP_FAT	GO:0019058~viral infectious cycle	3	3.7	0.01705	HTATSF1, DEK, HMGA1	0.32397
GOTERM_BP_FAT	GO:0006323~DNA packaging	4	4.94	0.01719	HIST1H1B, CHAF1B, HELLS, MCM2	0.31751
GOTERM_BP_FAT	GO:0051252~regulation of RNA metabolic process	16	19.8	0.0174	HMOX1, HTATSF1, NUFIP1, PA2G4, FOSL1, ATF2,THRAP3, RBL1, HELLS, SQSTM1, CHD8, MYBBP1A, DEK, IRX5, YBX3, HMGA1	0.31241
GOTERM_BP_FAT	GO:0043066~negative regulation of apoptosis	6	7.41	0.02432	HMOX1, HELLS, SQSTM1, BNIP2, CHD8, YBX3	0.39921
GOTERM_BP_FAT	GO:0045449~regulation of transcription	20	24.7	0.02467	HMOX1, HTATSF1, MCM2, NUFIP1, PA2G4, FOSL1, ATF2, HDGF,THRAP3, CHAF1B, RBL1, HELLS, MYBBP1A, SQSTM1, CHD8, DEK, IRX5, YBX3, HMGA1, CCNLI	0.39451
GOTERM_BP_FAT	GO:0043069~negative regulation of programmed cell death	6	7.41	0.02564	HMOX1, HELLS, SQSTM1, BNIP2, CHD8, YBX3	0.39763
GOTERM_BP_FAT	GO:0060548~negative regulation of cell death	6	7.41	0.02591	HMOX1, HELLS, SQSTM1, BNIP2, CHD8, YBX3	0.3923
GOTERM_BP_FAT	GO:0007049~cell cycle	9	11.1	0.02686	MAPRE1, CHAF1B, NUMA1, RBL1, HELLS, MCM2, MYH9, CLIP1, PA2G4	0.39507
GOTERM_BP_FAT	GO:0006259~DNA metabolic process	7	8.64	0.02991	RAD9A, CHAF1B, RRM2, HELLS, MCM2, TNKS1BP1, HMGA1	0.42067
GOTERM_BP_FAT	GO:0001525~angiogenesis	4	4.94	0.03162	HMOX1, MYH9, NCL,RTN4	0.43036
GOTERM_BP_FAT	GO:0022415~viral reproductive process	3	3.7	0.03375	HTATSF1, DEK, HMGA1	0.44359
GOTERM_BP_FAT	GO:0016032~viral reproduction	3	3.7	0.04319	HTATSF1, DEK, HMGA1	0.52074
GOTERM_BP_FAT	GO:0006457~protein folding	4	4.94	0.04941	CANX, ST13, RANBP2, STUB1	0.56136
GOTERM_BP_FAT	GO:0043065~positive regulation of apoptosis	6	7.41	0.04955	FOSL1, RPS6, HMOX1, RAD9A, PRKRA, SQSTM1	0.55389
GOTERM_BP_FAT	GO:0040029~regulation of gene expression, epigenetic	3	3.7	0.04997	HELLS, PRKRA, HMGA1	0.54873

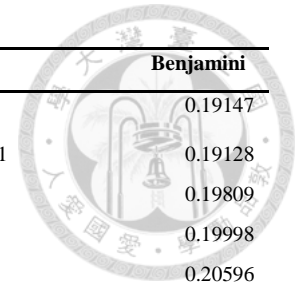


Table 7. The phosphosites on MCM2 identified in the phosphoproteome data

Uniprot ^a	Symbol ^b	Protein name ^c	Positions within proteins ^d	Amino acid ^e	Ratio H/L normalized MCM2 ^f	Ratio H/L normalized siMCM2 ^g	Localization prob MCM2 ^h	Localization prob siMCM2 ⁱ
P49736	MCM2	DNA replication licensing factor MCM2	27	S	13.627	0.19726	0.994583	0.999487
P49736	MCM2	DNA replication licensing factor MCM2	139	S	13.379	0.18847	1	1
P49736	MCM2	DNA replication licensing factor MCM2	108	S	7.4536	N/A	0.9653	N/A
P49736	MCM2	DNA replication licensing factor MCM2	26	S	N/A	0.2171	0.490244	0.814541

Table 8. The phosphosites on high mobility group (HMG) proteins identified in the phosphoproteome data

Uniprot ^a	Symbol ^b	Protein name ^c	Positions within proteins ^d	Amino acid ^e	Ratio H/L normalized MCM2 ^f	Ratio H/L normalized siMCM2 ^g	Localization prob MCM2 ^h	Localization prob siMCM2 ⁱ
P17096	HMGA1	High mobility group protein HMG-I/HMG-Y	99	S	2.7934	0.21118	1	1
P17096	HMGA1	High mobility group protein HMG-I/HMG-Y	102	S	1.2126	0.054961	1	1
P17096	HMGA1	High mobility group protein HMG-I/HMG-Y	103	S	0.97257	0.054961	1	1
P05114	HMGN1	Non-histone chromosomal protein HMG-14	86	S	0.44714	N/A	0.971379	N/A
P05114	HMGN1	Non-histone chromosomal protein HMG-14	89	S	0.44714	N/A	0.995472	N/A

^a The official protein Uniprot ID given to the identified protein.

^b The official gene symbol given to identified protein.

^c The official protein name obtained from Uniprot

^d The amino acid position sites to be phosphorylated within the identified phosphosites

^e The amino acid to be phosphorylated in the identified phosphosites

^f The normalized ratio between two medium and light label partners of the identified phosphosites in MCM2 overexpression experiment

^g The normalized ratio between two medium and light label partners of the identified phosphosites in silencing MCM2 experiment

^h The localization probability of the identified phosphosites in MCM2 overexpression experiment

ⁱ The localization probability of the identified phosphosites in silencing MCM2 experiment